5-2014

Molecular Characterization of Glioblastoma Cancer Stem Cells

Jo Meagan Garner
University of Tennessee Health Science Center

Molecular Characterization of Glioblastoma Cancer Stem Cells

DOI
10.21007/etd.cghs.2014.0106

Molecular Characterization of Glioblastoma Cancer Stem Cells

A Dissertation
Presented for
The Graduate Studies Council
The University of Tennessee
Health Science Center

In Partial Fulfillment
Of the Requirements for the Degree
Doctor of Philosophy
From The University of Tennessee

By
Jo Meagan Garner
May 2014

DEDICATION

This is dedicated to my loving husband and family for the endless support, encouragement and laughs they have provided me with to get through this journey.

ACKNOWLEDGEMENTS

I would like to thank my graduate advisor, Lawrence M. Pfeffer, Ph.D., and my advisory committee: Andrew Davidoff, M.D.; Meiyun Fan, Ph.D.; Charles Handorf, M.D., Ph.D. and Zhaohui Wu, M.D., Ph.D. for their instrumental comments, ideas, support and motivation. Additionally, I would like to acknowledge Ziyun Du, Ph.D.; Sue Pfeffer, Ph.D.; Michelle Sims and Chuan Yang, Ph.D. for their helpful assistance on all projects presented here. I would also like to thank Amira Ahmed, Ph.D.; Debolina Ganguly; Elena Paulus, M.D. and Aarti Sethuraman for providing me with daily discussions, whether they be scientific or senseless. Furthermore, I would like to recognize the VA Microarray Core, as well as, the Davidoff Lab, David Finkelstein, Ph.D. and David Ellison, M.D., Ph.D. at St. Jude Children's Research Hospital for helpful input and assistance. Finally, I would like to thank all of the faculty and staff of the University of Tennessee Health Science Center, Center for Cancer Research for providing a friendly environment for learning and research.

ABSTRACT

Malignant gliomas are locally aggressive, highly vascular tumors that have an overall survival time less than 14 months, and current therapies provide little improvement in the disease course and outcome. While glioblastoma multiforme (GBM) patients present uniform histological phenotypes, the molecular determinants of the disease vary considerably between individual cases resulting in complicated prognosis. The heterogeneity, aggressiveness and rapid tumor relapse of GBM is believed to be sustained by cancer stem-like cell populations that are able to initiate and maintain tumors. Although CSCs represent only a small fraction of cells within a tumor, their high tumor-initiating capacity and therapeutic resistance is believed to drive tumorigenesis. Therefore, it is imperative to improve our molecular understanding of the tumor initiating cells and identify pathways associated with CSCs in order to devise innovative strategies to selectively target them.

In this study, Glioma CSCs were isolated and maintained *in vitro* using an adherent culture system and shown to have constitutive activation of the STAT3/NF-κB signaling pathways and upregulation of STAT3 and NF-κB-dependent genes. Gene expression profiling also found components of the Notch pathway as being deregulated in glioma CSC, which were sensitive to treatment with STAT3 inhibitors. We also identified two CSC populations that produce Classical or Mesenchymal GBM tumors but display identical histological features. Adherent CSC-derived Mesenchymal GBM xenografts were found to exhibit high STAT3 and ANGPTL4 expression levels compared to Classical tumors. This subpopulation of glioma CSCs formed tumors with histopathological features of GBM and were enriched for stem cell markers, transcriptional networks and pro-angiogenic markers characteristic of the Mesenchymal subtype. Molecular characterization of aggressive Mesenchymal GBM xenografts identified high STAT3 and ANGPTL4 expression levels within the CD133+ CSC subpopulation, and these proteins were shown to colocalize within GBM stem cells. Elevated STAT3 and ANGPTL4 expression was found to correlate to short-term survival of human GBM patients, and a link in expression levels was observed between the genes in individual patient samples. The deregulated expression of these genes in glioma CSCs was sensitive to the kinase inhibitors, WP1066 and Sorafenib, and targeted inhibition of STAT3 and ANGPTL4 was found to decrease stem cell marker expression within tumors and lead to tumor regression.

Taken together, these studies reveal that multiple CSC populations exist within GBM that drive molecular heterogeneity and tumorigenesis. Establishing an adherent CSC culture that maintains a Mesenchymal GBM signature provides a valuable and accurate model of the human disease, which will give insight into the role in tumor progression of novel genes as well as their utility as new therapeutic targets. The constitutive activation of STAT3 and NF-κB signaling pathways found in glioma CSCs that regulates Notch signaling, as well as, the important relationship established between STAT3 and ANGPTL4 in Mesenchymal GBM stem cells provides potential therapeutic value as biomarkers in targeting the CSC subpopulation of GBM.

TABLE OF CONTENTS

LIST OF FIGURES

LIST OF ABBREVIATIONS

A20	Tumor necrosis factor, alpha-induced protein 3
AC133	Prominin 1
ADAM	ADAM metallopeptidase domain
Ad-CSC	Adherent cancer stem cell
AKT	V-akt murine thymoma viral oncogene homolog
ANGPTL	Angiopoietin-like protein
ANOVA	Analysis of variance
APH1	Anterior pharynx-defective 1
BAD	BCL2-associated agonist of cell death
BCA	Bicinchoninic acid
Bcl-2	B-cell lymphoma 2
Bcl-xL	B-cell lymphoma-extra large
bFGF	Basic fibroblast growth factor
bp	Base pair
BSA	Bovine serum albumin
CASP	Caspase
CBP	CREB binding protein
CCND2	Cyclin D2
CD133	Prominin 1
CDH1	Cadherin 1 type 1, E-cadherin
CDKN2A	Cyclin-dependent kinase inhibitor 2A
CHI3L1	Chitinase 3-like 1

ChIP	Chromatin immunoprecipitation
CNS	Central nervous system
COX-2	Cytochrome c oxidase subunit II
CREB	cAMP response element-binding protein
CSC	Cancer stem cell
CTBP1	C-terminal binding protein 1
CXCL	Chemokine (C-X-C motif) ligand
DAVID	Database for Annotation, Visualization and Integrated Discovery
DMEM	Dulbecco's modified eagle medium
DMSO	Dimethyl sulfoxide
DPBS	Dulbecco's phosphate buffered saline
DTX3	Deltex 3
DVL3	Dishevelled segment polarity protein 3
E.coli	Escherichia coli
EGF	Epidermal growth factor
EGFR	Epidermal growth factor receptor
ELAM-1	Selectin E
ELISA	Enzyme-linked immunosorbent assay
EP1	Prostaglandin E receptor 1
ERK	Elk-related tyrosine kinase
ETV1	Ets variant 1
FBS	Fetal bovine serum
FFPE	Formalin-fixed paraffin-embedded

FGF	Fibroblast growth factor
FGFR3	Fibroblast growth factor receptor
FITC	Fluorescein isothiocyanate
GBM	Glioblastoma multiforme
GFAP	Glial fibrillary acidic protein
GST	Glutathione S-transferase
GTPase	Hydrolyze guanosine triphosphate enzyme
H&E	Hematoxylin and eosin
HCL	Hydrochloric acid
Hes	Hairy enhancer of split family
Hey1	Hes-related family bHLH transcription factor with YRPW motif 1
HIF-1	Hypoxia-inducible factor 1
ICAM-1	Intercellular adhesion molecule 1
IDH1	Isocitrate dehydrogenase 1
IgG	Immunoglobulin G
IκB	Inhibitor of NF-kappa-B
IKK	IkappaB kinase
IL	Interluekin
IPA	Ingenuity Pathway Analysis
JAG1	Jagged 1
JAK	Janus kinase
KAT2A	K(lysine) acetyltransferase 2A
LYN	V-yes-1 Yamaguchi sarcoma viral related oncogene homolog

MAP2	Microtubule-associated protein 2
Mcl-1	Induced myeloid leukemia cell differentiation protein
Mcp-1	Monocyte chemoattractant protein-1
MMP	Matrix metalloproteinases
mTOR	Mechanistic target of rapamycin
MTT	3-(4,5-dimethylthiazol-2-yl)-2,5-diphenyltetrazolium bromide
Na3VO4	Sodium orthovanadate
NADPH	Nicotinamide adenine dinucleotide phosphate-oxidase
NaF	Sodium fluorid
NF1	Neurofibromin 1
NF-κB	Nuclear factor of kappa light polypeptide gene enhancer in B-cells
NICD	Notch intracellular domain
NQO1	NAD(P)H dehydrogenase, quinone 1
NRTK	Non-receptor tyrosine kinase
NSG	NOD.Cg Prkdcscid Il2rgtm1Wjl/SzJ
NUMBL	Numb homolog (Drosophila)-like
OCT	Optimal cutting temperature compound
OLIG2	Oligodendrocyte lineage transcription factor 2
PCA	Principal component analysis
PDGF	Platelet-derived growth factor
PDGFRA	Platelet-derived growth factor receptor, alpha
PDX	Patient-derived xenograft
PE	Phycoerythrin

PEN2	Presenilin enhancer gamma secretase subunit
PGE2	Prostaglandin E2
PI3K	Phosphatidylinositol-4,5-bisphosphate 3-kinase
PIAS3	Protein inhibitor of activated STAT3
PMSF	Phenylmethanesulfonyl fluoride
pol II	Polymerase II
pSTAT3	Phosphorylated STAT3
pTyr	Phospho-Tyrosine
PVDF	Polyvinylidene difluoride
qPCR	Quantitative polymerase chain reaction
Rac	Ras-related C3 botulinum toxin substrate
Ras	Rat sarcoma viral oncogene
Rb	Retinoblastoma 1
RBPJ	Recombination signal binding protein for IgG kappa J region
RIPA	Radioimmunoprecipitation assay buffer
RT-PCR	Real-time polymerase chain reaction
S100	S100 calcium binding protein
SDS-PAGE	Sodium dodecyl sulfate polyacrylamide gel electrophoresis
Ser-727	Serine-727
SH2	Src homology 2
Shh	Sonic hedgehog
siRNA	Small interfering RNA
SMA	Smooth muscle alpha actin

Sox2	Sex determining region Y-box 2
Sor	Sorafenib
Sp-C	Tumorsphere
SPP1	Secreted phosphoprotein 1
Src	V-src avian sarcoma (Schmidt-Ruppin A-2) viral oncogene
STAT	Signal transducers and activators of transcription
STRING	Search Tool for the Retrieval on Interacting Genes/Proteins
SYN	Synapsin
TCGA	The Cancer Genome Atlas
TF	Transcription factor
TGF-β	Transforming growth factor beta
TMZ	Temozolomide
TNF	Tumor necrosis factor
TNFR	Tumor necrosis factor receptor-associated factor
TP53	Tumor protein p53
TRADD	TNFRSF1A-associated via death domain
TRAF	Tumor necrosis factor receptor-associated factor
Tyr-705	Tyrosine-705
VCAM-1	Vascular cell adhesion molecule 1
VEGF	Vascular endothelial growth factor
VEGFR	Vascular endothelial growth factor receptor
Vel	Velcade
WP	WP1066

CHAPTER 1. INTRODUCTION

Significance of Transcription Factors in Tumorigenesis

Transcription factors (TFs) are important cellular components that control gene expression by gauging environmental cues to determine cell fate. Cells must recognize and respond appropriately to various internal and external stimuli to coordinate appropriate gene expression [1]. TFs bind to specific DNA sequences of genes and determine whether or not the gene will be transcribed. The control region of a gene includes specific segments of DNA called enhancers where transcription factors bind most often in multi-protein complexes. This attracts RNA polymerase II (pol II) and alters the chromatin structure by impacting histone proteins that package chromosomal DNA. An environment is then created that enables pol II to initiate and elongate an RNA transcript to regulate gene expression [2]. TFs can exercise great power since a single TF can simultaneously affect the expression of a large cohort of downstream genes. In maintaining expression of numerous genes, the transcriptional regulatory system plays a central part in controlling many biological processes such as cell cycle progression, cellular differentiation, and transformation [3-5]. It is through this same regulatory system that numerous diseases arise due to changes in the activity and regulatory specificity of TFs.

Deregulated expression and activation of TFs as well as mutations and translocations play critical roles in tumorigenesis. Most oncogenic signaling pathways converge on sets of transcription factors that ultimately control gene expression patterns that promote tumor formation, progression and metastasis [6]. Aberrant activation of these TFs is the result of numerous mechanisms such as changes in expression, protein stability, protein interactions and post-translational modifications, which leads to deregulated expression of multiple gene sets involved in cancer cell survival, proliferation, angiogenesis and metastasis [7]. Since transcriptional regulators are generally inactive in normal physiological conditions and their expression and activities are tightly regulated, TFs could serve as necessary and suitable therapeutic targets in inhibiting cancer development and progression. A limited number of transcription factors are overactive in a large percentage of cancers; of those are the latent cytoplasmic transcription factors STAT3, NF-κB and Notch intracellular domain (NICD) [8, 9].

STAT3 and Cancer

Signal Transducers and Activators of Transcription (STATs) are a family of latent cytoplasmic proteins that act as signal messengers and transcription factors and participate in normal cellular responses to cytokines and growth factors [6]. To date, there are seven STAT family members identified: STAT1, 2, 3, 4, 5a, 5b and 6; all of which are located in the cytoplasm in an inactive state in resting cells [10]. STAT3 was originally identified as the transcription factor responsible for the induction of acute phase response genes, but STAT3 is activated through tyrosine phosphorylation

(pSTAT3) by a wide variety of factors, suggesting that it integrates diverse signals into common transcriptional responses [11-13]. As shown in **Figure 1-1**, STAT3 activations begins most commonly when JAK tyrosine kinases associate with cytokine receptors and initiate a three-step tyrosine phosphorylation cascade: JAK(pTyr)-receptor(pTyr)-STAT(pTyr). G-protein coupled receptors as well as growth factor receptors can also activate STATs directly or by recruiting other non-receptor tyrosine kinases. Following tyrosine phosphorylation, the SH2 (src homology 2) domains of STAT3 dimerize by reciprocal phosphotyrosine interactions. STAT3 proteins then bind to importins and translocate to the nucleus and activate gene transcription [14, 15]. STAT3 has a diverse physiological role due to the many genes it regulates, such as: genes involved in cell cycle progression (Cyclin D1, D2, and cMyc), cell survival (Bcl-xL, Bcl-2, and Mcl-1), invasion (MMP2 and MMP9), and angiogenesis (VEGF and HIF-1). Due to the critical role of STAT3 in cells, it has a precise activation and deactivation cycle. Dysregulation at any level, whether it be cytokines, growth factors, or tyrosine kinases, can lead to increased activation and tumorigenesis [10, 16].

Constitutively active STAT3, that is tyrosine phosphorylated STAT3 (pSTAT3), has been found in a wide variety of human cancer cell lines and primary tumors. Normally, tyrosine phosphorylation of STAT3 protein is switched on and off in response to signals that control cell growth and development. However, in oncogenically transformed cells continuously activated STAT3 relays messages to the nucleus to promote transformation and tumorigenesis [17]. Gene knockout studies have revealed the importance of STAT3 in normal cells and development, as STAT3 null mice proved to be embryonic lethal [18]. It has also been demonstrated that cancer cells are addicted to STAT3 activity when compared to their normal counterpart. Several studies have revealed that inhibition of STAT3 signaling lead to apoptosis in tumor cells, while normal cells were able to survive at much lower levels through alternative mechanisms [19]. Evidence suggests that STAT3 activation plays a critical role in every step of tumor progression.

Malignant transformation of cells by various protein tyrosine kinases, oncogenes, and viruses are all mediated through STAT3 activation. STAT3 also promotes cellular proliferation and survival. Constitutive STAT3 signaling is associated with upregulation of Cyclin D1 and cMyc expression, resulting in accelerated cell-cycle progression [20]. Consistent with its role in proliferation, STAT3 signaling provides survival signals and suppresses apoptosis in cancer cells in part through the upregulation of Bcl-2, Bcl-xL, and Mcl-1 [21]. Invasion to the extracellular matrix is another key step in tumorigenesis that STAT3 actively participates in. Several studies reveal that overexpression of pSTAT3 correlates with increased invasion and metastasis through the direct regulation of matrix metalloproteinases (MMPs) [22-24]. Evidence also suggests that STAT3 activity plays a role in cellular migration under normal as well as pathological conditions. STAT3 is crucial to wound healing and cell migration and also controls the directional movements of cells through Rac1 and Rho GTPase regulation [25, 26]. Lastly, the constitutive activation of STAT3 promotes angiogenesis through direct transcriptional activation of vascular endothelial growth factor and hypoxia-inducible factor-1α [27-29].

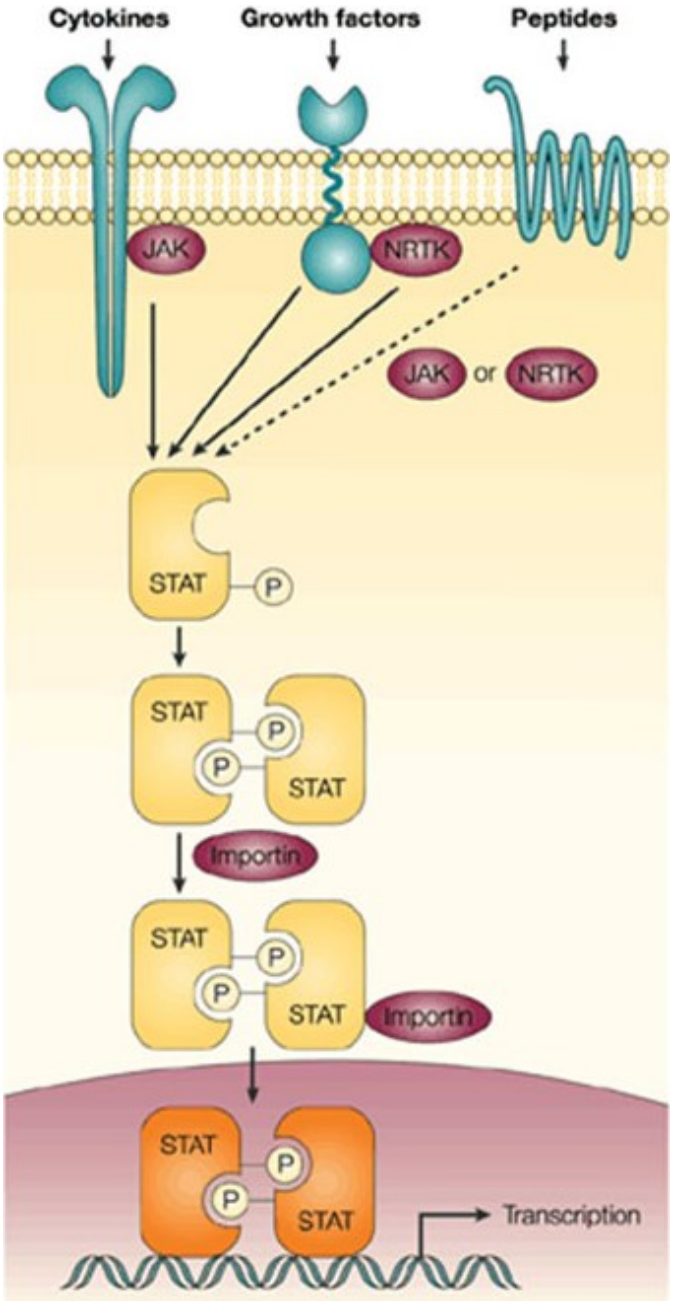

Figure 1-1. The STAT signaling pathway.

STAT transcription factors are activated via a tyrosine phosphorylation cascade following ligand binding. The activated STATs subsequently move into the nucleus where they bind specific DNA sites as homo or heterodimers to stimulate transcription of genes. Reprinted with permission from Darnell, J.E., Jr., *Transcription factors as targets for cancer therapy.* Nat Rev Cancer, 2002. 2(10): p. 740-9.

Due to widespread occurrence of persistent STAT3 activation in cancer and its various roles in tumor progression, the transcriptional activator is a prime anti-cancer target.

NF-κB and Cancer

Nuclear Factor of κB (NF-κB) is a family of latent transcription factors found inactive in the cytoplasm as homo- or heterodimers in cells. The NF-κB family includes at least five members: NFκB1 (constitutively processed to p50), NFκB2 (stimulus-induced processing to p52), RelA (p65), RelB and cRel, with the most common heterodimer being p50-p65 [14]. The NF-κB transcription factor was originally identified by its role in B-cell specific gene expression and is now known to be crucial in inflammatory and immune response to cellular injury. Further studies have shown that diverse stimuli converge on the NF-κB family in most cell types, leading to transcription and regulation of large genes sets involved in many biological processes [30]. Under most circumstances, NF-κB signaling is silent and sequestered in the cytoplasm through the binding of inhibitory proteins called IκBs. However, NF-κB is activated by diverse signaling pathways, including extracellular factors involved in inflammatory response, tumor necrosis factor-α (TNF-α), type I interferons, Interleukin-1 (IL-1), lipopolysaccharides, UV radiation, viruses, and reactive oxygen species [6]. As shown in **Figure 1-2**, various stimuli promote the dissociation of the cytosolic inactive NF-κB/IκB complexes via IκB kinase (IKK) activation, which results in the serine phosphorylation and degradation of IκB. The smaller NF-κB subunit, p50, is derived by proteolytic cleavage of a p100 translation product, which is retained in the cytoplasm. Upon release, the p50 subunit binds p65 in the cytoplasm to form an active transcription factor. The nuclear localization sequences that are exposed on p65 following IκB degradation allow the heterodimer to bind importins and translocate into the nucleus and participate in transcriptional activation [31-33].

NF-κB is involved in many biological processes by directly regulating the expression of inflammation response genes including cytokines and chemokines, acute phase proteins, cell adhesion proteins, immunoglobulins, viral genes as well as cell cycle regulatory and anti-apoptotic genes [34-37]. While activation of NF-κB is found in normal cells, it is constitutively activated in many human tumors. NF-κB binding activity is shown to be higher in 85% of nuclear extracts from mammary tumors when compared to normal mammary glands, and constitutive activation has been found in 83% of human pancreatic cancer cell lines [34]. Furthermore, the inhibition of p65 in thyroid cancer cell lines led to a decrease in cMyc expression and a reduction in cell growth. NF-κB is believed to contribute to tumorigenesis through the regulation of genes that promote tumor cell survival, proliferation, migration and therapeutic resistance [38-42].

A critical event in tumorigenesis is prolonged cell survival, and many studies prove that aberrant activation of NF-κB can provide this anti-apoptotic signal. A number of NF-κB-inducible genes that inhibit apoptosis have been identified, including Bcl-2, TRAF1, TRAF2 and A20 [43]. NF-κB can contribute to tumorigenesis in ways other than inhibition of apoptosis; it is shown to directly stimulate cell proliferation through

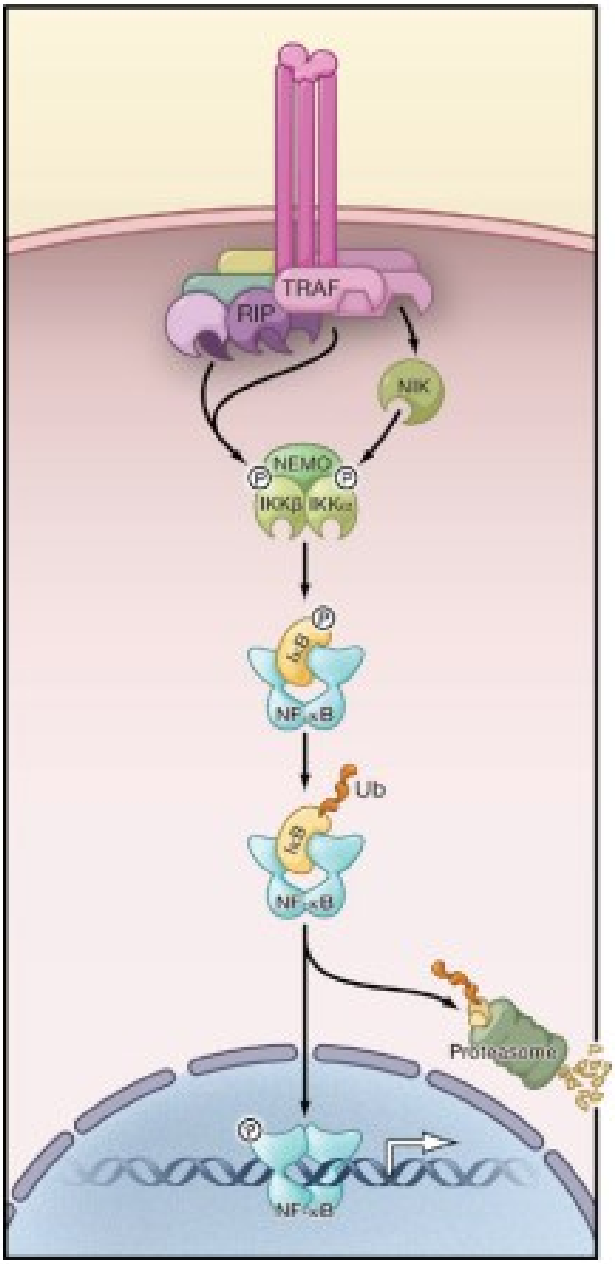

Figure 1-2. The NF-κB signaling pathway.

Following receptor ligation and recruitment of receptor proximal adaptor proteins, signaling to IKK proceeds through TRAF/Rip complexes, generally in conjunction with TAK1, leading to canonical NF-κB signaling. IKK activation results in IκB phosphorylation and degradation. Phosphorylated NF-κB dimers bind to DNA elements and induce transcription of target genes. Reprinted with permission from Hayden, M.S. and S. Ghosh, *Shared principles in NF-kappaB signaling.* Cell, 2008. **132**(3): p. 344-62.

activation of the proto-oncogenes cMyc and Cyclin D1 [44, 45]. The migration of cancer cells into and out of vessel walls that leads to metastasis is also attributed to constitutive activation of NF-κB. NF-κB regulates expression of cell adhesion molecules, so its activation leads to extravasation through increased gene expression of VCAM-1, ICAM-1 and ELAM-1 [46-48]. The dependence of cancer cells on oxygen for survival is also supported by NF-κB activity. The transcription factor regulates expression of angiogenic growth factors and cytokines, such as VEGF, TNF and MCP-1, to promote angiogenesis and tumor progression [49-51]. The constitutive NF-κB activity in many cancer types and its multiple roles in tumor development make this transcriptional activator an attractive target in treating cancer.

Transcription Factor Activity in Glioblastoma

Malignant gliomas are the most common type of primary brain tumor and the most prevalent cancer of the central nervous system. While the incidence of glioma is low compared to solid tumors in other organ systems, low survival rates make these tumors the leading cause of cancer-related death in the young to middle-aged populations [52]. Pathological studies indicate that gliomas arise in the cerebral hemispheres along the cortical/subcortical interface and feature enhanced mitoses and necrosis through histological analysis [53]. Malignant gliomas are locally aggressive, highly vascular tumors that are very difficult to treat. The median survival for patients with glioblastoma multiforme (GBM), the most common and aggressive subtype of glioma, has remained at around one year for several decades [54]. Surgical resection of GBM remains the primary treatment modality, as present adjuvant therapies provide little improvement in the disease course and outcome. It is believed that effective treatments can be developed once the genetic and molecular mechanisms that lead to glioma initiation and progression are discovered.

The malignant transformation of cells can be attributed to aberrant activation of STAT3, which leads to dysregulation of genes involved in the cell cycle and apoptosis. High persistent activation of STAT3 is found in diverse human tumors, including gliomas [15, 17]. Constitutively active STAT3, as assessed by tyrosine phosphorylation, is frequently expressed in high-grade gliomas and found to correlate with tumor grade and poor patient survival [55]. Elevated levels of pSTAT3 have been observed in GBM tissues compared with control tissue. Studies also show that STAT3 is one of the major regulators of mesenchymal transformation, which leads to the hallmark phenotype of tumor aggressiveness in GBM [56]. The activation of STAT3 and JAK2 in GBM can be attributed to the dysregulation of many proteins and pathways. The STAT3 activator, IL-6, is highly expressed in human GBMs and corresponds to increasing tumor grade and decreased patient survival [57]. IL-6 is also shown to act through STAT3 to regulate VEGF expression and promote angiogenesis [58]. Persistent STAT3 signaling in GBM is also a result of low expression levels of the protein inhibitor of activated STAT3 (PIAS3) in glioma samples [59]. The effective inhibition of STAT3 signaling in GBM animal models is found to decrease tumor growth and enhance apoptosis, confirming the importance of STAT3 activation in glioma progression [60].

The NF-κB family of transcription factors is also found to be aberrantly upregulated in a variety of human cancers, including gliomas [61]. Studies show that levels of NF-κB activity, as measured by serine phosphorylation, are much higher in GBM tissue compared to normal tissue and correlate with increasing grade in astrocytoma tumors [62, 63]. While the exact process leading to NF-κB activation in glioma is still unclear, there are numerous proteins and pathways dysregulated in glioma that result in constitutive NF-κB activity. TNF-α, one of the most common activators of NF-κB, is produced in the central nervous system (CNS) by microglia, neurons, astrocytes, and endothelial cells [64]. In GBM, TNF-α signals through TNFR1 to promote NF-κB activation and subsequent anti-apoptotic responses [65]. Furthermore, the levels of TNFR1 expression are elevated in GBM as compared with other low-grade gliomas, suggesting TNF-α and TNFR1 activate NF-κB signaling and gene transcription to promote tumor progression [66]. Numerous growth factors and signaling pathways dysregulated in gliomas, such as EGF and PDGF, also lead to the persistent activation of NF-κB. Through binding their respective receptors, both EGF and PDGF activate NF-κB by a PI3K-AKT-IKK dependent mechanism to promote glioma cell survival [67, 68]. In addition, the expression of the ubiquitin-editing protein A20, a negative regulator of NF-κB, is diminished in GBM and is associated with the acquired resistance of cancer cells to O6-alkylating agents like TMZ [69]. Studies reveal that inhibition of NF-κB activity and NF-κB-regulated genes leads to a reduction in GBM growth, invasion and angiogenesis, suggesting a strong correlation between NF-κB activation and gliomagenesis [70].

Activity of STAT3 and NF-κB in Glioma Cancer Stem Cells

For many cancers the tumorigenic process may be initiated and sustained by a rare, stem cell-like subpopulation, denoted cancer stem-like cells (CSCs) [71]. These cells behave similarly to normal stem cells in that they can self-renew and generate differentiated progeny, but they form tumors upon serial transplantation into host mice and recapitulate the tumor phenotype [72]. The stem cell markers Nestin, Sox2 and CD133 have been used to identify GBM CSCs [73]. A number of *in vitro* and *in vivo* studies have demonstrated that human tumor cells with stem cell properties are required for the growth and progression of glioma tumors. CD133 levels have even been shown to correlate with tumor grade and be a predictive marker of GBM survival [74]. Although CSCs represent a small population of cells within a tumor, their high tumor-initiating capacity and therapeutic resistance drives tumorigenesis. With the discovery of CSCs, new complexities in cancer therapy have been revealed. The ineffectiveness of current therapies probably reflects their lack of potency on the CSC subpopulation, which remains viable and commonly leads to tumor regeneration and metastasis [75].

Tumor-initiating cells in several solid tumor types including glioma, breast, colon, and lung cancer have been enriched using the classical tumorsphere culture system. To maintain cells in this culture condition, the exclusion of serum and the addition of growth factors are always required [76]. While stem cell expansion has been successful, the tumorsphere method has several important limitations. Sphere aggregation restricts true

clonal analysis, spontaneous cell differentiation commonly occurs, and there is a high percentage of apoptosis within the stem cell population. These problems limit the study of stem cell behavior and marker analysis, so the true nature of CSCs is difficult to determine [77]. Establishing an adherent culture system for GBM stem cells as shown in **Figure 1-3** that allows for long-term expansion of pure CSC populations would provide a valuable and accurate model of the human disease for future studies [78, 79]. Maintaining GBM stem cells *in vitro* that retain cancer-initiating properties is a critical step to understand the biological function and nature of these cells. The characterization of GBM stem-like cells will give insight into novel genes involved in glioma tumor progression and lead to the discovery of new molecular markers that are predictive of metastatic disease.

Recent studies have examined the roles of STAT3 and NF-κB in glioma CSCs. STAT3 is constitutively activated by virtue of its tyrosine phosphorylation in GBM CSCs and required for their proliferation and survival. Selective inhibition of STAT3 abrogates CSC proliferation, suggesting that self-renewal for GBM stem-likes cells depends on the presence of STAT3 [80]. Following treatment with targeted small molecule inhibitors of STAT3 DNA binding, single glioma cells could no longer form neurospheres. This same treatment also resulted in a loss of stem cell marker expression, suggesting STAT3 is required for maintenance of the stem-like characteristics of these cells [81]. Targeting STAT3 activity also sensitizes glioma CSCs to the inhibitory action of TMZ, which strongly demonstrates the therapeutic potential of STAT3-targeted therapy in treating GBM. The role of NF-κB signaling in glioma CSCs is not well defined. Studies reveal that genes regulated by NF-κB are more highly expressed in U87 glioma cells that are CD133 positive when compared to the CD133 negative population [82]. Recent findings suggest that activation of the NF-κB pathway plays a critical role in the maintenance of GBM stem cells. CD133 positive glioma CSCs were shown to undergo morphological changes following IKK inhibition and gene expression analysis under the same conditions revealed downregulation of stem cell markers while the astrocytic marker, GFAP, was upregulated [83]. Taken together, the two pathways regulate genes important to cell fate determination, survival, proliferation and maintenance of stem cells and represent potential therapeutic targets in treating GBM [84].

STAT3 and NF-κB Regulation of Notch Signaling

Studies suggest a complex relationship between the STAT3 and NF-κB pathways in glioma tumor progression [85]. Crosstalk between the two pathways has been demonstrated at multiple levels, including activation of STAT3 by NF-κB-inducible factors and STAT3 regulation of NF-κB processing and nuclear translocation [86]. Both transcription factors appear to regulate the expression of numerous overlapping genes that promote cell survival, proliferation and angiogenesis. Our studies in Chapter 2 reveal that adherent glioma CSCs show constitutive activation of the STAT3/NF-κB signaling pathways and upregulation of STAT3- and NF-κB-dependent genes. It was also found that crosstalk occurs between STAT3 and NF-κB in GBM stem cells, which leads to the

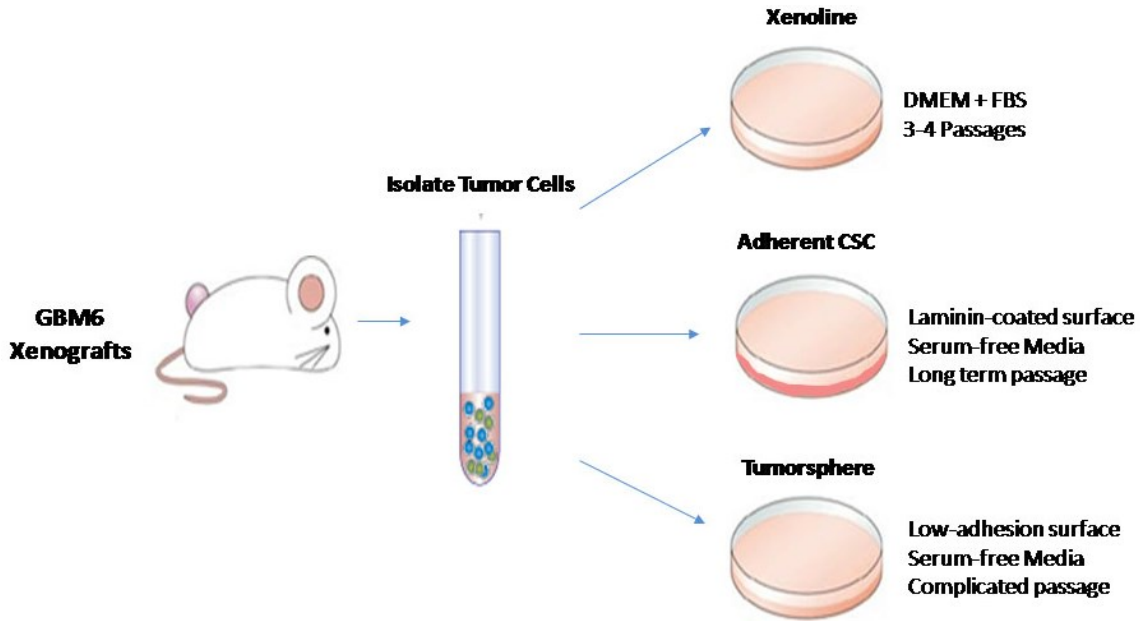

Figure 1-3. ***In vitro*** **expansion method of GBM cell lines.**

Human GBM patient-derived xenografts were maintained in mice. Cell were isolated from tissue and grown as short-term xenolines in DMEM media with fetal bovine serum or under adherent and low-adhesion stem cell conditions in serum-free media with additional growth factors.

activation of NOTCH signaling. The Notch family is a highly conserved cell signaling system expressed in most multicellular organisms. To date, four Notch genes have been identified (NOTCH 1-4) and five ligands (Delta-1, Delta-3, Delta-4, Jagged-1 and Jagged-2) that trigger Notch signaling.

Notch signaling is activated upon cell-cell contact as a result of interactions between Notch receptors and their ligands. At the molecular level, triggering of Notch receptor by ligand binding promotes two proteolytic cleavage events at the Notch receptor. The first cleavage is catalyzed by the ADAM-family of metalloproteases, whereas the second is mediated by g-secretase, an enzyme complex containing presenilin, nicastrin, PEN2 and APH1. The second cleavage releases the Notch intracellular domain (NICD), which translocates to the nucleus and activates transcription [87]. Several genes involved in cell proliferation and apoptosis have been identified as target genes of Notch, including the Hes family (Hairy enhancer of split family), NF-κB family (p65, p50, RelB and cREL), Cyclin D1 and c-Myc. Multiple oncogenic pathways, such as NF-κB, Shh, mTOR, Ras, Wnt, EGF and PDGF have been reported to crosstalk with Notch, suggesting an important role for Notch is tumorigenesis [88].

Notch signaling plays a key role in the normal development of many tissues and cell types through regulation of differentiation, survival and proliferation. Since dysregulation of these biological processes results in malignant transformation, Notch activation contributes to cancer development in various ways [89]. Aberrant activation of Notch signaling has been reported in many tumor types, including glioblastoma. In solid tumors, constitutive activation of the Notch pathway can occur through multiple mechanisms, such as overexpression of ligands or loss of negative regulators. Studies show that elevated expression of NOTCH-1 and JAGGED-1 is associated with poor prognosis and patient survival in breast and prostate cancer [90, 91]. It is through regulation of genes that promote survival and cell cycle progression like Bcl-xL, p21, Rb and NF-κB that Notch activation contributes to cancer [92]. Notch signaling also plays a major role in the maintenance and progression of tumors by promoting the epithelial-to-mesenchymal transition and angiogenesis. Elevated Notch expression in cancer cells is found to correlate with resistance to radiation and chemotherapeutic agents [93]. Recently, an emerging role of Notch in cancer stem cells has been revealed in which the Notch signaling pathway controls self-renewal and multi-potency.

Notch, STAT and NF-κB signaling pathways fulfill overlapping roles in the regulation of proliferation, differentiation and apoptosis, but no coordinated mechanism exists to explain their relationship [94]. Studies show that Hes binding mediates crosstalk between Notch and STAT signaling pathways. Constitutively active Notch upregulates the expression of Hes proteins that drive the interaction of JAK2 and STAT3, and subsequently results in STAT3 phosphorylation and activation [95]. In gastric cancer, the activated Notch1 receptor upregulates Twist and pSTAT3 to promote migration and invasion of tumor cells. It has also been reported that STAT3 acts through the Notch ligand Delta-like 1 to maintain neural precursors and potentially other stem cell populations. Growing evidence suggests a collaboration of Notch and NF-κB signaling in normal development and cancer. Increased Notch activation leads to induction of NF-κB

activity, while inhibition of Notch signaling decreases NF-κB. The same effect is observed in Notch signaling when NF-κB is activated or inhibited [96, 97]. Studies also reveal that the p65 subunit of NF-κB acts in synergy with NICD to remove co-repressors from the Hes-1 promoter and increase transcriptional activity [98]. Taken together, the overactivation of Notch signaling in cells and CSCs in combination with STAT3 and NF-κB play crucial roles in tumorigenesis and represent novel therapeutic targets in treating glioma.

Angiogenesis and STAT3

Angiogenesis is the formation of new blood vessels from the pre-existing vasculature. It is an essential process in reproduction, development and wound repair but is also involved in cancer progression [99]. Tumor angiogenesis is the proliferation of a network of blood vessels that penetrates into cancerous growths, supplying nutrients and oxygen and removing waste products. Tumor angiogenesis actually starts with cancerous tumor cells releasing molecules that send signals to surrounding normal host tissue. This signaling activates certain genes in the host tissue that, in turn, make proteins to encourage growth of new blood vessels. The complex multistage process is orchestrated by various pro- and anti-angiogenic factors, including vascular endothelial growth factor (VEGF), basic fibroblast growth factor (bFGF), thrombospondin, angiopoietins, and most recently angiopoietin-like proteins (ANGPTLs) [100, 101].

Angiogenesis is also regulated by a number of signal transduction pathways. Accumulating evidence reveals that STAT3 plays an important role in angiogenesis through regulation of pro-angiogenic genes. STAT3 is a direct transcriptional activator of vascular endothelial growth factor (VEGF), the most potent angiogenic molecule [102]. Studies indicate that constitutive activation of STAT3 upregulates VEGF expression and subsequently tumor angiogenesis in melanoma and pancreatic cancer cells [27, 103]. Furthermore, inhibition of STAT3 leads to a decrease in VEGF activity and angiogenesis. STAT3 is also involved in VEGF receptor signaling in endothelial cells, where upon its inhibition, migration and vessel formation is blocked [104]. Another key mediator of angiogenesis, hypoxia-inducible factor-1α (HIF-1α), is also shown to be induced by STAT3 signaling. In low oxygen or hypoxic conditions, STAT3 and HIF-1α bind simultaneously to the VEGF promoter, which leads to its maximum transcriptional activation and promotion of angiogenesis [28].

STAT3 and ANGPTL4 Activity in Tumorigenesis

ANGPTL4 is an extracellular-matrix-associated glycoprotein secreted by cells into the microenvironment. ANGPTL4 belongs to a family of 7 matricellular proteins that are considered orphaned ligands because their cognate receptors remain unknown [105]. However, ANGPTL4 is commonly activated by both VEGF and HIF-1α. While first identified for its involvement in lipid and glucose metabolism, a novel role for ANGPTL4 in cancer progression has emerged [106]. Notably, expression of ANGPTL4

has been identified in an *in vivo* hypoxia gene signature that predicts poor outcome in multiple tumor types [107, 108]. Evidence suggests ANGPTL4 provides signals to support several tumorigenic activities characteristic of the metastatic cascade, such as cell proliferation, migration, survival, angiogenesis, epithelial-to-mesenchymal transition, and the maintenance of stem cell niches [109].

As shown in **Figure 1-4**, tumor growth is promoted through a signaling pathway that upregulates the expression of ANGPTL4 as a result of enhanced expression of pro-inflammatory TGF-β via the SMAD pathway as well as COX-2–induced PGE2 signaling in carcinomas. ANGPTL4 subsequently activates NADPH oxidase to promote tumor cell proliferation via the Src/ERK/STAT1 pathway [110]. As the aberrant growth of cancer cells progresses, a mechanism to evade apoptosis via anoikis resistance ensures the survival of the tumor cells through ANGPTL4-mediated inhibition of pro-apoptotic Bcl-2 associated death promoter to activate BAD [111]. ANGPTL4 also triggers angiogenesis to support tumor survival by supplying oxygen and nutrients needed for growth. Studies of Kaposi sarcoma reveal that upon inhibition of ANGPTL4 by siRNA, neovascularization and tumor progression were prevented [112]. ANGPTL4 is also involved in tumor invasion and metastasis. ANGPTL4 was found to increase tumor vascular permeability through integrin-mediated signaling and binding cadherins and claudin-5 [110]. In addition, ANGPTL4 was shown to upregulate the expression of VCAM-1 on endothelial cells through an unknown mechanism facilitating the attachment of circulating metastatic cancer cells to endothelial cells, promoting their transendothelial extravasation and metastatic tumor formation [113]. With the various roles of ANGPTL4 in tumor progression, a better understanding of the underlying cellular and molecular mechanisms will reveal novel insights and the potential therapeutic value of ANGPTL4.

Studies have identified ANGPTL4 as being induced by constitutive activation of STAT3 [114]. Recent findings in breast and renal cell carcinoma suggest that this phenomenon is mediated by HIF-1 signaling. STAT3 was shown to activate HIF-1 target genes, such as ANGPTL4, by binding to their promoters, interacting with HIF-1α and recruiting the coactivators CREB binding protein (CBP), p300 and Pol II. Inhibition of STAT3 significantly reduced ANGPTL4 expression and other HIF-1 target genes, leading to decreased tumor growth. These results indicate that STAT3 and HIF-1 work together to drive tumorigenesis, specifically through the activation of ANGPTL4 [115]. Our studies in Chapter 4 reveal aberrant activation of STAT3 and ANGPTL4 in adherent GBM stem cells. STAT3 is bound to the ANGPTL4 promoter, and the proteins are co-expressed in GBM stem cell populations. Both STAT3 and ANGPTL4 appear to be important in stem cell maintenance and subsequent tumor initiation and progression.

Molecular Classification of Glioblastoma

Molecular subtypes of glioma as well as genes associated with tumor grade, progression and patient survival have been identified by microarray expression profiling [116-118]. While GBMs continue to be defined by histological criteria, reports indicate that expression profiles are more accurate in predicting patient outcome [119].

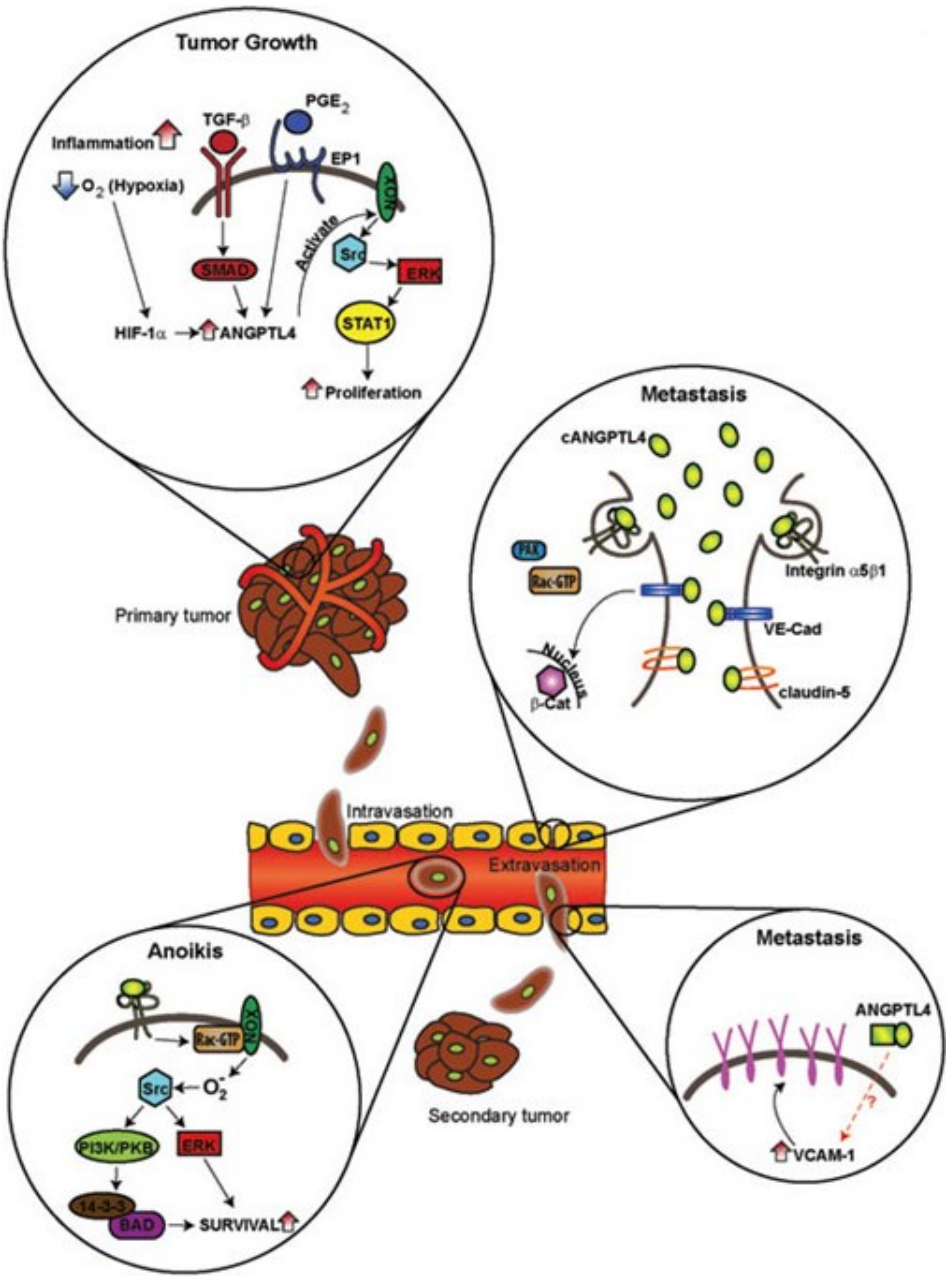

Figure 1-4. The roles of ANGPTL4 signaling in cancer progression.

There are diverse roles of ANGPTL4 in human cancer. ANGPTL4 promotes cell proliferation, helps cells evade apoptosis through anoikis resistance and promotes transendothelial extravasation and metastatic tumor formation by increasing vascular permeability. Reprinted with permission from Tan, M.J., et al., *Emerging roles of angiopoietin-like 4 in human cancer.* Mol Cancer Res, 2012. 10(6): p. 677-88.

Morphologically similar GBM tumors represent a mix of molecular subtypes, suggesting a possibility of different clinical responses. Furthermore, there is potential that GBMs in specific subtypes develop as a result of different causes or cells of origin [120]. Therefore, studying the behavior of the molecularly defined subclasses of GBM may further our understanding of glioma pathology and aid in the development of more effective therapies.

Genomic profiling has identified four subtypes of GBM based on robust gene expression: Proneural, Neural, Classical and Mesenchymal. The Proneural subtype has been associated with PDGFRA abnormalities, IDH1 and TP53 mutations and correlates with younger patients. Most gliomas are classified as Proneural due to their oligodrendrocytic signature, specifically secondary GBMs [121-123]. The gene expression of the Neural class of glioma most closely resembles normal brain tissue. These tumors have a strong enrichment for genes differentially expressed by neurons, associating with neural, astrocytic and oligodendrocytic signatures. The Classical glioma subtype has an astrocytic signature; commonly EGFR amplification is observed in this tumor type along with low levels of CDKN2A and TP53. The neural precursor and stem cell marker Nestin as well as NOTCH3 and Shh signaling pathways are highly associated with the Classical subtype. Gliomas classified as Mesenchymal exhibit higher activity of mesenchymal and astrocytic markers, which mimics cells undergoing the epithelial-to-mesenchymal transition [124]. The subtype is characterized by the high expression of the mesenchymal markers, MET and CHI3L1, as well as deletion of NF1 [125, 126]. Markers of proliferation and angiogenesis also distinguish the Mesenchymal phenotype, suggesting an aggressive GBM tumor subtype with poor prognosis.

Emerging evidence suggests a role of transcriptional networks in regulating the cellular transition into the Mesenchymal phenotype of GBM. STAT3 is believed to be an initiator and major regulator of mesenchymal transformation through the reprogramming of neural stem cells into an aberrant mesenchymal lineage. Constitutive STAT3 activation results in a loss of neuronal differentiation and increased expression of mesenchymal proteins and genes, like smooth muscle alpha actin (SMA), fibronectin and CHI3L1. Studies reveal that the inhibition of STAT3 leads to a collapse in the Mesenchymal signature and reduces GBM aggressiveness [56]. The transition of glioma cells to a mesenchymal state is also reported to be dependent on NF-κB signaling. Findings indicate that TNF-α promotes mesenchymal differentiation through the enrichment of CD44 positive stem cells in an NF-κB-dependent manner. NF-κB also mediates mesenchymal reprogramming by inducing other transcription factors. While NF-κB and STAT3 are both upregulated in Mesenchymal GBMs, TNF-α-induced p65 activation was found to precede STAT3 activation, suggesting that STAT3 acts downstream of the NF-κB pathway [127]. A robust angiogenesis gene signature has been shown to correlate with the Mesenchymal subtype of GBM as well. Gene expression analysis revealed that Mesenchymal GBMs exhibit overexpression of the angiogenesis markers VEGF, VEGFR1, VEGFR2 and ANGPTL4 [125].

The highly proliferative, pro-angiogenic and de-differentiated state of Mesenchymal GBM tumors make them highly aggressive. The Mesenchymal signature

has been found to correlate with poor radiation response and shorter survival in patients with GBM. Therefore, a more detailed molecular understanding of this GBM subtype is crucial to improve therapeutic design and patient outcome. In chapter 3, we describe glioma CSCs that retain the Mesenchymal gene signature *in vitro* and in mouse xenografts. This subpopulation of glioma cells forms tumors with histopathological features of GBM and is enriched for stem cell markers, transcriptional networks and angiogenesis markers. In establishing a culture system that represents the Mesenchymal GBM subtype, it provides a valuable and accurate model of the human disease for future studies. The characterization of the Mesenchymal subclass will give insight into novel genes involved in glioma tumor progression and lead to the discovery of new therapeutic targets in treating GBM.

Hypothesis and Specific Aims

Our hypothesis is that cancer stem-like cells are responsible for the generation, growth and progression of glioblastoma multiforme (GBM). Additionally, several cancer stem-like cell populations exist, and these cells have distinct molecular signatures. The genes associated with these tumor-initiating subpopulations serve as molecular biomarkers for disease prognosis and therapeutic targets in treating GBM progression. Three aims were designed to investigate this hypothesis:

1. To characterize GBM cancer stem cells and investigate the role of transcription factors in the tumor initiating subpopulation of GBM.
2. To examine the contribution of different GBM stem cell populations to the promotion of tumor heterogeneity and define their specific molecular signatures.
3. To identify CSC molecular biomarkers that drive gliomagenesis and determine whether targeting them has therapeutic potential in treating GBM.

CHAPTER 2. CONSTITUTIVE ACTIVATION OF STAT3 AND NF-κB SIGNALING IN GLIOBLASTOMA CANCER STEM CELLS REGULATES THE NOTCH PATHWAY*

Introduction

Malignant gliomas are locally aggressive, highly vascular tumors that have a dismal prognosis, and present therapies provide little improvement in the disease course and outcome. Many types of malignancies, including glioblastoma, originate from a population of cancer stem cells (CSCs) that are able to initiate and maintain tumors. Although CSCs only represent a small fraction of cells within a tumor, their high tumor-initiating capacity and therapeutic resistance drives tumorigenesis. Therefore, it is imperative to identify pathways associated with CSCs in order to devise strategies to selectively target them. In this study, we describe a novel relationship between glioblastoma CSCs and the Notch pathway, which involves the constitutive activation of STAT3 and NF-κB signaling. Glioma CSCs were isolated and maintained *in vitro* using an adherent culture system, and the biological properties were compared to the traditional cultures of CSCs grown as multicellular spheres under nonadherent culture conditions. Interestingly adherent glioma CSCs show constitutive activation of the STAT3/NF-κB signaling pathway and upregulation of STAT3- and NF-κB-dependent genes. Gene expression profiling also identified components of the Notch pathway as being deregulated in glioma CSCs, and the deregulated expression of these genes was sensitive to treatment with STAT3 inhibitors. This finding is particularly important because Notch signaling appears to play a key role in CSCs in a variety of cancers, and controls cell fate determination, survival, proliferation and the maintenance of stem cells. The constitutive activation of STAT3 and NF-κB signaling pathways that leads to regulation of Notch pathway genes in glioma CSCs identifies novel therapeutic targets for the treatment of glioma.

Methods

Cell Culture

GBM6 (provided by Dr. C. David James, Department of Neurological Surgery, University of California, San Francisco) and MT330 (provided Dr. Christopher Duntsch, Department of Neurosurgery, UTHSC) human glioma cell lines were grown in

---

* Reprinted with permission. Garner, J.M., et al., *Constitutive activation of signal transducer and activator of transcription 3 (STAT3) and nuclear factor kappaB signaling in glioblastoma cancer stem cells regulates the Notch pathway.* J Biol Chem, 2013. 288(36): p. 26167-76.

monolayer culture in DMEM (Cellgro, Hemdon, VA) supplemented with 10% heat-inactivated fetal bovine serum (Hyclone Labs, Thermo Scientific, Rockford, IL), 100 units/mL penicillin and 100 μg/mL streptomycin. GBM6 cells were continuously maintained as subcutaneous xenografts in NSG mice, and monolayer and CSC cultures were derived from freshly harvested tumor tissue. Adherent and spheroid glioma CSCs were maintained in NeuroBasal-A medium (Invitrogen, Carlsbad, CA) containing 2% B27 supplement, 2 mM L-glutamine, 100 units/mL penicillin, 100 μg/mL streptomycin, EGF (20 ng/ml), and basic FGF (40 ng/ml). For isolation of adherent CSCs, culture flasks were coated with 100 μg/mL poly D-lysine (Sigma-Aldrich, St. Louis, MO) for 1 hr followed by coating with 10 μg/mL laminin (Gibco, Life Technologies Inc., Grand Island NY) for 2 hr prior to use. Adherent CSCs were plated at 1 X 10^5 cells per 75 cm2 flask, grown to confluence, dissociated with HyQTase (Thermo Scientific, Scientific, Rockford, IL), and split 1:3. For isolation of spheroid CSCs, glioma cells were dissociated with HyQtase and plated at ~ 1 x 10^5 cells/mL in ultra-low adhesion flasks.

Quantitative RT-PCR

Total RNA was extracted using the QIAshredder and RNeasy mini kits (Qiagen Inc., Valencia, CA) according to manufacturer's protocol. RT-PCR was performed on an iCyclerIQ (Bio-Rad, Richmond, CA) using an iScript One-Step RT-PCR kit with SYBR Green (Bio-Rad, Richmond, CA). Reaction parameters were as follows: cDNA synthesis at 50 °C for 20 min, transcriptase inactivation at 95°C for 5 min, PCR cycling at 95°C for 10 sec, and 60°C for 30 sec for 40 cycles. The following primers were used for RT-PCR: β-actin, 5′-AGAAGGAGATCACTGCCCTG-3′ (forward), 5′-CACATCTGCTGGAAGGTGGA-3′ (reverse); CD133 5'-CATCCACAGATGCTCCTAAGG-3' (forward), 5'-AAGAGAATGCCAATGGGTCCA-3' (reverse); SOX2 5′-GCCGAGTGGAAACTTTTGTCG-3′ (forward), 5′-GCAGCGTGTACTTATCCTTCTT-3′ (reverse); IL8 5'-TAGCAAAATTGAGGCCAAGG-3' (forward), 5'-AGCAGACTAGGGTTGCCAGA-3' (reverse); Trail 5'-GAGCTGAAGCAGATGCAGGAC-3' (forward), 5'-TGACGGAGTTGCCACTTGACT-3' (reverse); CXCL11 5'-ATGAGTGTGAAGGGCATGGGC-3' (forward), 5'-TCACTGCTTTTACCCCAGGG-3' (reverse); Bcl-2 5'-CCGGAGGCGCTTTACTACC-3" (forward), 5'-TAGGGGTGTAGGCAGGTTCAC-3' (reverse); Bcl-X 5'-GGTCGCATTGTGGCCTTTTTC-3' (forward), 5'-AGGGGCTTGGTTCTTACCCA-3' (reverse); Caspase-3 5'-CATGGAAGCGAATCAATGGACT-3' (forward), 5'-CTGTACCAGACCGAGATGTCA-3' (reverse); NOTCH1 5′-GAGGCGTGGCAGACTATGC-3′ (forward), 5′- CTTGTACTCCGTCAGCGTGA-3′ (reverse); HES5 5′-AGTCCCAAGGAGAAAAACCGA-3′ (forward), 5′-GCTGTGTTTCAGGTAGCTGAC-3′ (reverse); JAG1 5'-GTCCATGCAGAACGTGAACG-3' (forward);

5’-GCGGGACTGATACTCCTTGA-3’ (reverse), NUMBL
5’-TGGTGGACGACAAAACCAAGG-3’ (forward),
5’-ACGACAGATATAGGAAGCCT-3’ (reverse); DTX3
5’-TCGTTCGTCCTGTCCAGAATG-3’ (forward),
5’-AAGTCTCGCCATCTATGAGGAT-3’ (reverse); DVL3
5’-GACGCCGTACCTTGTGAAG-3’ (forward); 5’-CGCTGCAAAACGCCCTTAAA-3’ (reverse); RBPJ 5’-CGGCCTCCACCTAAACGAC-3’ (forward),
5’-TCCATCCACTGCCCATAAGAT-3’ (reverse).

Immunoblot Analysis

For preparation of whole cell extracts, cells were lysed in RIPA buffer (Thermo Scientific, Rockford, IL), containing 1 mM NaF, 1 mM Na3VO4, 1 mM PMSF and protease inhibitor cocktail (Sigma-Aldrich, St. Louis, MO) at 4°C for 30 minutes, and pre-cleared by centrifugation (12,000×g, 15 minutes). Nuclear extracts were prepared using a nuclear extract kit (Active Motif, Carlsbad, CA) as previously described [31]. The amount of protein was determined using a BCA protein assay kit (Thermo Scientific, Pierce, Rockford, IL). Extracts (25 μg) were separated by SDS-PAGE, transferred to polyvinylidenedifluoride membranes (Millipore Co., Bedford, MA) and immunoblotted with antibodies against the following proteins: β-Tubulin III and GFAP (Sigma-Aldrich, St. Louis, MO); Nestin (Abcam, Cambridge, MA); STAT3 and phospho-STAT3 (Cell Signaling Technology, Beverly, MA); p65 and lamin (Santa Cruz Biotechnology Inc., Santa Cruz, CA). Followed by addition of IRDye800CW goat anti-mouse IgG or IRDye680 goat anti-rabbit IgG antibodies(LI-COR Biosciences, Lincoln, NE). Blots were visualized on an Odyssey Infrared Imaging System (LI-COR Biosciences, Lincoln, NE).

Immunofluorescence and Confocal Microscopy

Cells grown in 8-well chamber slides (Millipore Co., Bedford, MA) to ~50% confluence were washed with PBS, fixed with 4% paraformaldehyde and methanol, and permeabilized with 1% Triton X100. After blocking with 5% goat serum, cells were incubated with nestin, STAT3, pSTAT3, and p65 antibodies, and subsequently stained with goat anti-mouse Alexa Fluor 488 and goat anti-rabbit Alexa Fluor 555 (Invitrogen, Carlsbad, CA). Cell were counterstained with Vectashield mounting media with DAPI (Vector Laboratories, Burlingame, CA). Images were captured on a Zeiss LSM700 laser scanning confocal microscope (Zeiss, New York, NY).

Tumor Xenografts in Mice

All animal experiments were performed in accordance with a protocol approved by the Institutional Animal Care and Use Committee of the University of Tennessee Health Science Center. Cells were dissociated with HyQTase, resuspended in PBS, enumerated in a Coulter Counter Analyzer, and resuspended in 100 μl of PBS at the

desired cell number for subcutaneous injections. Tumor xenografts were established in five-week-old male NOD.CgPrkdcscid Il2rgtm1Wjl/SzJ (NSG) mice (Jackson Laboratory, Bar Harbor, ME) by direct injection of glioma cells into the flanks. Tumors were measured bi-weekly until reaching a volume of ~400 mm^3; mice were then sacrificed and tumors harvested.

Colony Formation Assay

Single cell suspensions of 5,000 cells in 1 ml of 0.4% agarose in tissue culture medium were added to triplicate wells of ultralow adhesion 6-well plates. Cells were fed twice a week with an additional 0.5 ml media. At day 14, plates were stained with MTT (10 μg/ml) for 3 hours and colonies were counted on a light microscope.

MTT Cell Viability Assay

Glioma monolayer cells or adherent CSCs in 96-well plates were treated with varying concentrations of WP1066 or S3I-201 (Selleckchem, Houston, TX). After 72 hr, 10 μl of MTT stock solution (10 mg/ml) was added to each well and incubated at 37°C for 2-4 hr. MTT was solubilized by adding 100 μl of 10% SDS in 0.01N HCL and plates incubated at 37°C for 4 hr in a humidified chamber. Plates were read at 570 nm on a Bio-Rad plate reader.

Apoptosis Assay

The induction of apoptosis was monitored by flow cytometry on an Accuri C6 (BD Bioscience, San Jose, CA) using the Annexin V-FITC apoptosis detection kit (BD Pharmingen, San Diego, CA), according to the manufacturer's instructions.

p65-GST Pulldown Assay

The p65 cDNA was cloned into pGEX-KG expressed in E.coli strain BL21 and affinity-purified in glutathione-sepharose beads as previously described [128]. For pulldown assays, nuclear extracts from glioma monolayer cells or adherent CSCs were incubated with the p65-GST fusion protein bound to glutathione-agarose beads at 4°C overnight. The bound proteins were washed extensively and eluted with Laemmli buffers, resolved by SDS-PAGE (10%), blotted on PVDF membranes, and probed with anti-STAT3.

Microarray Analysis

Total cellular RNA was extracted from cells with TRIzol reagent (Invitrogen, Carlsbad, CA) and submitted to the UTHSC Center of Genomics and Bioinformatics (Memphis, TN) for labeling and hybridization to Human-HT12 BeadChips (Illumina, Inc., San Diego, CA). Microarray data analysis was then carried out using GenomeStudio 3.4.0 (Illumina Inc., San Diego, CA) and GeneSpring software 7.0 (Silicon Genetics, Inc., RedWood City, CA), and expression values for each gene were normalized as described previously [129]. The average fold-change in gene expression from three independent sets of GeneChip data for glioma monolayers and adherent CSCs was subjected to non-parametric t testing. The microarray data were subjected to Gene Ontology modular enrichment analysis using the Database for Annotation, Visualization and Integrated Discovery (DAVID) [130] and the protein-protein interaction network of the Notch pathway was determined by STRING (Search Tool for the Retrieval on Interacting Genes/Proteins) analysis [131].

Chromatin Immunoprecipitation

Chromatin Immunoprecipitation (ChIP) was carried out using the ChIP-ITTM Express Enzymatic kit (ActiveMotif, Carlsbad, CA) according to the manufacturer's instructions. In brief, chromatin from cells was cross-linked with 1% formaldehyde (10 min at 22^{o}C), sheared to an average size of 200 bp, and then immunoprecipitated with anti-p65 or STAT3 (Santa Cruz Biotechnology Inc., Santa Cruz, CA). ChIP-PCR primers were designed to amplify a proximal promoter region containing putative STAT3 (-1940 to -1919) and NF-κB (-2145 to -2135) binding sites in the Notch1 promoter. The primers used were: for STAT3 site, 5'-CACTGGCTGTTTCCAGAGTG-3' (forward), 5'-GGGAGGGACCTAGGACTGTG-3' (reverse); for NF-κB site, 5'CTACTTGCCAGGGGCCTAC-3' (forward), 5'-GCTCATAAGCCCGCGTTAC-3' (reverse).

Statistical Analysis

At least three independent experiments were performed in duplicate, and data are presented as means ± sd. ANOVA and post-hoc least significant difference analysis or Student t tests were performed.p values < 0.05 (*) were considered statistically significant.

Results

Expression of CSC Markers and Tumorigenicity of Adherent CSCs

CSCs are often generated based on their ability to grow as multicellular, nonadherent spheres in low adhesion flasks, which we denote spheroid CSCs [132, 133]. Alternatively, CSCs can also be grown in laminin-coated flasks, which we denote as adherent CSCs [77]. To define the biological properties of adherent and spheroid CSCs derived from glioma lines, we examined the expression of two classical stem cell markers CD133 and Sox2. In brief, total RNA was prepared from GBM6 and MT330 gliomas, which were grown in monolayer or under the two different CSC conditions, and the expression of CD133 and Sox2 was determined by qPCR. As shown in **Figure 2-1A**, CD133 and Sox2 gene expression was greater in both adherent and spheroid glioma CSCs when compared to glioma cells grown in monolayer. Furthermore, as determined by immunostaining, nestin (neural stem cell marker) was highly expressed in adherent and spheroid glioma CSCs when compared to glioma monolayers, while βIII-tubulin (neural differentiation marker) and glial fibrillary acid protein (astrocyte differentiation marker) were more highly expressed in glioma monolayers (**Figure 2-1B**).

Since CSCs are believed to have enhanced tumorigenicity, we next compared the tumor initiating capacity of GBM6 glioma cells grown in monolayer or as adherent CSCs. In brief, initially 1 x 10^6 cells were injected subcutaneously in the flanks of NSG mice and tumor engraftment determined by caliper measurement. As shown in **Figure 2-1C**, adherent glioma CSCs formed tumors rapidly and grew to ~400 mm^3, while only small tumors developed in mice injected with monolayer cultures at 40 days. The tumorigenic potential of adherent glioma CSCs was further characterized by performing a limiting dilution analysis. We found that as few as 10,000 glioma CSCs were capable of consistently forming tumors, and most interestingly that the adherent CSCs were nearly 100-times more potent in inducing tumors than the glioma monolayer cultures. Soft-agar assays for anchorage independent growth, which is used as an *in vitro* correlate for tumorigenic potential, show that adherent CSCs have a 68-fold greater colony formation potential than glioma monolayer cells, 6.8% versus 0.1%, respectively. (**Figure 2-1D**). Thus, the adherent glioma cells grown in laminin-coated plates exhibit characteristics previously ascribed to cancer stem cells, i.e. they self-renew, display neural stem cell markers, form tumors upon serial transplantation that recapitulate the tumor phenotype, and exhibit enhanced tumorigenicity.

Constitutive Activation of the STAT3 and NF-κB Signaling Pathways in Glioma CSCs

The STAT3 and NF-κB signaling pathways have been found to be constitutively active in various human cancers including glioma, and their activation is believed to play a critical role in the stem cell phenotype. To characterize the NF-κB and STAT3 signaling pathways in glioma CSCs, we examined the intracellular localization of STAT3

Figure 2-1. Expression of CSC markers and tumorigenicity of adherent CSCs.

A. RNA was prepared from monolayer, and adherent and spheroid CSC cultures of GBM6 and MT330 gliomas, and CD133 and SOX2 expression quantified by qPCR and normalized to actin expression (n=3). Error bars, S.D. ** $p < 0.01$; *** $p < 0.001$. **B**. GBM6 monolayer cells and adherent CSCs were fixed and immunostained for Nestin, tubulin, or GFAP (green) and counterstained with DAPI (blue), and analyzed by confocal microscopy. **C**. Mice were subcutaneously injected with varying concentrations of GBM6 cells grown in monolayer (GBM6-M) or adherent CSCs in laminin-coated plates (GBM6 Ad-C), and tumor volume was determined by caliper measurement three times per week (n=10 per group). **D**. GBM6 monolayer and adherent CSC cultures were plated in soft-agar (10,000 cells per well of 6-well plates) and the colony formation potential was assessed.

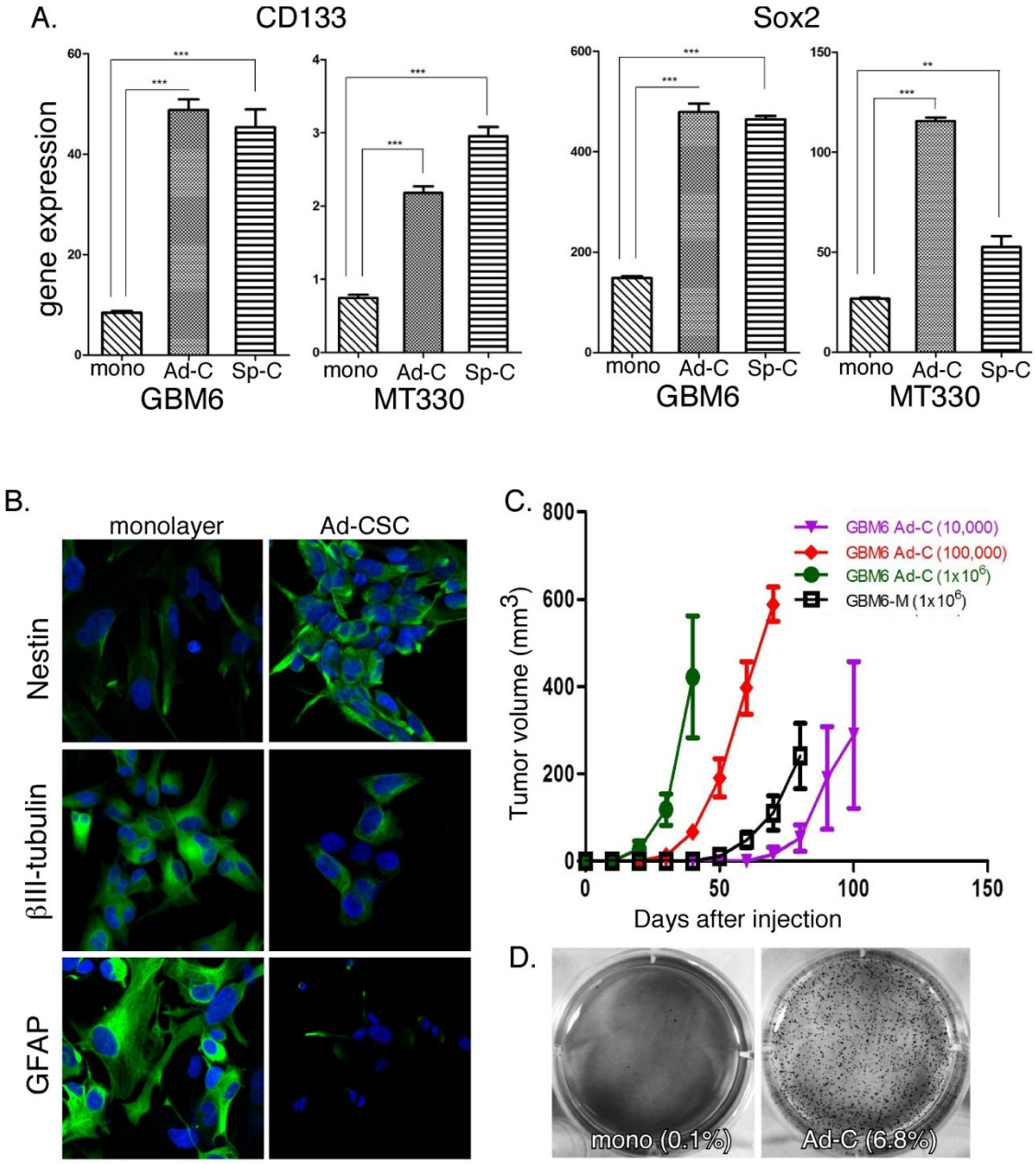
A.
CD133
Sox2
gene expression
mono
Ad-C
Sp-C
GBM6
MT330
B.
monolayer
Ad-CSC
Nestin
βIII-tubulin
GFAP
C.
Tumor volume (mm3)
Days after injection
GBM6 Ad-C (10,000)
GBM6 Ad-C (100,000)
GBM6 Ad-C (1x10^6)
GBM6-M (1x10^6)
D.
mono (0.1%)
Ad-C (6.8%)

and the p65 subunit of NF-κB by confocal microscopy. GBM6 glioma cells were grown as monolayers or adherent glioma CSCs on glass slides and immunostained with antibodies specific for STAT3, pSTAT3 (as a measure of transcriptionally active STAT3), and p65. Cells were counterstained with DAPI to define nuclear localization of proteins. As shown in **Figure 2-2A**, although STAT3 and p65 are present in the cytoplasm and nucleus of both GBM6 glioma monolayers and adherent CSCs, their colocalization is only evident in the nucleus of adherent CSCs. Moreover as shown in **Figure 2-2B**, while tyrosine phosphorylated STAT3 is undetectable in glioma monolayer cultures, pSTAT3 is clearly present in glioma CSCs and is selectively colocalized in the nucleus with p65.

To further characterize the activation of the STAT3 signaling pathway in gliomas, nuclear extracts were prepared from GBM6 cells grown under the different culture conditions and analyzed by immunoblotting for phopho-STAT3 and STAT3. As shown in **Figure 2-2C** and consistent with immunostaining results, both STAT3 and pSTAT3 were clearly detectable in nuclear extracts of glioma cells irrespective of whether they were grown as monolayers or CSCs. However, basal activation of STAT3, as determined by the nuclear levels of tyrosine-phosphorylated STAT3, was markedly greater in CSCs. This finding is in contrast to normal (untransformed) cells such as fibroblasts, where basal activation of STAT3 is undetectable. Moreover, nuclear expression of p65 is higher in both adherent and spheroid CSCs. Thus, we provide strong evidence that the STAT3 (as measured by nuclear STAT3 and phospho-STAT3 levels) and NF-κB (as measured by nuclear p65 levels) signaling pathways are constitutively activated in glioma cells, and activation is markedly greater in glioma CSCs. In addition, as shown in **Figure 2-2D**, the interaction between STAT3 and p65 in the nucleus is further borne out by pulldown assays with p65-GST, which show a greater interaction of STAT3 with p65 in nuclear extracts from adherent and spheroid CSCs.

To characterize the functional significance of constitutive activation of these signaling pathways, we examined the expression of several STAT3 and NF-κB regulated genes in glioma monolayer and CSCs. As shown in **Figure 2-2E**, the expression of several NF-κB regulated genes (IL8, CXCL11and Trail) was significantly higher in both adherent and spheroid glioma CSCs when compared to monolayer cultures. Most notably, IL8 gene expression was 6-8 fold-higher in CSCs. In addition, the expression of known STAT3-regulated genes (Bcl-2, Bcl-X and Caspase 3) was also markedly elevated in both adherent and spheroid CSCs (**Figure 2-2F**). These results suggest that, since the transcriptionally-active forms of p65 and STAT3 are colocalized in the nucleus of glioma CSCs, the constitutively activated forms of these important transcription factors may interact and drive the expression of critical STAT3 and NF-κB regulated genes.

The Effects of Specific STAT3 Inhibitors on Glioma Monolayers and Glioma CSCs

We next sought to determine the efficacy of STAT3 inhibitors on the constitutively activated STAT3 pathway in CSCs. Adherent GBM6 CSCs were plated and treated with a pharmacological inhibitor of STAT3 (WP1066 or S3I-201) for 2 hrs at

Figure 2-2. Constitutive activation of STAT3 and NF-κB signaling pathways in glioma adherent CSCs.

GBM6 monolayer, and adherent CSC cultures or cultures were fixed and immunostained with antibodies as indicated and analyzed by confocal microscopy. **A.** STAT3 and **B.** phospho-STAT3 staining is represented in green, p65 in represented in red, and nuclear DAPI staining in blue. White pixels represent the colocalization of STAT3 or phospho-STAT3 and p65 proteins within the cells. **C.** The expression of STAT3, pSTAT3, and p65 in nuclear extracts prepared glioma cells was determined by immunoblotting. **D.** GST-p65 pulldown assays were performed to assess the interaction of STAT3 and p65 in glioma CSCs. **E.** RNA was prepared from GBM6 monolayer and adherent CSC cultures, and the expression of IL8, Trail, CXCL11, Bcl-2, Bcl-X and Caspase-3 was quantified by qPCR and normalized to actin expression (n=3). Error bars, S.D. * $p < 0.05$; ** $p < 0.01$.

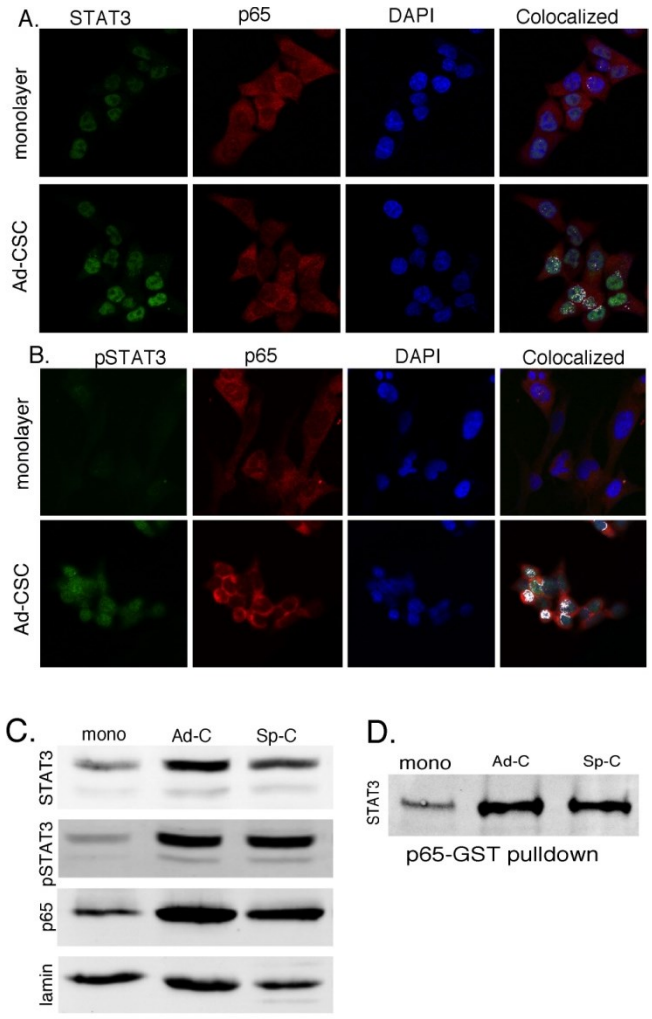
A.
STAT3
p65
DAPI
Colocalized
monolayer
Ad-CSC
B.
pSTAT3
p65
DAPI
Colocalized
monolayer
Ad-CSC
C.
mono
Ad-C
Sp-C
STAT3
pSTAT3
p65
lamin
D.
mono
Ad-C
Sp-C
STAT3
p65-GST pulldown
E
NF-κB regulated genes
IL8
Trail
CXCL11
gene expression
mono
Ad-C
Sp-C
STAT3 regulated genes
Bcl-2
Bcl-X
Caspase-3
gene expression
mono
Ad-C
Sp-C

varying concentrations. Nuclear extracts were prepared and STAT3 and pSTAT3 expression was determined by immunoblotting. As shown in **Figure 2-3A**, both WP1066 and S3I-201 were extremely effective in inhibiting STAT3 tyrosine phosphorylation in CSCs, with nearly complete inhibition of pSTAT3 at 50 μM WP1066 and 300 μM S3I-201. However, both inhibitors had little or no effect on nuclear STAT3 levels. We then examined the effects of WP1066 (50 μM for 2 hr) on intracellular localization of STAT3 and the p65 subunit of NF-κB in glioma CSCs by confocal microscopy. As shown in the upper panel of **Figure 2-3B** and previously in **Figure 2-2A**, STAT3 and p65 are colocalized in the nucleus of adherent CSCs. In contrast, treatment with WP1066 markedly inhibited the nuclear colocalization of STAT3 with p65 in GBM6 glioma CSCs (lower panel of **Figure 2-3B**). Similar results were obtained when cells were immunostained for pSTAT3 and p65, i.e. the STAT3 inhibitor ablated the nuclear colocalization of pSTAT3 with p65.

We then examined the effects of WP1066 or S3I-201 on the cell viability or proliferation of glioma monolayers and adherent CSCs. In brief, cells in 96-well plates were treated with varying concentrations of the pharmacological STAT3 inhibitors for 72 hr, and cell proliferation was determined by MTT assays. As shown in **Figure 2-3C**, although both inhibitors induced a dose-dependent reduction in cell number in both glioma monolayers and adherent CSCs, there was a markedly enhanced effect of both inhibitors on adherent CSCs. Moreover, flow cytometric analysis of Annexin V stained cells demonstrated that treatment with the STAT3 inhibitor WP1066 had a greater effect on the induction of apoptosis in adherent CSCs than in glioma monolayers (**Figure 2-3D**). Taken together these results show that STAT3 activation is greater in adherent CSCs.

Microarray Analysis Identifies Upregulation of the Notch Pathway in Glioma CSCs

To identify genes differentially expressed in glioma CSCs, we performed a preliminary microarray analysis. In brief, whole genome expression profiling was performed on RNA prepared from three independent biological replicates of MT330 and GBM6 grown as monolayers and spheroid glioma CSCs. The samples were submitted to the UTHSC Center of Genomics and Bioinformatics (Memphis, TN) for labeling and hybridization to HT-12 expression BeadChips (Illumina Inc., San Diego, CA). RNA integrity was validated on an Agilent bioanalyzer, and all samples showed distinct peaks corresponding to intact 28S and 18S ribosomal RNA. Hybridization signals were processed using Illumina GenomeStudio software (annotation, background subtraction, Quantile normalization and presence call filtering). GeneSpring GX software (Agilent Technologies, Palo Alto, CA) was used for statistical computing. Functional annotation of the genes differentially expressed in glioma CSCs revealed that genes in the Notch signaling pathway were significantly enriched ($P<0.05$, DAVID Bioinformatics Resources 6.7). The expression of these Notch pathway genes is shown in **Figure 2-4A**, and their interaction with the STAT3 and NF-κB signaling pathways shown schematically in **Figure 2-4B**. Most notably while Notch1, Notch3, Notch4, Hes5, Hey1

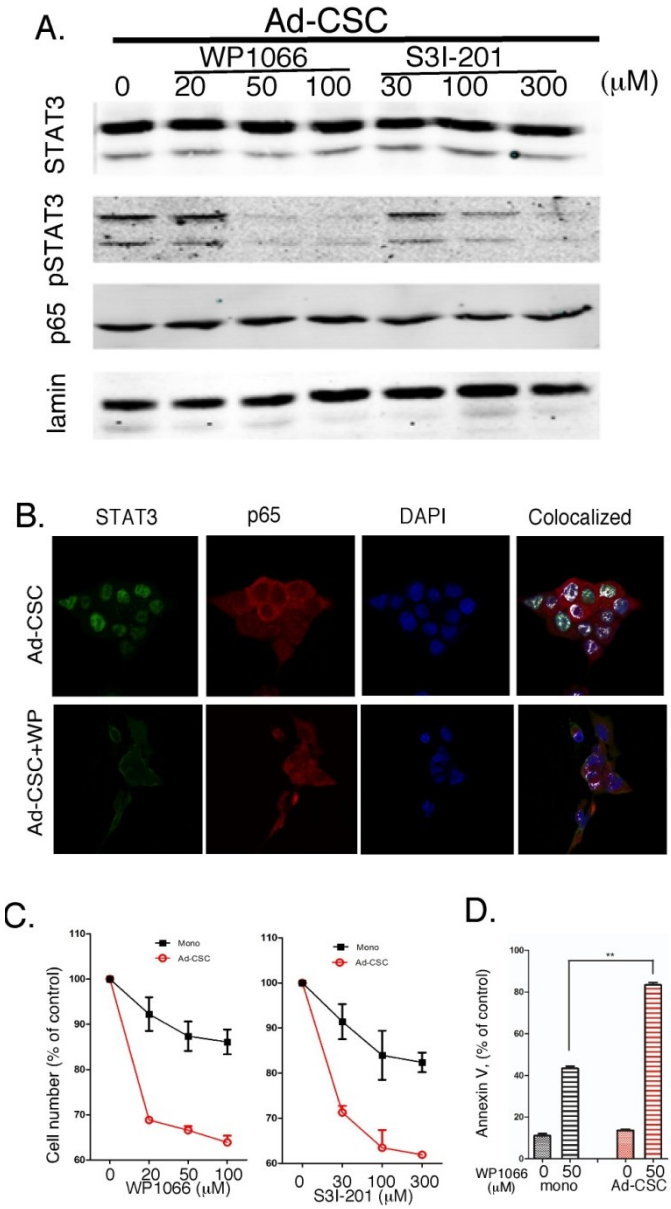

Figure 2-3. Effects of selective STAT3 inhibitors on adherent glioma CSCs.

A. GBM6 cells were treated with WP1066 and S3I-201 at the indicated concentrations and the expression of STAT3, pSTAT3, and p65 proteins was determined by immunoblotting. **B**. Cells were treated with WP1066 (50 μM for 2 hrs) or vehicle, and colocalization of STAT3 and p65 was determined by immunostaining. **C**. Proliferation of GBM6 monolayer and adherent CSC cultures was measured by MTT assay after treatment (72 hr) with WP1066 or S3I-201 at the indicated concentrations. **D**. At 48 hrs after treatment with 50 μM WP1066, apoptosis was determined by Annexin V staining and quantified by flow cytometry.

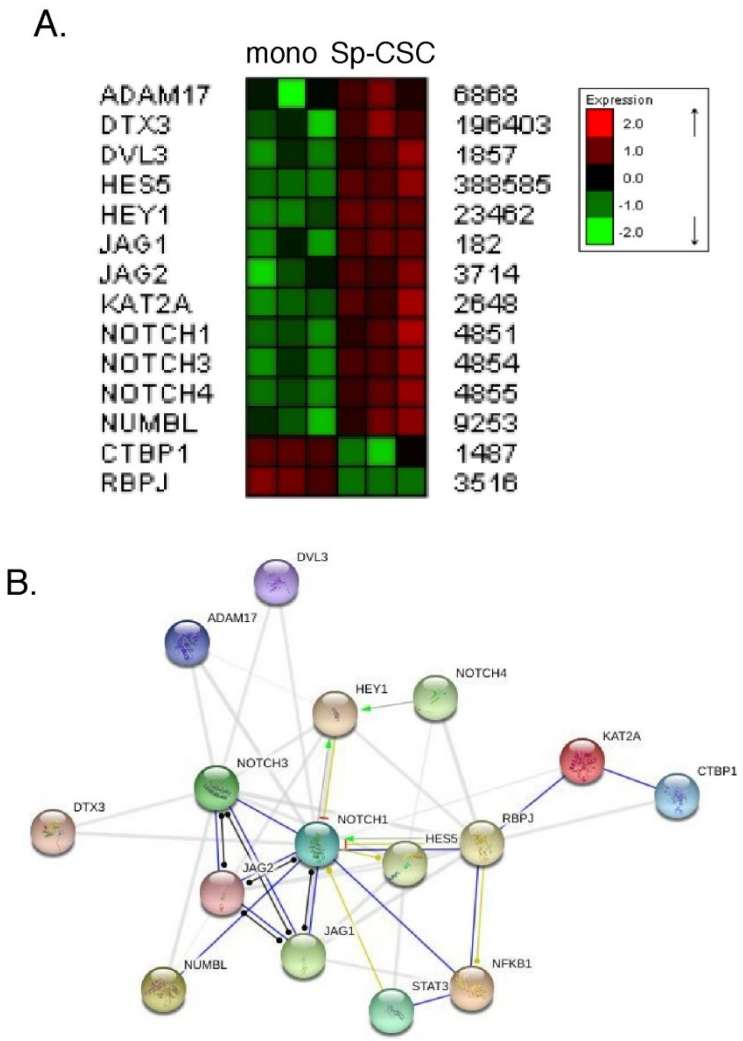

Figure 2-4. Enrichment of the Notch signaling pathway in glioma CSCs.

A. RNA from MT330 and GBM6 monolayer and spheroid CSC cultures was prepared and microarray analysis performed. **B**. Schematic representation of the interaction of the Notch pathway with STAT3 and NF-κB signaling pathways using STRING analysis.

and Jag1, known positive regulators of this pathway, were upregulated in glioma CSCs, negative regulators of this pathway, CTBP1 and RBPJ, were downregulated.

The Roles of STAT3 and p65 in the Upregulation of the Notch Pathway in Glioma CSCs

To confirm that these genes were indeed differentially regulated in CSCs, qPCR was performed on RNA extracted from GBM6 monolayers and adherent glioma CSCs. As shown in **Figure 2-5**, expression of Notch1, Hes5, Jag1, Numbl, Dtx3 and Dvl3 was upregulated in adherent glioma CSCs, while RBPJ was downregulated. Most interestingly, pretreatment with either STAT3 inhibitor or the NF-κB inhibitor Velcade reduced the expression level of the genes upregulated in the CSCs to levels observed in monolayer cultures, while these inhibitors increased the level of RBPJ expression in glioma CSCs. Thus, these genes in the Notch pathway are regulated both by STAT3 and NF-κB.

In addition, treatment with DAPT (γ-secretase inhibitor), which blocks Notch activation, also reduced the expression level of the genes upregulated in CSCs, while it increased the level of expression of RBPJ in glioma CSCs. These results are consistent with the critical role that Notch receptor plays in the regulating multiple genes in both normal neural stem cells and glioma CSCs [134, 135]. Since p65 and STAT3 appear to be involved in Notch1 expression, we next examined whether they directly bind to the Notch1 promoter. Examination of putative transcription binding sites revealed a STAT3 and a NF-κB binding site proximal to the Notch1 promoter. Specific primers were designed and synthesized for each of these potential binding sites in the Notch1 promoter and the binding of STAT3 and p65 was demonstrated by ChIP analysis. In brief, protein-DNA complexes were crosslinked with formaldehyde, chromatin was sheared to average of 200 bp and immunoprecipitated with anti-STAT3 or -p65, crosslinking reversed and the resulting DNA sequences detected by PCR and qPCR. As shown in **Figure 2-6A**, significantly increased binding of STAT3 to the Notch1 promoter was observed in adherent CSCs as compared to glioma monolayer cultures. We then examined whether p65 bound to the NF-κB binding site that was nearby the STAT3 site in the Notch1 promoter. As shown in **Figure 2-6B**, significantly increased binding of p65 to the Notch1 promoter was also observed in adherent CSCs. Taken together these results show that STAT3 and p65 regulate Notch1 expression in adherent CSCs by directly binding to the Notch1 promoter.

Discussion

Numerous studies support the concept that many types of malignancies, including glioblastoma, originate from a CSC population that is able to initiate and maintain tumors [8, 136]. Although CSCs only represent a small fraction of cells within a tumor, their high tumor-initiating capacity and therapeutic resistance drives tumorigenesis. Therefore, it is imperative to identify pathways associated with CSCs in order to devise strategies to

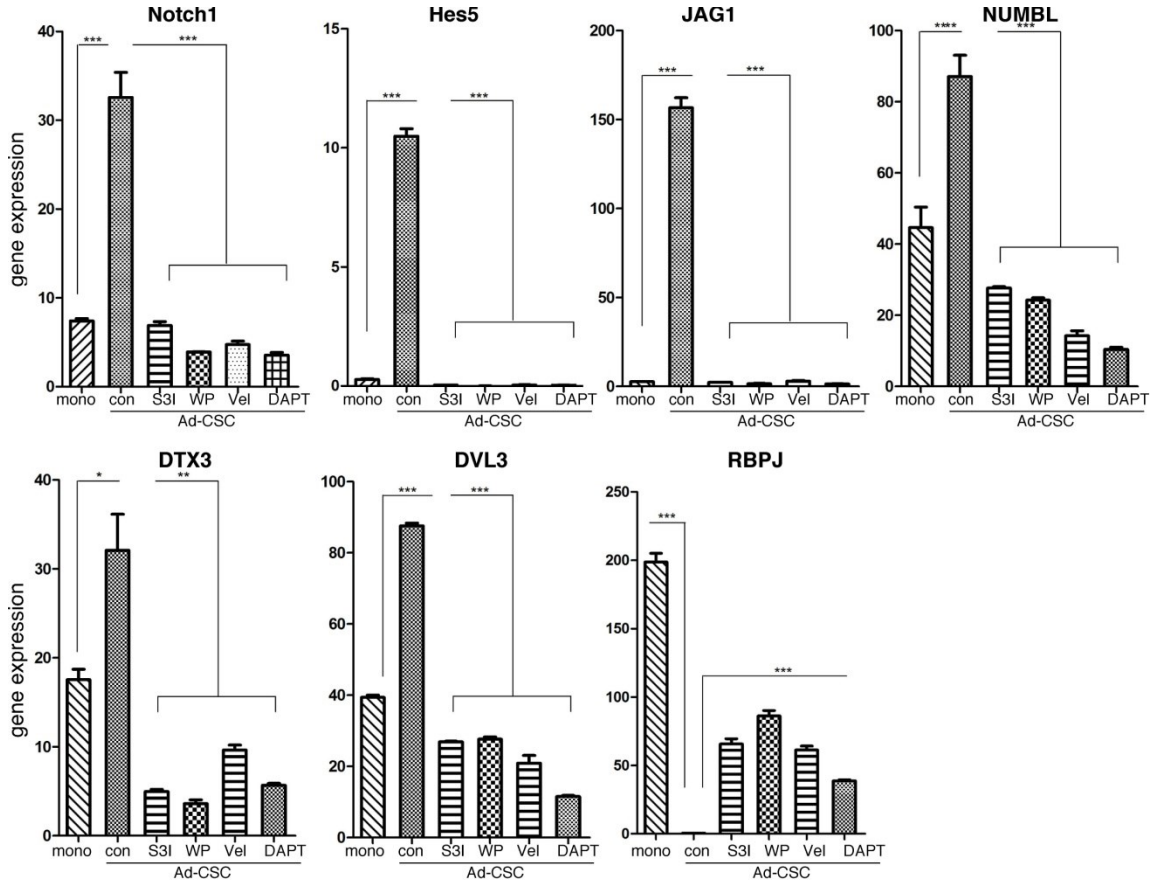

Figure 2-5. Effects of STAT3 and NF-κB inhibitors on the expression of components in the Notch signaling cascade *in vitro*.

GBM6 cells were treated with STAT3 (50 μM WP1066 and 300 μM S3I-201), NF-κB (10 nM Velcade) or γ-secretase (10 μM DAPT) inhibitors. RNA was prepared and the gene expression of Notch1, Hes5, JAG1, NUMBL, DTX3, DVL3 and RBPJ quantified by qPCR and normalized to actin expression (n=3). Error bars, S.D. * $p < 0.05$; **, $p < 0.01$; *** $p < 0.001$.

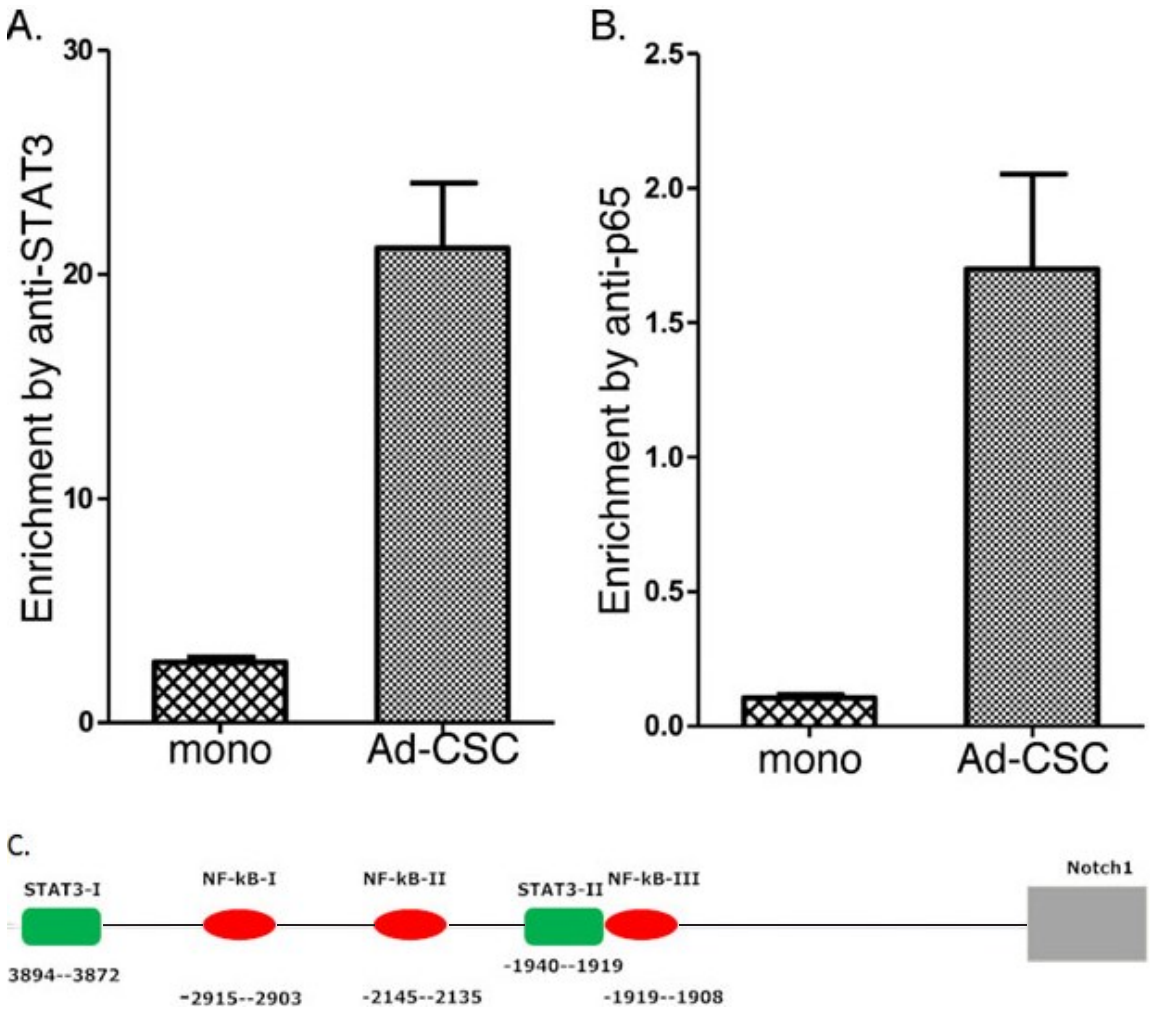

Figure 2-6. The binding of STAT3 and the p65 subunit of NF-κB to the Notch1 promoter.

ChIP analyses of **A**. STAT3 and **B**. p65 binding to Notch1 promoter. The ChIP-enriched DNA levels analyzed by qPCR were normalized to input DNA, followed by subtraction of non-specific binding determined by control IgG. **C**. The location of STAT3 and NF-κB binding sites on the Notch promoter; STAT3-II and NF-κB-III were used for this study.

selectively target them. In this study, we describe a novel relationship between glioblastoma CSCs and the Notch pathway, which involves the constitutive activation of STAT3 and NF-κB signaling. Glioma CSCs were isolated and maintained *in vitro* using the previously described adherent culture system [77], and the biological properties were compared to the traditional cultures of CSCs grown as multicellular spheres under nonadherent culture conditions [132, 133]. Under the different CSC growth conditions, the expression of CD133, Sox2 and Nestin, which are markers of neural and brain cancer stem cells [137], were similar but increased when compared to glioma cells grown in monolayer. Examination of the tumorigenicity of the adherent glioma CSCs *in vivo* by limiting dilution analysis showed that these cells were ~100 times more tumorigenic than monolayer cultured glioma cells. These findings are consistent with previous studies, which showed that CD133 expression correlated with chemoresistance of short-term cultures of glioma cells isolated from patients with primary or recurrent tumors, and the percentage of tumor cells expressing CD133 increased in all recurrent patient tumors compared to the primary tumor [138]. Furthermore, 100-fold fewer CD133 positive cells of the murine GL261 glioma line were sufficient to initiate tumors in the brain of mice when compared to CD133-negative cells [139]. Taken together, these findings demonstrate that adherent glioma CSCs exhibit characteristics previously described for CSCs grown in suspension culture and thus provide a valuable model for studying glioma CSC behavior.

The STAT3 and NF-κB pathways have been linked to cancer, and they trigger critical target genes regulating cell proliferation and survival. Both pathways have been found to be constitutively active in a number of human cancers including glioma, but their role in the glioma CSC subpopulation is not well understood [140]. For example, aberrant nuclear expression of NF-κB was found in a panel of GBM cell lines, while untransformed glial cells did not display NF-κB activity [141]. In addition, constitutively high STAT3 activity has been observed in a number of glioma cell lines and correlated with poor prognosis [142]. In this study, although the STAT3 and NF-κB signaling pathways are constitutively activated in glioma lines, we found that these pathways are dramatically activated in glioma CSCs. For example, nuclear STAT3 and phosph-STAT3 levels found in glioma CSCs were similar to the high cytokine-induced levels found in glioma monolayers, which at baseline were low but detectable. Moreover, NF-κB activation in glioma CSCs was demonstrated by high levels of the p65 subunit of NF-κB present in nuclear extracts. Furthermore constitutive activation of the STAT3 and NF-κB pathways and their direct interaction in glioma CSCs was evidenced by confocal microscopy of glioma CSCs stained for STAT3, pSTAT3, and p65. These STAT3 and NF-κB proteins were colocalized in the nuclei of glioma CSCs, with the transcriptionally active form of STAT3 (i.e pSTAT3) and p65 exclusively found in the nucleus. Evidence of the functional significance of STAT3 and NF-κB activation in glioma CSCs was provided by the finding that some of their known target genes (Bcl-2, Bcl-X, IL8, CXCL11, Trail and Caspase3) were overexpressed in adherent and spheroid glioma CSCs relative to glioma monolayers. Since targeting these signaling pathways in glioma CSCs would be a novel approach in glioma treatment, we examined the effects of two STAT3 inhibitors, WP1066 and S3I-203, in glioma CSCs. The inhibitors blocked STAT3 tyrosine phosphorylation, thereby preventing its nuclear translocation [143]. This was

confirmed by its ability to reduce the high basal nuclear levels of pSTAT3 in glioma CSCs. Treatment with the STAT3 inhibitor led to loss of nuclear colocalization of these proteins as well as their interaction. In addition, treatment with either STAT3 inhibitor resulted in growth suppressive effect on monolayer and adherent CSC cultures, but there was a markedly greater growth suppressive effect on glioma CSCs, suggesting that targeted therapy of these key pathways in glioma CSCs may be possible.

To further investigate potential biomarkers in glioma CSCs, microarray analysis was performed and revealed deregulation of the Notch signaling pathway. Notch is involved in cell fate decisions throughout normal brain development and in stem cell proliferation and maintenance, and its role in glioma is firmly established [84]. While the expression of Notch1, Hes5, Jag1, Numbl, Dtx3 and Dvl3 was upregulated in glioma CSCs, the expression of CTBP1 and RBPJ, negative regulators of Notch signaling, was downregulated in glioma CSCs. The differential expression of these genes was validated by qPCR. The identification of Hes5 as a potential glioma CSC biomarker is of great interest because Hes5 appears to play an important role in neural development [144].

In addition, we defined molecular crosstalk between the STAT3, NF-κB and Notch signaling pathways in glioma CSCs. While STAT3 inhibitors reduced expression of Notch-related genes in glioma CSCs, they increased expression of the negative regulator of Notch, RBPJ. It has been previously reported that in the developing central nervous system there is crosstalk between Notch and STAT3 pathways. For example, the activation and phosphorylation of STAT3 is mediated by the direct binding of several Hes family members (Notch effectors) to STAT3 [95]. Interestingly, activation of the Notch pathway leads to serine phosphorylation (Ser-727) but not tyrosine phosphorylation (Tyr-705) of STAT3, suggesting that the constitutive activation of STAT3 in glioma CSCs as determined by its tyrosine phosphorylation lies upstream of Notch pathway activation [135]. These results on STAT3 activation are consistent with previous studies on the Notch pathway in neural stem cells [134]. In addition, Notch and NF-κB signaling pathways apparently collaborate throughout normal brain development and function, and may regulate stem cell renewal and differentiation [94]. We hypothesize that the interactions of STAT3, NF-κB, and Notch signaling pathways that occur during normal brain development are deregulated in glioma CSCs. As shown in this study, there is crosstalk between these signaling pathways in the glioma CSC subpopulation that drives gliomagenesis. The constitutive activation of STAT3 and NF-κB signaling pathways, and the upregulation of the Notch pathway in glioma CSCs identifies novel therapeutic targets for the treatment of glioma. Future studies will be required to validate these findings *in vivo* and decipher the underlying molecular mechanisms.

Summary

In conclusion, we characterized the properties of glioblastoma cancer stem cells (CSCs) grown as adherent cultures in neurobasal medium on laminin-coated plates. Glioma CSCs have markedly enhanced tumor-initiating activity when compared to the

glioma monolayers from which they were derived. These adherent glioma CSCs share many properties with CSCs grown as traditional tumorspheres. Interestingly adherent glioma CSCs show constitutive activation of the STAT3/NF-κB signaling pathway and upregulation of STAT3- and NF-κB-dependent genes. Gene expression profiling also identified components of the Notch pathway as being deregulated in glioma CSCs, and the deregulated expression of these genes was sensitive to treatment with STAT3 inhibitors. This finding is particularly important because Notch signaling appears to play a key role in CSCs in a variety of cancers, and controls cell fate determination, survival, proliferation and the maintenance of stem cells [84].

CHAPTER 3. DISTINCT CANCER STEM CELL POPULATIONS PROMOTE TUMOR HETEROGENEITY AND DETERMINE THE MOLECULAR SIGNATURE OF GLIOBLASTOMA

Introduction

Although glioblastoma patients present uniform histological phenotypes, the molecular determinants of the disease vary considerably between individual cases. Genomic profiling of GBM samples in the TCGA database has identified four subtypes of GBM based on robust gene expression, which may develop as a result of different cancer stem cells driving tumorigenesis. Since few biomarkers show prognostic promise or predict therapeutic response in GBM, improved molecular understanding of the tumor initiating cells that drive cancer heterogeneity will advance treatment strategies for the distinct molecular subclasses of GBM. In the present study, we identify two stem cell populations that produce Classical or Mesenchymal GBM tumors but display identical histological features. Gene expression analysis revealed that GBM xenografts derived from tumorsphere cultured glioma CSCs produced a Classical GBM phenotype like that of the bulk tumor cells, while adherent CSCs retained a Mesenchymal gene signature *in vitro* and *in vivo*. Adherent GBM stem cell-derived xenografts also exhibited high STAT3 and ANGPTL4 expression levels compared to Classical tumors. This subpopulation of glioma CSCs formed tumors with histopathological features of GBM and is enriched for stem cell markers, transcriptional networks and pro-angiogenic markers characteristic of the Mesenchymal subtype. These results were verified in subcutaneous and intracranial tumors, and confirm the existence of multiple tumor initiating cell populations within GBM. Taken together, establishing a CSC culture that maintains a Mesenchymal GBM subtype provides a valuable and accurate model of the human disease, which will give insight into the role in tumor progression of novel genes, such as STAT3 and ANGPTL4, as well as their utility as new therapeutic targets.

Methods

Cell Culture

The human GBM6 patient-derived xenograft (PDX) of adult GBM tissue was provided by Dr. C. David James, (Department of Neurological Surgery, University of California, San Francisco) and continuously maintained as subcutaneous xenografts in NSG mice. Monolayer and CSC cultures of GBM6 cells were derived from freshly harvested tumor tissue. Short-term GBM6 xenolines were grown as monolayer cultures in DMEM (Cellgro, Hemdon, VA) supplemented with 10% heat-inactivated fetal bovine serum (Hyclone Labs, Thermo Scientific, Rockford, IL), 100 units/mL penicillin and 100 µg/mL streptomycin. Adherent and spheroid glioma CSCs were maintained in NeuroBasal-A medium (Invitrogen, Carlsbad, CA) containing 2% B27 supplement, 2 mM L-glutamine, 100 units/mL penicillin, 100 µg/mL streptomycin, EGF (20 ng/ml),

and basic FGF (40 ng/ml). For isolation of adherent CSCs, culture flasks were coated with 100 µg/mL poly D-lysine (Sigma-Aldrich, St. Louis, MO) for 1 hr followed by coating with 10 µg/mL laminin (Gibco, Life Technologies Inc., Grand Island NY) for 2 hr prior to use. Adherent CSCs were plated at 1 X 10^5 cells per 75 cm^2 flask, grown to confluence, dissociated with HyQTase (Thermo Scientific, Scientific, Rockford, IL), and split at a 1:3 ratio. For isolation of spheroid CSCs, glioma cells were dissociated with HyQtase and plated at ~ 1 x 10^5 cells/mL in ultra-low adhesion flasks.

Subcutaneous Xenografts

Animal experiments were performed in accordance with a study protocol approved by the Institutional Animal Care and Use Committee of the University of Tennessee Health Science Center. Glioma cancer xenografts were established in five-week-old male NOD.Cg-*Prkdc*^{scid} *Il2rg*^{tm1Wjl}/SzJ (NSG) mice (Jackson Laboratory, Bar Harbor, ME) by direct flank injection of 1×10^6 GBM6 cells transduced with luciferase lentivirus constructs. For bioluminescence imaging, mice were injected intraperitoneally with d-luciferin, imaged on the IVIS *in vivo* imaging system (Caliper Life Sciences, Hopkinton, MA), and photonic emissions assessed using Living image® software.

Orthotopic Injections

Animal studies were performed under established guidelines and supervision by the St. Jude Children's Research Hospital's Institutional Animal Care and Use Committee, as required by the United States Animal Welfare Act and the National Institutes of Health's policy to ensure proper care and use of laboratory animals for research. Anesthetized animals (ketamine/xylazine) were placed on stereotactic equipment where the scalp was prepped using alcohol and iodine swabs and artificial tear gel applied to the eyes. Following scalp excision, a rectangular window was carved out and the dura was completely removed from the surface of the brain, and $1x10^6$ cells suspended in 10 uL of media were injected approximately 2.5 mm deep in the right motor cortex. The excision was closed with skin glue, and all animals were monitored closely 24 hrs post-operatively. For bioluminescence imaging, mice were injected intraperitoneally with d-luciferin, imaged on the IVIS *in vivo* imaging system (Caliper Life Sciences, Hopkinton, MA), and photonic emissions assessed using Living image® software.

Gene Expression Analysis

Total RNA was isolated by treating tissue homogenates with Trizol followed by isolation with the RNeasy Mini kit (Qiagen Inc., Valencia, CA). Samples were submitted for complete mRNA expression profiling to the UTHSC Center of Genomics and Bioinformatics (Memphis, TN) for labeling and hybridization to Human-HT12

BeadChips (Illumina Inc.). Gene expression was also measured on the nCounter Analysis System (Nanostring Technologies, Seattle, WA) using the panel of 230 human cancer-related genes. In brief, total RNA was mixed with pairs of capture and reporter probes, hybridized on the nCounter Prep Station, and purified complexes were measured on the nCounter digital analyzer. To account for differences in hybridization and purification, data was normalized to the average counts for all control spikes in each sample and analyzed with nSolver software. Gene expression analysis was performed in collaboration with Dr. David Finkelstein in the Division of Research Informatics at St. Jude Children's Research Hospital. Gene expression patterns were compared by principal component analysis. Statistically significant genes were then identified by volcano plot, which is a scatter-plot used to quickly identify changes in large datasets composed of replicate data. It plots significance versus fold-change on the y- and x-axes, respectively. Bonferroni correction was also used to calculate an adjusted probability of comparison-wise type I error from the desired probability of family-wise type I error.

Ingenuity Pathway Analysis (IPA)

IPA (Qiagen Inc., Valencia, CA was used to identify canonical signaling pathways and functional pathways as well as to produce networks of related genes derived from genes changed in the analyzed comparisons. Here, the rank-product-generated gene lists using a 50% false discovery rate were uploaded into the IPA server as input data. IPA uses pathway libraries derived from the scientific literature. Statistics for functional analysis were carried out by Fischer's exact test (as done automatically by the software).

Histopathology

Tissue derived from bulk tumor cells, adherent CSCs and tumorspheres (four separate tumors for each condition) were fixed in 10% neutral buffered formalin for 24 hours, embed in paraffin, and sectioned at 5um thickness. For each sample, sections were stained using a standard hematoxylin and eosin (H&E) protocol, or for the common GBM neural markers GFAP, S100, OLIG2, MAP2 and the neuronal marker SYN. Sections were analyzed by Dr. David Ellison at St. Jude Children's Research Hospital. Representative images of each sample/stain combination was captured at 20x original magnification on a Nikon S1 digital camera.

Quantitative RT-PCR

Gene expression of RNA used for microarray analysis was measured by q-PCR on an iCyclerIQ (Bio-Rad Laboratories, Richmond, CA) using an iScript One-Step RT-PCR kit with SYBR Green (Bio-Rad Laboratories, Richmond, CA). Reaction parameters were as follows: cDNA synthesis at 50°C for 20 min, transcriptase inactivation at 95°C for 5 min, PCR cycling at 95°C for 10 sec, and 60°C for 30 sec for

40 cycles. The following primers were used for RT-PCR: β-actin
5'-AGAAGGAGATCACTGCCCTG-3′ (forward),
5'-CACATCTGCTGGAAGGTGGA-3′ (reverse); CHI31
5'-GTGAAGGCGTCTCAAACAGG-3' (forward),
5'-GAAGCGGTCAAGGGCATCT-3' (reverse); TRADD
5'-GCTGTTTGAGTTGCATCCTAGC-3' (forward),
5'-CCGCACTTCAGATTTCGCA-3' (reverse); NF1
5'-AGATGAAACGATGCTGGTCAAA-3' (forward),
5-CCTGTAACCTGGTAGAAATGCGA-3' (reverse); RelB
5'-CAGCCTCGTGGGGAAAGAC-3' (forward),
5'-GCCCAGGTTGTTAAAACTGTGC-3' (reverse); CASP4
5'-TTTCTGCTCTTCAACGCCACA-3' (forward),
5'-AGCTTTGGCCCTTGGAGTTTC-3' (reverse); FGFR3
5'-TGCGTCGTGGAGAACAAGTTT-3' (forward),
5'-GCACGGTAACGTAGGGTGTG-3' (reverse); PDGFA
5'-GCAAGACCAGGACGGTCATTT-3' (forward),
5'-GGCACTTGACACTGCTCGT-3' (reverse); EGFR
5'-CTACGGGCCAGGAAATGAGAG-3' (forward),
5'-TGACGGCAGAAGAGAAGGGA-3' (reverse); AKT2
5'-ACCACAGTCATCGAGAGGACC-3' (forward),
5'-GGAGCCACACTTGTAGTCCA-3' (reverse); Nestin
5'-GGCGCACCTCAAGATGTCC-3' (forward), 5'- CTTGGGGTCCTGAAAGCTG-3' (reverse).

Statistical Analysis

At least three independent experiments were performed in duplicate, and data are presented as means ± sd. ANOVA and post-hoc least significant difference analysis or Student *t* tests were performed. p values < 0.05 (*) were considered statistically significant.

Results

Diverse Molecular Signatures Found in GBM Cells and Subcutaneous Xenografts

Glioblastoma is characterized by extensive heterogeneity at the cellular and molecular levels [145]. Our previous findings revealed upregulation of the STAT3, NF-κB and Notch signaling pathways within GBM stem cells, so we then molecularly characterized xenograft tumors formed by GBM bulk tumor cells and CSCs. In brief, we prepared RNA from biological replicates of GBM6 cells grown as monolayers, adherent CSCs, and tumorspheres as well as tumor tissue derived from each condition and performed gene expression analysis. We concentrated our studies on genes analyzed in the TCGA database, which contains mRNA expression profiles from large-scale

multi-dimensional analysis of human GBM biospecimens [146]. We found that *in vitro* the bulk tumor cells have a different molecular signature compared to cells grown under both CSC conditions. In contrast, the tumors formed from the tumorsphere and adherent CSCs showed distinct differences in gene expression pattern as shown in **Figure 3-1A**. Most interesting, tumors that arose from bulk tumor cells and turmorspheres had similar expression profiles while tumors that arose from adherent CSCs had a markedly different expression profile. We then examined the mathematical variance among the data samples by PCA mapping. **Figure 3-1B** shows that bulk tumor cells and tumors that arose from them are relatively similar in expression profiles as well as adherent CSCs and their derived tumors. However, the expression profile of tumorsphere samples is very different. While the gene expression of spheroid cells is similar to adherent CSC samples, the molecular signature of the tumor tissue that arose from these CSCs is completely different. These results suggest that distinct stem cell populations exist and promote tumor heterogeneity during GBM tumor initiation and progression.

Distinct Stem Cell Populations Drive GBM Molecular Subclassification

Genomic profiling has identified four subtypes of GBM based on patterns of gene expression: Proneural, Neural, Classical and Mesenchymal. Heterogeneity of GBM tumors is thought to be attributed to different causes or cells of origin [120]. To determine if the distinct molecular signatures found between tumors derived from GBM stem cells grown as adherent CSCs or tumorspheres corresponds to a specific subtype of GBM, we analyzed "core" genes of each subtype that have been defined previously. Verhaak and colleagues performed microarray analysis on two hundred GBMs and two normal samples from the TCGA database and applied hierarchical clustering to assess subclass cross validation error and find gene signatures for each class of GBM. We used this information to categorize the genes within our array by their association with the Classical, Neural, Proneural or Mesenchymal subclass. The PCA maps in **Figure 3-2A** reveal how GBM bulk tumor cells, CSCs and the subsequent tumor tissue correspond to the four subtypes of GBM. The distinct gene signatures among GBM tumor tissue (202 samples) from Classical (in white), Neural (in black), Proneural (in blue) and Mesenchymal (in gray) subclasses is represented and matched to our samples. *In vitro*, the gene expression profile of adherent CSCs (red) and tumorspheres (yellow) associate with the Mesenchymal type of GBM, while the expression profile of bulk tumor cells (orange) fall within the Classical subtype. The different gene signatures observed between tumors derived from adherent CSCs and tumorspheres is also shown in association with the GBM subclasses. While the adherent CSC-derived tumors maintain a Mesenchymal gene signature, tumorspheres form tumors of a Classical subtype that mimics the gene signature of tumors derived from bulk tumor cells.

To further illustrate the molecular subclassification of our GBM xenografts, we measured some of the classic genes used to define the Classical and Mesenchymal GBM subtypes by qPCR. In brief, RNA was extracted and pooled from 3 individual subcutaneous tumors derived from monolayers, adherent CSCs or tumorspheres. As shown in **Figure 3-2B**, the Mesenchymal markers CHI3L1, TRADD and RelB are

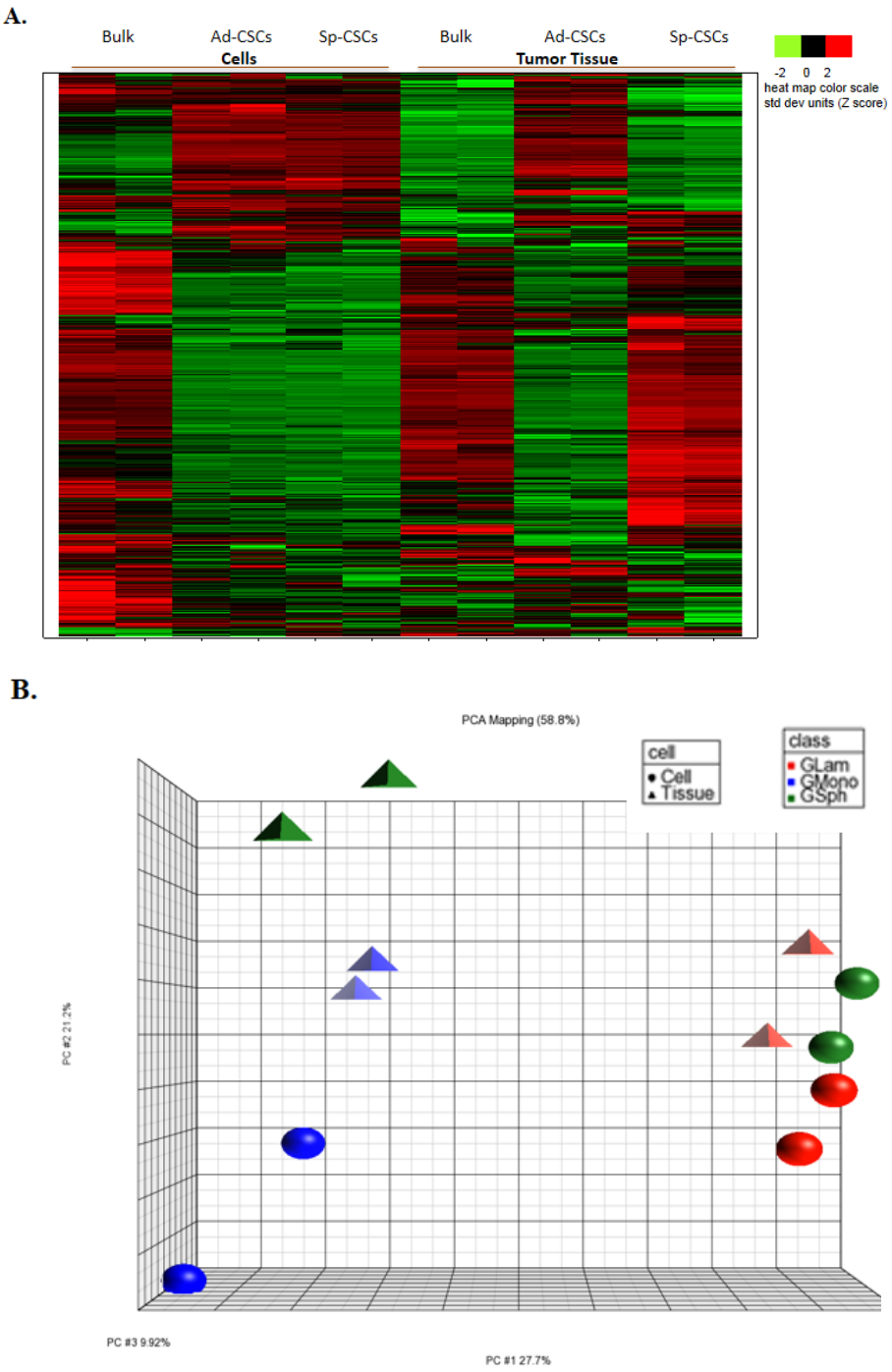

Figure 3-1. Illumina array analysis of GBM6 cells and tumor tissue.

RNA was prepared from GBM6 monolayer, adherent CSC, and tumorsphere cell cultures as well as from subcutaneous tumors derived from each condition. Biological duplicates were ran for each sample and data was collected and analyzed. **A.** Gene expression was measured by Illumina array and genes reported in the TCGA database were analyzed. **B.** The PCA plot represents the comparison of gene signatures from each condition.

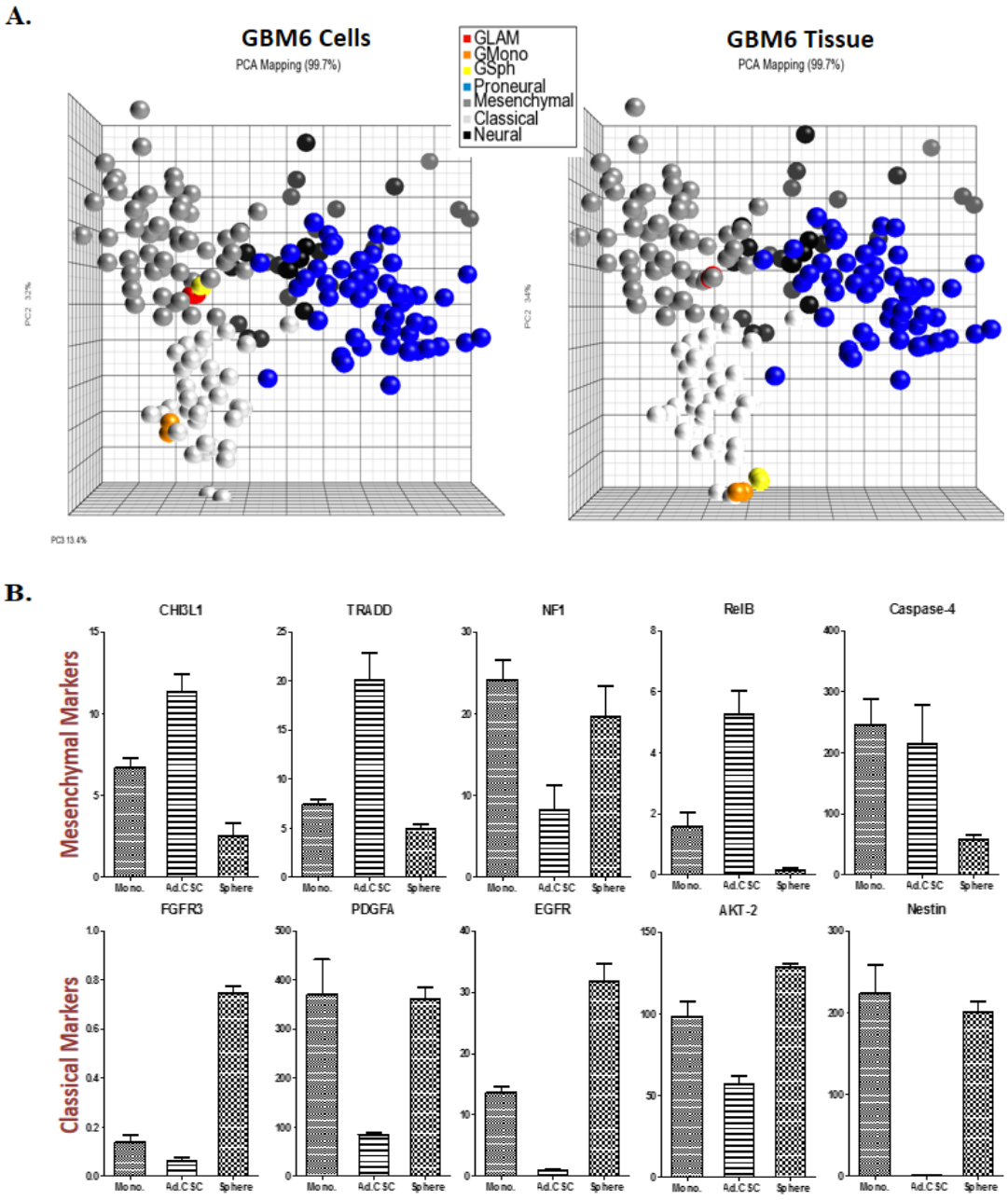

Figure 3-2. Molecular classification of GBM6 cells and tissue.

A. Array analysis was performed and compared to GBM molecular subclasses; PCA map depicts the classical, mesenchymal, neural, and proneural gene signatures and the gene signature of GBM6 cells and tumor tissue derived from glioma monolayer, adherent CSC, and spheroid cells. **B.** RNA was pooled from three individual tumor tissues derived from GBM6 bulk tumor cells, adherent CSCs, and tumorspheres to determine gene expression of molecular markers of GBM. Mesenchymal (CHI3L1, TRADD, NF1, RelB & Caspase-4) and Classical genes (FGFR3, PDGFA, EGFR, AKT2 & Nestin) were measured by qPCR and normalized to actin expression (n=3).

significantly elevated in tissue derived from adherent CSCs compared to the other tumors, and NF1, which is a tumor suppressor commonly downregulated in Mesenchymal GBM, is decreased. The mesenchymal marker CHI3L1 in combination with astrocytic markers is indicative of an epithelial-to-mesenchymal transition that has been linked to aggressive, dedifferentiated tumors [124]. Genes in the TNF and NF-κB pathways, such as TRADD and RelB, are highly expressed in this subtype as well, potentially as a consequence of increased necrosis and associated inflammatory infiltrates [127]. We also found that Classical markers PDGFA, EGFR, AKT and Nestin are highly expressed in tumor tissue derived from bulk tumor cells and tumorspheres, while there is relatively low expression in adherent CSC tumors. Most notably, EGFR and Nestin expression are almost non-existent. Significant EGFR amplification is observed in 97% of Classical GBMs in the TCGA database and infrequently in other subtypes along with the neural precursor and stem cell marker, Nestin. This finding is of significant importance as the GBM6 patient xenograft is from a patient with overexpression of the VIII mutant of EGFR, and consistent with our finding of high EGFR expression in bulk tumor cells and in tumors derived from them. These studies indicate that GBM stem cells maintained in adherent culture conditions are a different tumor initiating subpopulation than that of traditional tumorspheres. The adherent GBM CSCs exhibit a mesenchymal gene signature and promote the initiation and progression of the Mesenchymal GBM subtype *in vivo*.

Indistinguishable Histopathology among Heterogeneous GBM Xenografts

While GBM tumors represent different molecular subtypes, there is commonly no distinction in histologic phenotype, which complicates the prognosis and treatment of this malignancy [147]. The molecular heterogeneity observed in our GBM xenografts derived from bulk tumor cells, adherent CSCs and tumorspheres lead us to examine the histopathology of these tumors. Four individual subcutaneous tumors derived from each cell culture condition were formalin-fixed, paraffin-embedded, and sectioned. Each sample was stained for H&E analysis, and immunohistochemistry was performed to measure immunoreactivity with antibodies for the common GBM markers GFAP, S100, OLIG2, MAP2 and SYN. As shown in **Figure 3-3A**, the Classical GBM tumors derived from bulk tumor cells and tumorspheres and the Mesenchymal tumors derived from adherent GBM stem cells were all determined to be high-grade gliomas and morphologically indistinguishable. Tumor cells with a high nuclear:cytoplasmic ratio and little nuclear pleomorphism showed the morphology of relatively undifferentiated high-grade gliomas. Neural markers used in glioma classification were also analyzed and found to be indistinguishable among the molecularly heterogeneous GBM xenografts (**Figure 3-3B**). There was strong immunoreactivity for GFAP and OLIG2 in many tumor cells, while all tumor cells expressed S-100 and MAP-2. In neural tumors, GFAP, OLIG-2 and MAP-2 are generally expressed by gliomas, while the neuronal marker Synaptophysin is negative [148-151]. These findings reveal the similarity at the microscopic level between the molecularly distinct xenografts of the Classical and Mesenchymal subclasses derived from bulk tumor cells and adherent CSCs, respectively.

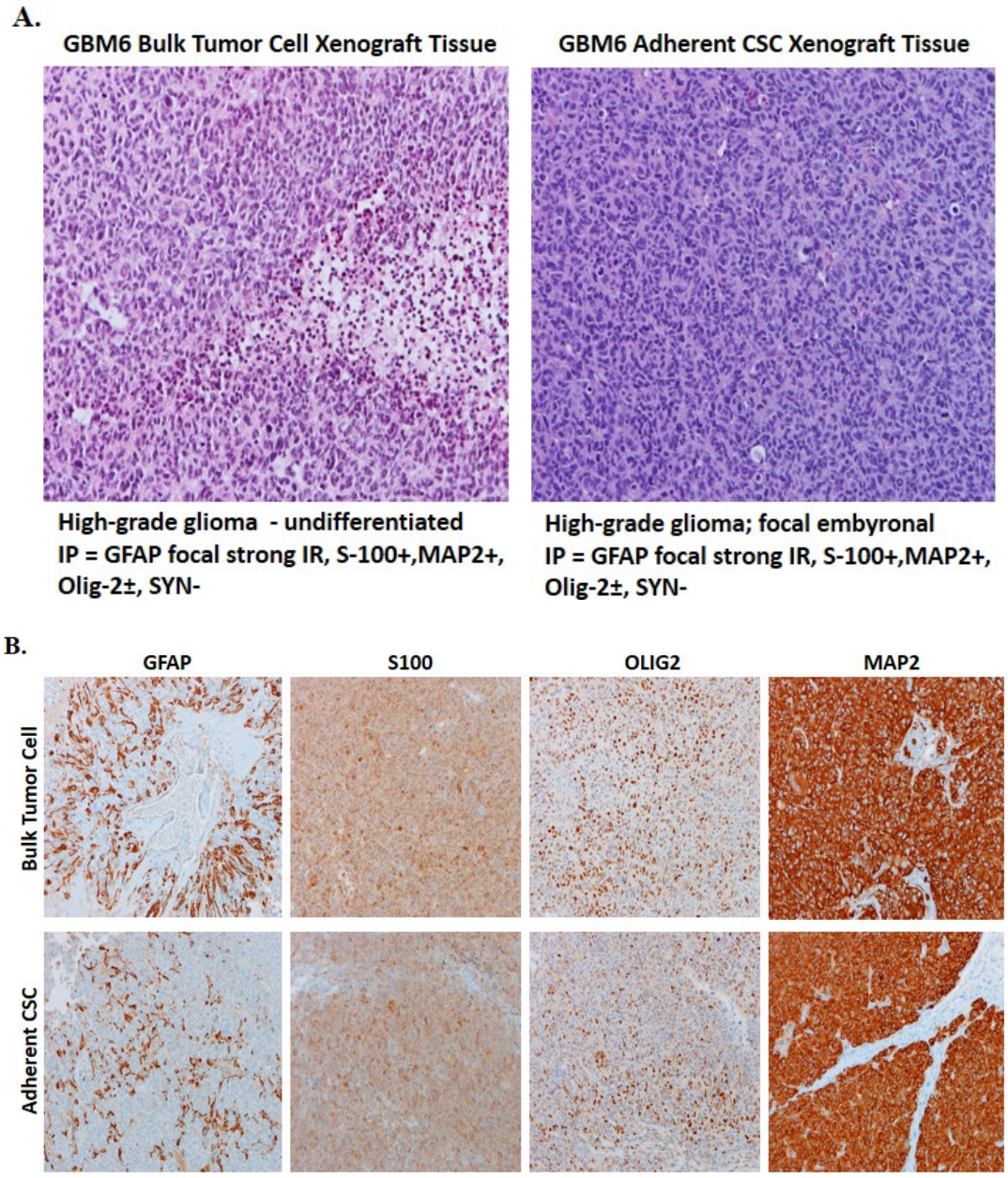

Figure 3-3. Pathological review of GBM6 tumor xenografts.

Cells from monolayer and adherent CSC culture conditions were injected subcutaneously and allowed to grow to a diameter of ~400mm^3. Tumors were extracted and paraffin embedded for histology services. **A.** H&E staining as well as **B.** immunoreactivity of the markers GFAP, S100, OLIG2, MAP2, and SYN was carried out and reviewed by Dr. David Ellison at SJCRH. Tumor cells with a high nuclear:cytoplasmic ratio and little nuclear pleomorphism showed the morphology of relatively undifferentiated high-grade gliomas. There was strong immunoreactivity for GFAP or OLIG2 in many tumor cells, while all tumor cells expressed S-100 and MAP-2. (All photomicrographs taken at 200x)

It also demonstrates the importance of integrative histological and molecular classification of gliomas in establishing effective treatment regimens for GBM patients.

Adherent CSCs Promote Mesenchymal Signature in Intracranial GBMs

In order to understand the role of the "true" tumor microenvironment on gene expression in GBM we then performed our analysis in an orthotopic animal model by intracranial injection of tumor cells. The human glioblastoma orthotopic mouse model results in invasive growth in mice and allows users to quantitate intracranial tumor growth [152]. To determine if our findings were also observed in the conventional microenvironment of GBM, we performed intracranial injections of 1×10^6 luciferase-expressing GBM6 cells grown as short-term monolayer cultures, adherent CSCs or tumorspheres. We first compared the tumor initiating capacity of the GBM bulk tumor cells to both CSC conditions by bioluminescence imaging. As shown in **Figure 3-4A**, both CSC subpopulations formed tumors more rapidly than bulk tumor cells, and survival was shorter in the more aggressive tumors. This is consistent with our previous subcutaneous studies that revealed adherent CSCs were nearly 100-times more potent in inducing tumors than the glioma monolayer cultures.

We next examined the histological phenotypes and molecular heterogeneity of the different intracranial GBM xenografts. As shown in **Figure 3-4B**, the GBM tumors derived from bulk tumor cells, adherent CSCs and tumorspheres were all determined to be High-Grade Glioma and exhibit no distinction in H&E staining as before. All of the tissue displayed characteristics of GBM, such as hypercellularity, atypical nuclei, pseudopalisading necrosis and microvascular proliferation [153]. The traditional GBM prognostic markers GFAP, S100, OLIG2, MAP2 and SYN were also analyzed and found to be indistinguishable among the GBM xenografts.

To further refine the molecular subclassification of the intracranial GBM xenografts, we measured the expression of genes used commonly to define the Classical and Mesenchymal GBM subtypes by qPCR. In brief, RNA was extracted from 3 individual intracranial tumors derived from monolayers, adherent CSCs or tumorspheres. As shown in **Figure 3-4C**, the Mesenchymal markers CHI3L1, TRADD, RelB and Caspaase4 are significantly elevated in intracranial tumors derived from adherent CSCs compared to the other xenografts, while NF1 is decreased. We also found that the Classical markers FGFR3, PDGFA, EGFR, AKT-2 and Nestin are highly expressed in tumor tissue derived from bulk tumor cells and tumorspheres, while there is little expression in adherent CSC tumors. These orthotopic studies support our previous finding that GBM stem cells maintained in adherent culture conditions are a different tumor initiating subpopulation than that of traditional tumorspheres. The adherent GBM CSCs exhibit a mesenchymal gene signature and promote the initiation and progression of the Mesenchymal GBM subtype *in vivo*.

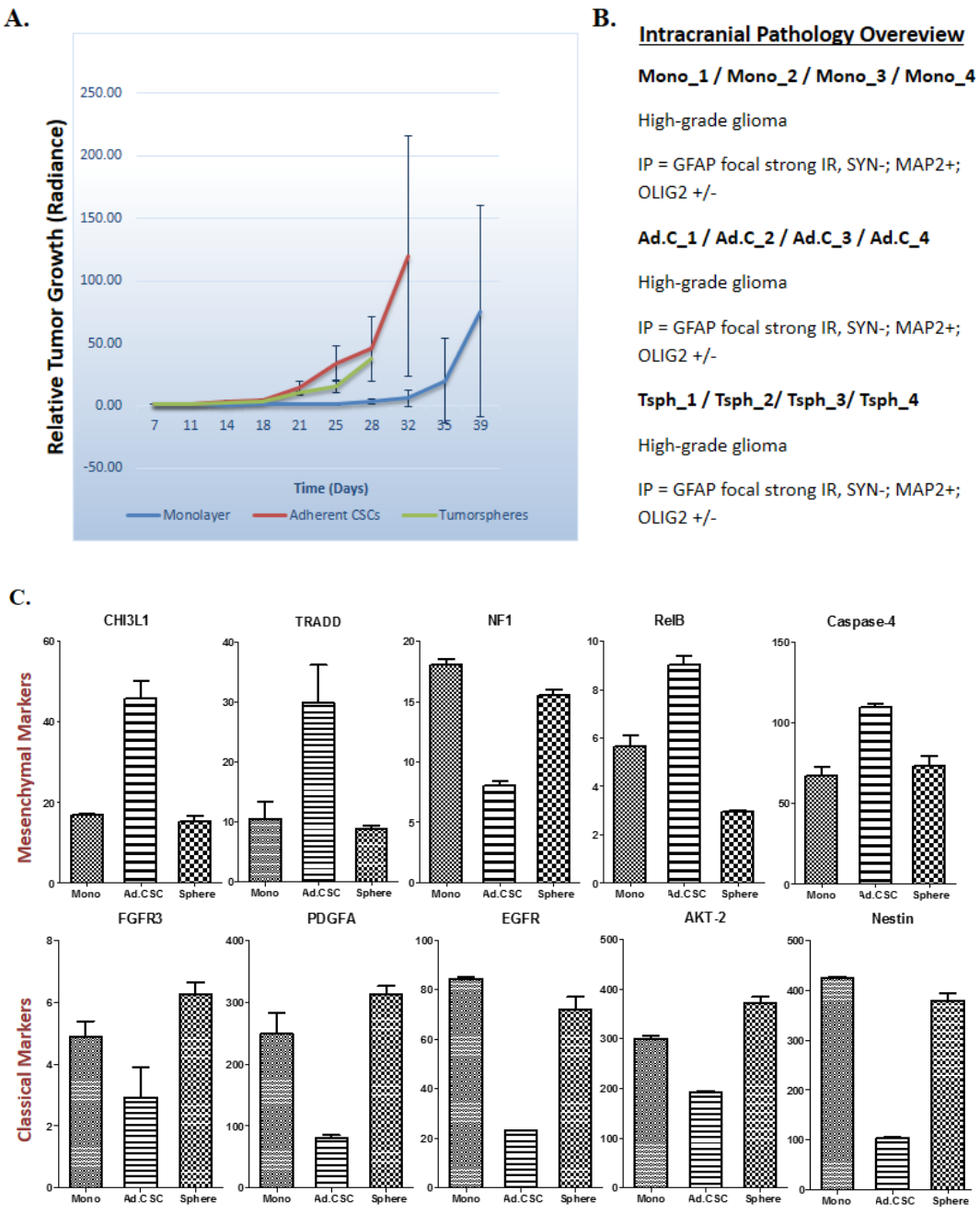

Figure 3-4. Characterization of orthotopic GBM6 tumors

A. NSG mice were orthotopically injected with $1x10^6$ luciferase-tagged GBM6 cells grown as monolayers, adherent CSCs or tumorspheres and tumor burden was measured by Xenogen imaging twice a week (n=10 per group). **B.** Tumor-bearing brains were extracted and paraffin embedded for histology services. H&E staining as well as analysis of the markers GFAP, S100, OLIG2, MAP2, and SYN was carried out and reviewed by Dr. David Ellison at SJCRH. **C.** RNA extracted from intracranial tumors was extracted and submitted for array analysis. (n=3)

Upregulation of STAT3 and ANGPTL4 in Mesenchymal GBM Xenografts

To identify specific genes differentially expressed in Mesenchymal GBM tumors derived from adherent CSC cultures of GBM6 xenografts, we further analyzed the mRNA expression profiling. The samples were also evaluated on the nCounter Analysis System (Nanostring Technologies, Seattle, WA) using the human cancer-related panel of 230 genes. RNA was mixed with pairs of capture and reporter probes, hybridized on the nCounter Prep Station, and purified complexes were measured on the nCounter digital analyzer. To account for differences in hybridization and purification, data was normalized to the average counts for all control spikes in each sample and analyzed with nSolver software. **Figure 3-5A** reveals the different molecular signature observed between bulk tumor cell and CSC-derived GBM tumors. Individual biological replicates of tumor tissue showed little variation in gene expression, but there were clear differences in the gene expression pattern in Classical and Mesenchymal tumors derived from short-term monolayer cultures vs. adherent CSCs, respectively. Significant genes upregulated or downregulated that passed the Bonferroni threshold in the adherent CSC-derived tumors are shown in **Figure 3-5B** by Volcano Plot, with verified mRNA levels of SPP1, ETV1, CCND2, CDH1, NQO1, STAT3 and LYN shown in **Figure 3-5C.** Notably, the enhanced expression of STAT3 in Mesenchymal GBM6 tumors derived from CSCs confirms *in vitro* results that we previously published [154]. One other report has shown STAT3 to be an initiator and master regulator of mesenchymal transformation in GBM [56]. Elevated expression of CDH1, NQO1 and LYN has also previously been identified in GBM, with each contributing to the growth and invasion of this aggressive brain tumor subtype in different ways [155-157].

Functional annotation of the genes differentially expressed in GBM tumors of the Mesenchymal subclass formed from adherent CSCs also reveals that genes involved in angiogenesis are significantly enriched ($P<0.05$, Ingenuity Pathway Analysis). The schematic expression of these pro-angiogenic genes is shown in **Figure 3-5D,** and the qPCR validation of ANGPTL4, IL8, CDKN2A and CXCL1 mRNA levels in adherent CSC-derived tumors is shown in **Figure 3-5E.** Most interestingly, our lab has observed the elevated expression of ANGPTL4 in xenografts derived from CSCs in other cancer types [unpublished]. ANGPTL4 upregulation has also previously been identified in a robust angiogenesis gene signature shown to correlate with the Mesenchymal subtype of GBM [125]. The chemokine IL-8 has been found to be expressed and secreted at high levels in GBM both *in vitro* and *in vivo*, and recent experiments suggest it is critical to glial tumor neovascularity and progression [158]. Another chemokine, CXCL1, has been implicated as an oncogenic factor in glioma and directly related to attenuated angiogenic activity through NF-κB regulation [159]. These pro-angiogenic genes have been shown to contribute to the vascularization of highly aggressive GBM tumors and therefore represent therapeutic interests.

Figure 3-5. Enrichment of pro-survival and pro-angiogenic genes in GBM tumor tissue derived from adherent CSCs.

A. RNA was prepared from three separate tumors generated from GBM6 monolayer or adherent CSCs and nanostring analysis was performed. **B.** Volcano plot depicting the genes of interest within the CSC tumors that passed the Bonferroni test. **C.** Verification of significant deregulated genes found in Nanostring analysis. The RNA used for Nanostring analysis was prepared and the gene expression of SPP1, ETV1, CCND2, CDH1, NQO1, and LYN was quantified by qPCR and normalized to actin expression. **D.** RNA was prepared from tumor tissue derived from GBM6 bulk tumor cells and adherent CSCs to perform microarray analysis; schematic representation of Ingenuity pathway analysis showing the upregulation of genes involved in angiogenesis. **E.** qPCR validation of pro-angiogenic genes (ANGPTL4, IL8, CDKN2A and CXCL1) upregulated in GBM6 adherent CSC-derived tumor tissue normalized to actin expression (n=3).

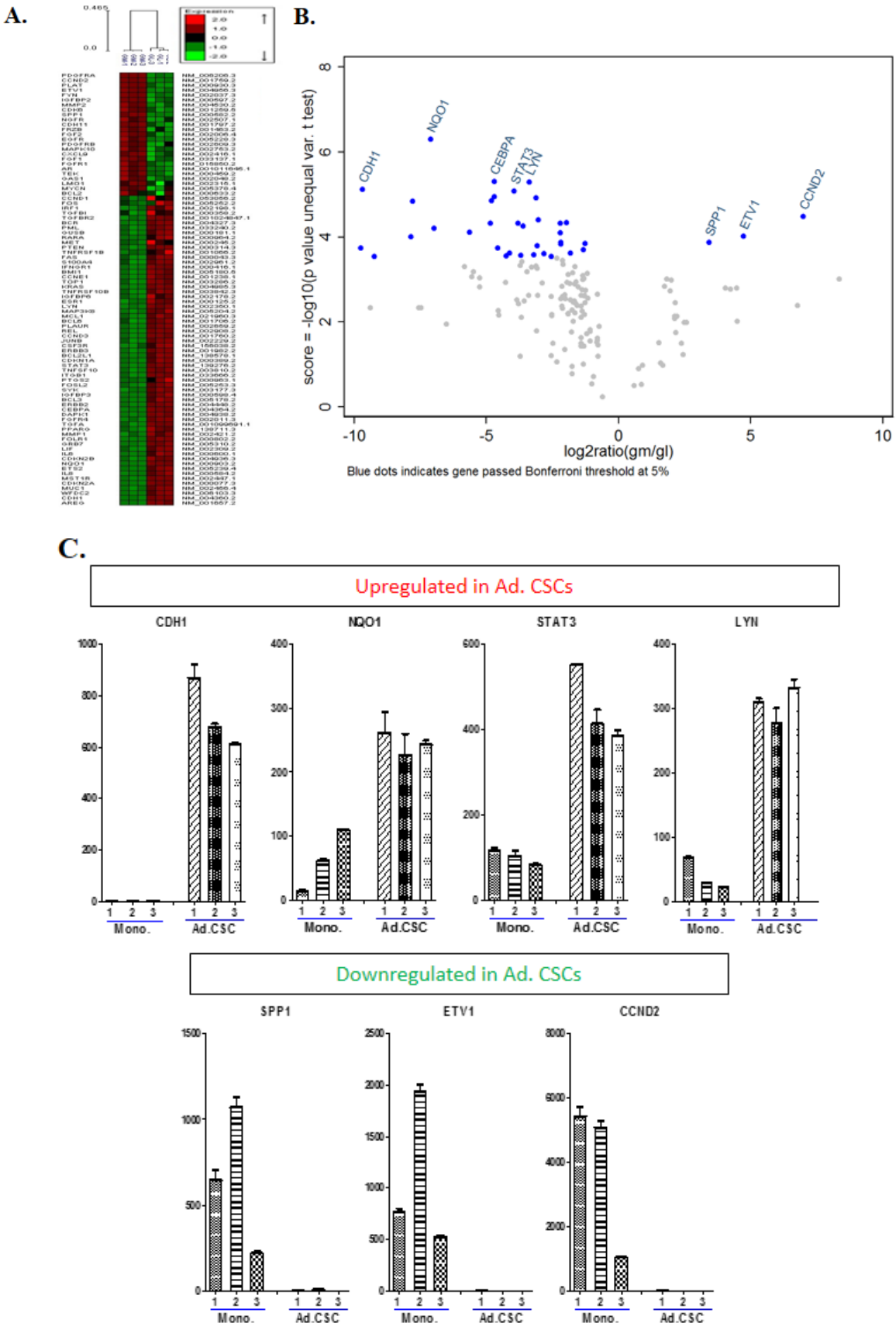
A.
B.
score = -log10(p value unequal var. t test)
log2ratio(gm/gl)
Blue dots indicates gene passed Bonferroni threshold at 5%
CDH1
NQO1
CEBPA
STAT3
LYN
SPP1
ETV1
CCND2
C.
Upregulated in Ad. CSCs
CDH1
NQO1
STAT3
LYN
Downregulated in Ad. CSCs
SPP1
ETV1
CCND2
Mono.
Ad.CSC

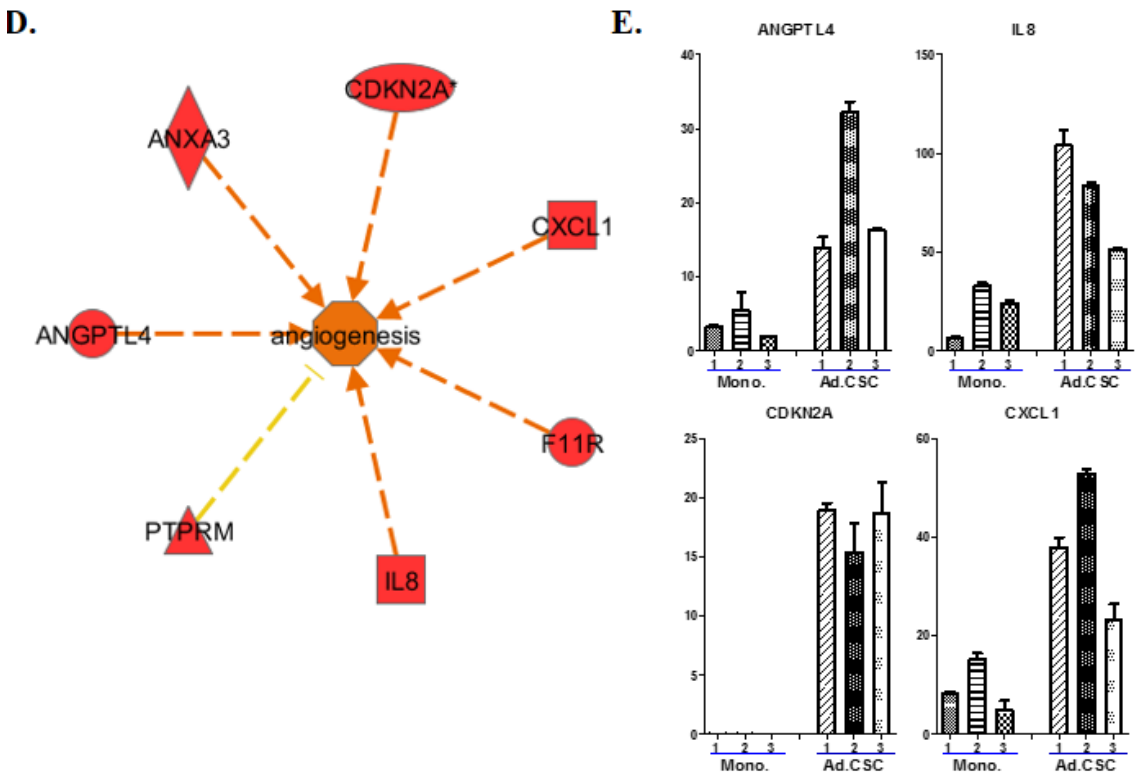

Figure 3-5. Continued.

Discussion

Although most glioblastoma multiforme (GBM) patients present uniform histological phenotypes, the molecular determinants of disease aggressiveness vary considerably between individual cases. The name "multiforme" is derived from the histopathologic description of the varied morphologic features of this tumor and the presence of heterogeneous cell populations within a single tumor, in which lesions with a high degree of cellular and nuclear polymorphism and numerous giant cells coexist with areas of high cellular uniformity [160]. Genomic profiling of GBM samples in the TCGA database has identified four subtypes of GBM, Classical, Neural, Proneural and Mesenchymal, based on robust gene expression, which are thought to develop as a result of different cancer stem cells driving tumorigenesis [120]. Since few biomarkers show prognostic promise or predict therapeutic response, improved molecular understanding of the tumor initiating cells that drive cancer heterogeneity will advance treatment strategies for the distinct molecular subclasses of GBM. In the present study, we demonstrate two distinct stem cell populations that produce Classical or Mesenchymal GBM tumors but display identical histological features.

We began our studies by performing microarray analysis to molecularly characterize GBM bulk tumor cells, adherent CSCs and tumorspheres, as well as, the tumors derived from each cell type. The results revealed that *in vitro* the bulk tumor cells exhibited a different molecular signature compared to both CSC conditions, however the tumor tissue displayed a distinct difference in gene expression pattern between the CSC cultures. Our findings support recent studies proposing that tumor heterogeneity is a result of cancer stem cells that are able to self-renew and generate differentiated progeny that compose the bulk of the tumor. CSCs have been identified in several types of cancer, including GBM. Initially, the expression of CD133 seemed to be the robust marker of brain tumor stem cells. However, numerous studies have since shown that this marker does not consistently distinguish tumorigenic and non-tumorigenic glioma cells, suggesting that distinct CSC subpopulations exist to drive GBM tumorigenesis [161, 162]. To determine whether the two stem cell populations (adherent CSCs and tumorspheres) we employed in our studies promote tumor heterogeneity corresponding to a specific subtype of GBM, we analyzed traditional markers of the Classical, Neural, Proneural and Mesenchymal subtypes. The different gene signatures observed between tumors derived from adherent CSCs and tumorspheres were classified, and adherent CSC-derived tumors were found to promote a Mesenchymal GBM gene signature, while tumorspheres promoted the Classical GBM subtype like that of the bulk tumor cells. These results were confirmed by qPCR and reveal that GBM stem cells maintained in adherent culture conditions represent a different tumor initiating subpopulation than that of traditional tumorspheres. The extensive heterogeneity at the cellular and molecular levels of GBM that are found in tumors produced by CSCs has great significance for the general outcome of the malignancy; it confounds our understanding of the disease and also contributes to tumor aggressiveness and poses obstacles to the design of effective therapies [163]. Therefore, establishing an adherent CSC culture method that exhibits a mesenchymal gene signature and promotes the initiation and progression of the

aggressive Mesenchymal GBM subtype *in vivo*, provides a valuable model of the human disease for future studies.

Most GBMs are distinguished pathologically from low grade gliomas by the presence of necrosis and microvascular hyperplasia, but there is no distinction between molecular subtypes, which complicates prognosis and therapeutic strategies [164]. To study the pathology of the Classical and Mesenchymal GBM tumors derived from our different GBM6 cell cultures, each sample was stained for H&E analysis, and immunohistochemistry was performed to review the common GBM markers GFAP, S100, OLIG2, MAP2 and SYN. The Classical GBM tumors derived from bulk tumor cells and tumorspheres and the Mesenchymal tumors derived from adherent GBM stem cells were all diagnosed as high-grade glioma and displayed no differences in H&E staining or marker expression. These findings reveal the pathological likeness between the molecularly distinct Classical and Mesechymal xenografts derived from bulk tumor cells and adherent CSCs, respectively. It also demonstrates the importance of integrative histological and molecular classification of gliomas in establishing effective treatment regimens for GBM patients

To determine if the molecular heterogeneity found in our High-Grade Glioma xenografts is maintained in the conventional microenvironment of GBM, we performed intracranial injections of GBM6 cells grown as short-term monolayers, adherent CSCs or tumorspheres. The tumor initiating capacity of the GBM CSCs by intracranial injection was comparable to our previous studies performed by subcutaneous injection. Both CSC subpopulations formed tumors more rapidly than bulk tumor cells, and survival was shorter in the more aggressive tumors [154]. We next examined the histological phenotypes and molecular heterogeneity of the different intracranial GBM xenografts. The GBM tumors derived from bulk tumor cells, adherent CSCs and tumorspheres were all diagnosed as High-Grade Glioma and had no distinction in H&E staining or traditional glioma markers as before. The common genes used to define the Classical and Mesenchymal GBM subtypes were measured by qPCR, and the Mesenchymal markers were significantly elevated in intracranial tumors derived from adherent CSCs compared to the other xenografts, while NF1 was decreased. The Classical markers were also highly expressed in tumor tissue derived from bulk tumor cells and tumorspheres, with little expression in adherent CSC tumors. These orthotopic studies confirm our previous finding that GBM stem cells maintained in adherent culture conditions represent a different tumor-initiating subpopulation than that of traditional tumorspheres. The adherent GBM CSCs exhibit a mesenchymal gene signature and promote the initiation and progression of the Mesenchymal GBM subtype intracranially.

To identify novel genes specifically deregulated in Mesenchymal GBM tumors derived from adherent CSC cultures of GBM6 xenografts, we re-analyzed our microarray analysis on RNA prepared from GBM xenografts derived from bulk tumor cells, adherent CSCs and tumorspheres and found that gene expression was markedly different between GBM xenografts derived from these different cell populations. Most interestingly, the expression of STAT3 was shown be elevated in the more aggressive stem cell-derived tumors. This is consistent with our previous findings *in vitro*, in which we identified

STAT3 as a potential therapeutic target due to its constitutive activation in GBM stem cells [154]. STAT3 is a master regulator of genes involved in various steps of tumor progression, so we sought to identify pathways that STAT3 could potentially regulate within CSCs to promote gliomagenesis. IPA analysis revealed significant upregulation of several genes involved in the angiogenic pathway, with ANGPTL4 being of great interest since our lab has previously observed elevated expression of ANGPTL4 in xenografts derived from CSCs in other cancer types [unpublished]. While previous reports suggest EGFR induces ANGPTL4 expression and promotes tumor angiogenesis in malignant gliomas, we find ANGPTL4 activation to be independent of EGFR upregulation in Mesenchymal GBM xenografts [165]. The important roles of STAT3 and ANGPTL4 in promoting GBM progression and vascularization represent potential therapeutic targets in treating GBM and warrant further molecular characterization.

Summary

In conclusion, we performed gene expression profiling on subcutaneous xenografts derived from GBM bulk tumor cells and two different stem cell cultures and found distinct molecular signatures among the tissue. While monolayer and tumorsphere cultured glioma cells produced a Classical GBM tumor, adherent CSCs retained the Mesenchymal gene signature *in vitro* and in mouse xenografts. Mesenchymal GBM xenografts derived from adherent CSCs also exhibited high STAT3 and ANGPTL4 expression levels compared to Classical tumors. This subpopulation of glioma cells formed tumors with histopathological features of high-grade glioma and was enriched for stem cell markers, transcriptional networks and angiogenesis markers. These results were verified intracranially and confirm the existence of multiple tumor initiating cell populations within GBM. Taken together, establishing a culture system that represents the Mesenchymal GBM subtype provides a valuable and accurate model of the human disease for future studies. The characterization of the Mesenchymal subclass will give insight into novel genes, such as STAT3 and ANGPTL4, that are involved in glioma tumor progression and lead to the discovery of new therapeutic targets in treating GBM.

CHAPTER 4. STAT3 AND ANGPTL4 WORK TOGETHER IN CANCER STEM CELLS TO DRIVE MESENCHYMAL GLIOBLASTOMA

Introduction

Despite multimodality therapeutic strategies developed over the past three decades, patients with glioblastoma multiforme (GBM) still have a dismal prognosis and overall survival time less than 14 months. The aggressiveness and rapid tumor relapse of GBM is believed to be sustained by a cancer stem-like cell population that is able to initiate and maintain tumors. Although CSCs represent only a small fraction of cells within a tumor, their high tumor-initiating capacity and therapeutic resistance is believed to drive tumorigenesis. Therefore, it is imperative to identify pathways associated with CSCs in order to devise innovative strategies to selectively target them. In the present study, we describe a novel relationship between STAT3 and ANGPTL4 within the cancer stem-like cell population of GBM that drives tumor initiation and progression. Molecular characterization of aggressive Mesenchymal GBM xenografts identified high STAT3 and ANGPTL4 expression levels within the CD133+ CSC subpopulation, and these proteins were shown to colocalize within GBM stem cells. Elevated STAT3 and ANGPTL4 expression was found to correlate to short-term survival of human GBM patients, and a link in expression levels was observed between the genes in individual patient samples. The deregulated expression of these genes in glioma CSCs was sensitive to the kinase inhibitors, WP1066 and Sorafenib. Targeted inhibition of STAT3 and ANGPTL4 was found to decrease stem cell marker expression within tumors and lead to tumor regression. Taken together, we have identified an important relationship between STAT3 and ANGPTL4 in GBM stem cells, as well as potential therapeutic value as biomarkers in targeting the CSC subpopulation of Mesenchymal GBM.

Methods

Tumor Studies in Mice

All animal experiments were performed in accordance with a study protocol approved by the Institutional Animal Care and Use Committee of the University of Tennessee Health Science Center. Glioma cancer xenografts were established in five-week-old male NOD.Cg-*Prkdc*^{scid} *Il2rg*^{tm1Wjl}/SzJ (NSG) mice (Jackson Laboratory, Bar Harbor, ME) by direct flank injection of 1×10^6 GBM6 cells transduced with luciferase lentivirus constructs. For gene expression analysis, tumors were measured bi-weekly until reaching a volume of ~400mm^3; mice were then sacrificed and tumors harvested for RNA. For bioluminescence imaging, mice were injected intraperitoneally with d-luciferin, imaged on the IVIS *in vivo* imaging system (Caliper Life Sciences, Hopkinton, MA), and photonic emissions assessed using Living image® software. At ~7 days after cell injection, when tumors formed in all mice, mice were given intraperitoneal injections of WP1066 (44 mg/kg) and Sorafenib (20 mg/kg) in 1% DMSO every other

day. For survival analysis mice were observed daily after injection and were sacrificed at the first sign of shortness of breath, decreased locomotion or reduced body weight (>20% of total body weight). Tumors were measured weekly with a handheld caliper and by bioluminescence imaging. At the end of treatment the animals were sacrificed, and the tumors were removed, weighed and processed for further study.

Quantitative RT-PCR

Total RNA was extracted as described before for xenografts; RNA was also extracted from curls of formalin fixed paraffin-embedded tissue blocks of brain biopsy specimens from GBM patients obtained from UTHSC Pathology Tissue Core using RecoverAll Total Nucleic Acid Isolation Kit (Ambion Inc., Austin, TX). Gene expression was measured by RT-PCR performed on an iCyclerIQ (Bio-Rad Laboratories, Richmond, CA) using an iScript One-Step RT-PCR kit with SYBR Green (Bio-Rad Laboratories, Richmond, CA). Reaction parameters were as follows: cDNA synthesis at 50°C for 20 min, transcriptase inactivation at 95°C for 5 min, PCR cycling at 95°C for 10 sec and 60°C for 30 sec for 40 cycles. The following primers were used for RT-PCR: β-actin 5-AGAAGGAGATCACTGCCCTG-3′ (forward), 5-CACATCTGCTGGAAGGTGGA-3′ (reverse); SPP1 5’-CTCCATTGACTCGAACGACTC-3’ (forward), 5’-CAGGTCTGCGAAACTTCTTAGAT-3’ (reverse); ETV1 5’-TACCCCATGGACCACAGATT-3’ (forward), 5’-CACTGGGTCGTGGTACTCCT-3’ (reverse); CCND2 5’-ACCTTCCGCAGTGCTCCTA-3’ (forward), 5’-CCCAGCCAAGAAACGGTCC-3’ (reverse); CDH1 5’-CGAGAGCTACACGTTCACGG-3’ (forward), 5’-GGGTGTCGAGGGAAAAATAGG-3’ (reverse); NQO1 5’-GAAGAGCACTGATCGTACTGGC-3’ (forward), 5’-GGATACTGAAAGTTCGCAGGG-3’ (reverse); STAT3 5’-CAGCAGCTTGACACACGGTA-3’ (forward), 5’-GCCCAATCTTGACTCTCAATCC-3’ (reverse); LYN 5’-GCTTTTGGCACCAGGAAATAGC-3’ (forward), 5’-TCATGTCGCTGATACAGGGAA-3’ (reverse); ANGPTL4 5’-GGCTCAGTGGACTTCAACCG-3’ (forward), 5’-CCGTGATGCTATGCACCTTCT-3’ (reverse); IL8 5’-TAGCAAAATTGAGGCCAAGG-3’ (forward), 5’-AGCAGACTAGGGTTGCCAGA-3’ (reverse); CDKN2A 5’-GGGTTTTCGTGGTTCACATCC-3’ (forward), 5’-CTAGACGCTGGCTCCTCAGTA-3’ (reverse); CXCL1 5’-ATGAGTGTGAAGGGCATGGGC-3’ (forward), 5’-TCACTGCTTTTACCCCAGGG-3’ (reverse); VEGFR-1 5’-TTTGCCTGAAATGGTGAGTAAGG-3’ (forward), 5’-TGGTTTGCTTGAGCTGTGTTC-3’ (reverse); VEGFR-2 5’-GGCCCAATAATCAGAGTGGCA-3’ (forward), 5’-CCAGTGTCATTTCCGATCACTTT-3’ (reverse*);* CD133 5’-CATCCACAGATGCTCCTAAGG-3’ (forward), *5’-AAGAGAATGCCAATGGGTCCA-3’* (reverse); SOX2

5′-GCCGAGTGGAAACTTTTGTCG-3′ (forward),
5′-GCAGCGTGTACTTATCCTTCTT-3′ (reverse); Nestin
5’-GGCGCACCTCAAGATGTCC-3’ (forward), 5’-CTTGGGGTCCTGAAAGCTG-3’ (reverse)

Immunofluorescence and Confocal Microscopy

Tissue was embedded in OCT compound and cryosectioned at 10 μm prior to fixation with 4% paraformaldehyde and blocking with 5% BSA. Tissue was incubated with antibodies directed against STAT3 (Cell Signaling Technology, Beverly, MA) and ANGPTL4 (Invitrogen, Carlsbad, CA), and subsequently stained with goat anti-mouse Alexa Fluor 488 and goat anti-rabbit Alexa Fluor 555 (Invitrogen, Carlsbad, CA). Sections were counterstained with Vectashield mounting media with DAPI (Vector Laboratories, Burlingame, CA). Cells were grown in 8-well chamber slides (Millipore Co., Bedford, MA) to ~50% confluence. The cells were then washed with PBS, fixed with 4% paraformaldehyde and methanol, and permeabilized with 1% Triton X-100. After blocking with 5% goat serum, cells were stained as described above. Images were captured on a Zeiss LSM700 laser scanning confocal microscope (Zeiss, New York, NY).

Tumor Digestion and Flow Sorting

All glioma tumors used for flow-sorting experiments were harvested from NSG mice when they reached a size of ~400 mm3. Tumor tissue was chopped finely with razor blades and the resultant cell suspension was passed through a 40μm filter insert. Cells were washed with dPBS and resuspended in DMEM containing 10% FBS. The percentage of human CD133 cells was determined using antibodies labeled with either fluoresceinisothiocyanate (FITC) or phycoerythrin (PE). The anti-CD133 antibody conjugated to PE (clone: AC133/2 (293C3)) was obtained from (Miltenyi-Biotec, Bergisch Gladbach, Germany). Clone AC133/2 (293C3) recognizes epitope 2 and does not overlap with clone AC133 used in the selection. Flow cytometric analysis was performed using a LSR flow cytometer (BD Biosciences, San Jose, CA). Briefly, 10x106 cells were incubated with antibodies, and data acquisition and analysis was performed on a three-laser LSR (Becton-Dickinson) flow cytometer using CellQuest software. Cells negative for CD133 were placed in monolayer culture conditions, while CD133+ cells were grown as adherent CSCs.

Cell Culture

The human GBM6 patient-derived xenograft (PDX) of adult GBM tissue was provided by Dr. C. David James, (Department of Neurological Surgery, University of California, San Francisco) and continuously maintained as subcutaneous xenografts in NSG mice. Monolayer and CSC cultures of GBM6 cells were derived from freshly harvested tumor tissue. Short-term GBM6 xenolines were grown as monolayer cultures in

DMEM (Cellgro, Hemdon, VA) supplemented with 10% heat-inactivated fetal bovine serum (Hyclone Labs, Thermo Scientific, Rockford, IL), 100 units/mL penicillin and 100 µg/mL streptomycin. Adherent and spheroid glioma CSCs were maintained in NeuroBasal-A medium (Invitrogen, Carlsbad, CA) containing 2% B27 supplement, 2 mM L-glutamine, 100 units/mL penicillin, 100 µg/mL streptomycin, EGF (20 ng/ml), and basic FGF (40 ng/ml). For isolation of adherent CSCs, culture flasks were coated with 100 µg/mL poly D-lysine (Sigma-Aldrich, St. Louis, MO) for 1 hr followed by coating with 10 µg/mL laminin (Gibco, Life Technologies Inc., Grand Island NY) for 2 hrs prior to use. Adherent CSCs were plated at 1 X 10^5 cells per 75 cm^2 flask, grown to confluence, dissociated with HyQTase (Thermo Scientific, Scientific, Rockford, IL), and split at a 1:3 ratio. For isolation of spheroid CSCs, glioma cells were dissociated with HyQtase and plated at ~ 1 x 10^5 cells/mL in ultra-low adhesion flasks.

Chromatin Immunoprecipitation

Chromatin Immunoprecipitation (ChIP) was carried out using the ChIP-IT™ Express Enzymatic kit (Active Motif, Carlsbad, CA) according to the manufacturer's instructions. In brief, chromatin from cells was cross-linked with 1% formaldehyde (10 min at 22ºC), sheared to an average size of ~200 bp with a Biorupter sonicator (Diagenode, Sparta, NJ), and then immunoprecipitated with antibodies against STAT3 (Santa Cruz Biotechnology, Santa Cruz, CA). ChIP-PCR primers were designed to amplify a proximal promoter region containing putative STAT3 (-1348 to -1369) binding sites in the ANGPTL4 promoter. The primers used were: for STAT3 site, 5'-CATTAAAGACCCTGGCGGTA-3' (forward), 5'-GGATCACAGTCGTGTGAGGA-3' (reverse).

TCGA Data Analysis

To examine the relationship between STAT3 and ANGPTL4 expression in human GBM brain tissue, we queried the TCGA data portal for all low-grade glioma and GBM samples with gene expression (BI_HT_HG-U113A Array Data Set) data available as well as accompanying clinical data. The data set was filtered for samples having expression data for STAT3, ANGPTL4 and clinical data, yielding a final set of 265 individual low-grade glioma samples and 328 independent GBM patient samples. The samples were then grouped according to glioma grade and Karnofsky Performance Status, which takes into account the patient performance in general daily life activities. The Karnofsky score runs from 100 to 0, where 100 is defined as "perfect" health and 0 as death. Statistical analysis was performed using Graphpad Prism.

Apoptosis Assay

The induction of apoptosis was monitored by flow cytometry (Accuri Model 6C) using the Annexin V-FITC apoptosis detection kit (BD Pharmingen, San Diego, CA), according to the manufacturer's instructions.

WP1066 and Sorafenib Studies *in vivo*

$1x10^6$ GBM6 cells grown as monolayers or adherent CSCs were subcutaneously injected in to the flanks of NSG mice, and animals were monitored for tumor growth twice a week by caliper measurement. Upon induction of detectable tumors as determined by caliper measurement, WP1066 (40 mg/kg) and Sorafenib (15 mg/kg) in DMSO/Polyethylene gycol were delivered daily by intra-tumoral injection. The effect of these drugs on tumor progression was measured by caliper measurement and Xenogen live animal imaging.

Statistical Analysis

At least three independent experiments were performed in duplicate, and data are presented as means ± sd. ANOVA and post-hoc least significant difference analysis or Student *t* tests were performed. p values < 0.05 (*) were considered statistically significant.

Results

Constitutive Activation of STAT3 and ANGPTL4 in the CSC Subpopulation of Mesenchymal GBM Tumors

Aberrant activation of STAT3 and ANGPTL4 has been found to be associated with tumor progression in blood malignancies and a variety of human solid tumors such as breast, prostate, renal, and head and neck cancers [166-168]. Our previous studies reveal the upregulation of these genes within Mesenchymal GBM xenografts. To characterize the combined roles of STAT3 and ANGPTL4 in the CSC subpopulation of Mesenchymal GBM tumors, we examined the intracellular localization of STAT3 and ANGPTL4 by confocal microscopy. Mesenchymal GBM6 tumors derived from cells grown as adherent glioma CSCs were sectioned and immunostained with antibodies specific for STAT3 and ANGPTL4; cells were counterstained with DAPI to define nuclear localization of proteins. As shown in **Figure 4-1A**, STAT3 and ANGPTL4 are present in the cytoplasm and nucleus of various cells throughout Mesenchymal GBM tissue, but their colocalization is only evident in the nucleus of a few cells. To determine if the interaction of STAT3 and ANGPTL4 is specific to the CSC subpopulation of GBM tumors, single cells were isolated from Mesenchymal xenografts and flow sorted by the

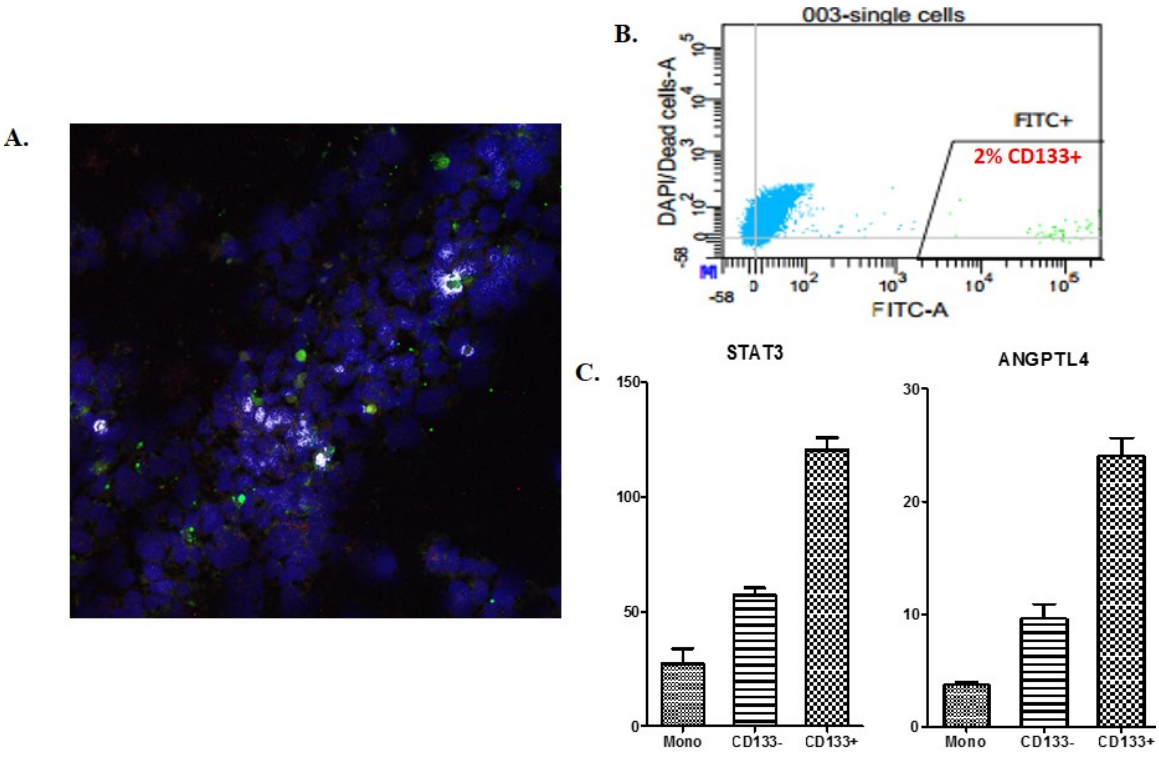

Figure 4-1. Enhanced ANGPTL4 expression correlates with STAT3 activation in the GBM CD133+ CSC subpopulation.

A. Tumor tissue derived from GBM6 adherent CSCs was sectioned and stained with antibodies as indicated and analyzed by confocal microscopy. STAT3 is represented in green, ANGPTL4 is represented in red, and nuclear DAPI staining in blue. White pixels represent the colocalization of STAT3 and ANGPTl4 proteins within the tissue. **B**. Cells were isolated from GBM6 xenografts and sorted for CD133+ and CD133- populations. **C.** RNA was extracted from cells and STAT3 and ANGPTL4 gene expression levels were measured by qPCR and normalized to actin. (n=3).

stem cell marker CD133. **Figure 4-1B** displays the sorted CD133+ and CD133- cell populations and reveals that 2% of cells within the Mesenchymal GBM xenografts are CD133+ stem cells. Since studies have shown that CD133 does not consistently distinguish tumorigenic and non-tumorigenic glioma cells [161, 162], CD133- cells were placed in monolayer and adherent CSC culture conditions while CD133+ cells were grown only as adherent CSCs. RNA was then prepared from bulk tumor cells, CD133- stem cells and CD133+ stem cells and analyzed by qPCR for STAT3 and ANGPTL4 expression. As shown in **Figure 4-1C**, both STAT3 and ANGPTL4 are detectable in glioma cells regardless of whether they are bulk tumor cells or CSCs. However, activation of STAT3 and ANGPTL4 is markedly greater in CD133+ CSCs, suggesting that the proteins are constitutively activated in glioma cells but exhibit increased activity in the CD133+ CSC subpopulation of Mesenchymal GBM.

To further characterize the activation of STAT3 and ANGPTL4 in glioma CSCs that promote the formation of Mesenchymal GBM tumors, GBM6 cells were grown *in vitro* as monolayers or adherent CSCs on glass slides and immunostained with antibodies for STAT3 and ANGPTL4 as above. As shown in **Figure 4-2A**, although STAT3 and p65 are present in the cytoplasm and nucleus of both GBM6 bulk tumor cells and adherent CSCs, their colocalization is only evident in the nucleus of adherent CSCs. Since both STAT3 and ANGPTL4 may play important roles in CSC maintenance, we next examined whether they interact. Examination of putative transcription binding sites revealed three STAT3 binding sites proximal to the ANGPTL4 promoter. As shown in **Figure 4-2B**, specific primers were designed and synthesized for each of these potential binding sites in the ANGPTL4 promoter, and STAT3 binding was detected by ChIP analysis for site-II. In brief, protein-DNA complexes were crosslinked with formaldehyde, chromatin was sheared to average of 200bp and immunoprecipitated with anti-STAT3, crosslinking reversed and the resulting DNA sequences detected by PCR and qPCR. As shown in **Figure 4-2C**, significantly increased binding of STAT3 to the ANGPTL4 promoter was observed in GBM adherent CSCs as compared to bulk tumor cells. Also, the STAT3 inhibitor WP1066 is shown to decrease STAT3 binding to ANGPTL4 in CSCs. Taken together, these results show that STAT3 regulates ANGPTL4 expression in adherent CSCs by directly binding to its promoter, and this interaction can be blocked with targeted STAT3 inhibitors.

Additionally to confirm that ANGPTL4 is indeed important to GBM CSCs, other GBM cell lines were analyzed for ANGPTL4 expression as well as members of the VEGF signaling cascade, a known activator of ANGPTL4. qPCR was performed on RNA extracted from GBM6, U87, SJG2 and MT330 monolayers and adherent CSCs. As shown in **Figure 4-2D**, expression of ANGPTL4, VEGFR-1 and VEGFR-2 are significantly upregulated in 3 out of the 4 adherent CSC cultures when compared to bulk monolayers cultures of glioma cells, suggesting that ANGPTL4 alongside STAT3 could play an important role in stem cell maintenance and subsequent GBM tumor initiation and progression. While constitutively activated STAT3 has previously been found in glioma CSCs and required for their proliferation and survival, the role of ANGPTL4 in GBM stem cells is unknown and represents a highly novel finding. The upregulation of

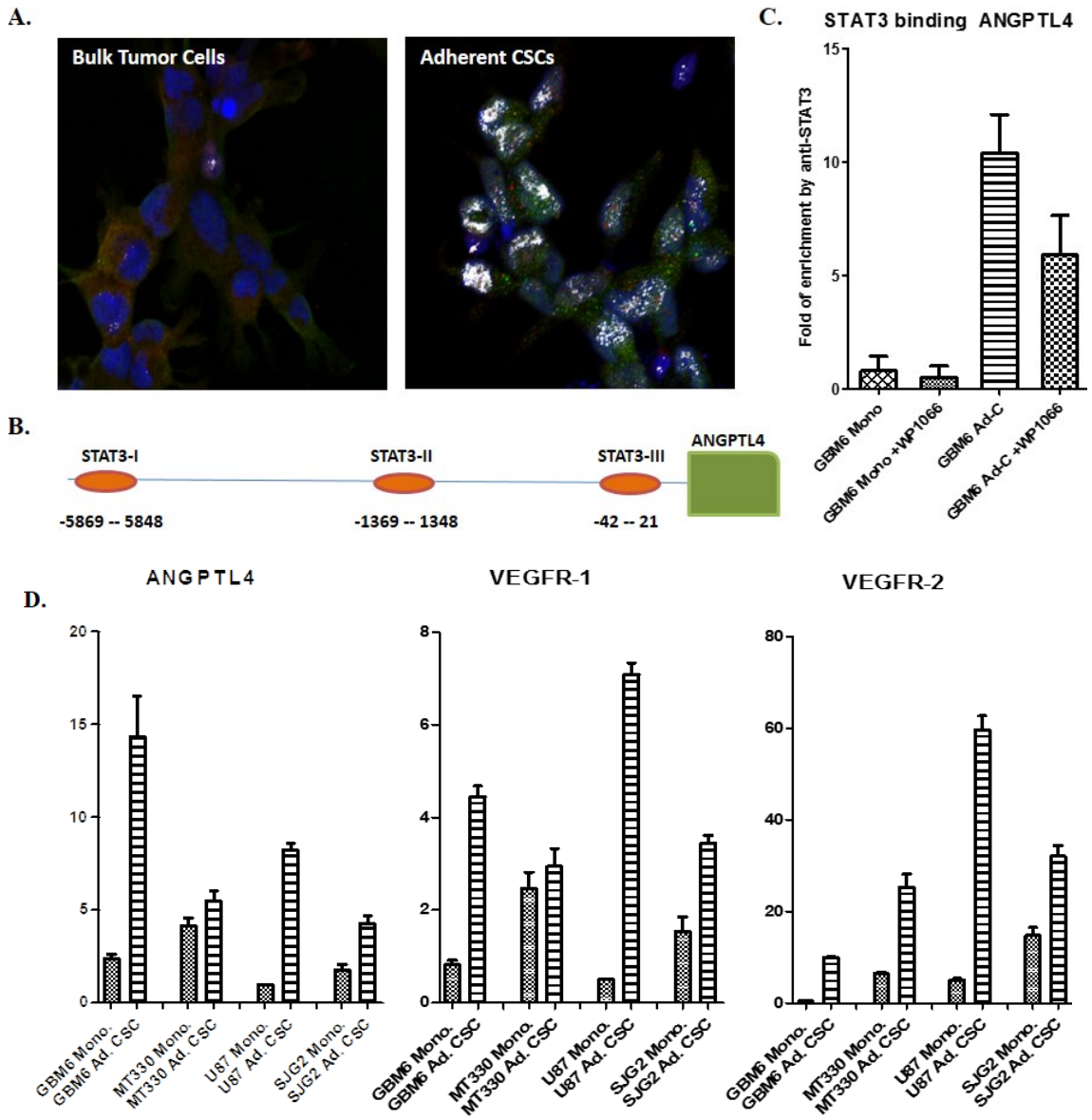

Figure 4-2. Crosstalk between STAT3 and ANGPTL4 in CSCs.

A. GBM6 bulk tumor cells (Mono) and adherent CSC cultures were fixed and immunostained with antibodies as indicated and analyzed by confocal microscopy; STAT3 is represented in green, ANTPL4 is represented in red and nuclear DAPI staining in blue. White pixels represent the colocalization of STAT3 and ANGPTL4 proteins within the cells. **B**. STAT3 binding sites on ANGPTL4 promoter; site 2 was used for the assay. **C**. ChIP analyses of STAT3 to Notch1 promoter; the ChIP-enriched DNA levels analyzed by qPCR were normalized to input DNA, followed by subtraction of non-specific binding determined by control IgG. **D**. Gene expression of the pro-angiogenic genes ANGPTL4, VEGFR-1 and VEGFR-2 was measured by qPCR in GBM6, MT330, U87 and SJG2 bulk tumor cells (mono) and adherent CSCs and normalized to actin expression (n=3).

ANGPTL4 in the tumor initiating subpopulation of Mesenchymal GBM is a novel finding, and its biological relationship with STAT3 is of great therapeutic interest.

The Relationship between STAT3 and ANGPTL4 Expression to Glioma Grade and Patient Performance Status in Clinical Specimens

To examine STAT3 and ANGPTL4 expression in human glioma, we analyzed information in the TCGA database for the correlation between glioma grade and the expression of STAT3 and ANGPTL4. Gene expression of STAT3 and ANGPTL4 was examined in 10 normal brain samples, 265 individual low grade glioma patients and 328 individual GBM patients for comparison. As shown in **Figure 4-3A**, both STAT3 and ANGPTL4 levels are significantly increased in GBM samples when compared to normal tissue and even lower grade gliomas. We also analyzed GBM specimens in the TCGA database to investigate the relationship between patient performance status and STAT3 and ANGPTL4 levels. The 328 GBM patients were placed into groups according to their Karnofsky performance status, and their gene expression was compared to the 10 normal brain samples. As shown in **Figure 4-3B**, the levels of ANGPTL4 are similar among groups, while a significant increase in STAT3 expression was found in lower performing patients when compared to those with good performance.

We then independently determined whether the expression of STAT3 and ANGPTL4 correlates with patient survival. Brain biopsy specimens from 24 GBM patients that represented long-term and short-term survival after diagnosis were obtained from the UTHSC tissue core, and RNA was isolated from FFPE tissue blocks to determine expression of STAT3 and ANGPTL4. As shown in **Figure 4-3C**, although there was significant patient-to-patient variability as expected, there was a direct relationship between STAT3 and ANGPTL4 expression and patient survival. A statistically significant increase in STAT3 and ANGPTL4 gene expression was observed in GBM patients that survived less than one year when compared to long-term survivors. Interestingly, several patients exhibited elevated expression of both STAT3 and ANGPTL4, while others were shown to have low levels of both genes. The direct correlation of the expression of these genes in GBM is shown in **Figure 4-3D**. We next looked at the potential of STAT3 and ANGPTL4 in predicting survival of GBM patients. In **Figure 4-3E** we show that high levels of STAT3 significantly correlate with short-term survival, while high ANGPTL4 levels appear to correlate with poor patient survival but this was found to be not statistically significant.

The Effects of Specific STAT3 and VEGF Inhibitors on GBM CSCs

We next sought to determine the effect of STAT3 and VEGF inhibitors on the intracellular localization of STAT3 and ANGPTL4 in GBM stem cells. Adherent GBM6 CSCs were plated on 8-well slides and treated for 2 hours with a pharmacological inhibitor of STAT3 (25 μM WP1066) and/or VEGF inhibitor (5 μM Sorafenib), and then immunostained for STAT3 and ANGPTL4. As shown in **Figure 4-4A** and previously in

Figure 4-3. Upregulation of STAT3 and ANGPTL4 expression in human GBM samples.

A. Gene expression of STAT3 and ANGPTL4 was obtained from the TCGA database to compare normal brain tissue (n=10), low grade glioma samples (n=265) and GBM samples (n=328). **B**. Gene expression of STAT3 and ANGPTL4 was obtained from the TCGA database for normal brain tissue (n=10) and GBM samples (n=328) to compere levels based on patient performance. **C**. Human GBM tissue samples were obtained from UTHSC Pathology and RNA was extracted; gene expression of STAT3 and ANGPTL4 was measured by qPCR and normalized to actin expression (n=12) to study correlation to patient survival. **D**. Correlation of STAT3 and ANGPTL4 expression within human GBM samples. **E**. Survival analysis of GBM patients expressing high or low STAT3 and ANGPTL4.

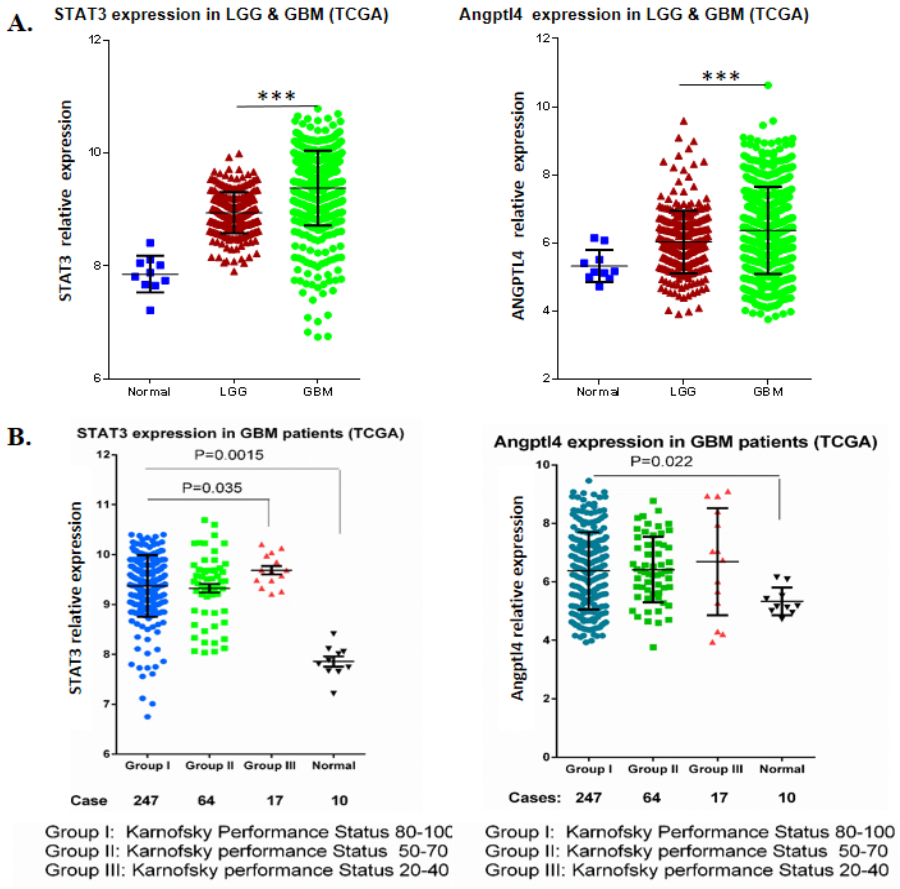
A.
STAT3 expression in LGG & GBM (TCGA)
STAT3 relative expression
***
Normal
LGG
GBM
Angptl4 expression in LGG & GBM (TCGA)
ANGPTL4 relative expression
***
Normal
LGG
GBM
B.
STAT3 expression in GBM patients (TCGA)
P=0.0015
P=0.035
STAT3 relative expression
Group I
Group II
Group III
Normal
Case 247 64 17 10
Angptl4 expression in GBM patients (TCGA)
P=0.022
Angptl4 relative expression
Group I
Group II
Group III
Normal
Cases: 247 64 17 10
Group I: Karnofsky Performance Status 80-100
Group II: Karnofsky performance Status 50-70
Group III: Karnofsky performance Status 20-40
Group I: Karnofsky Performance Status 80-100
Group II: Karnofsky performance Status 50-70
Group III: Karnofsky performance Status 20-40

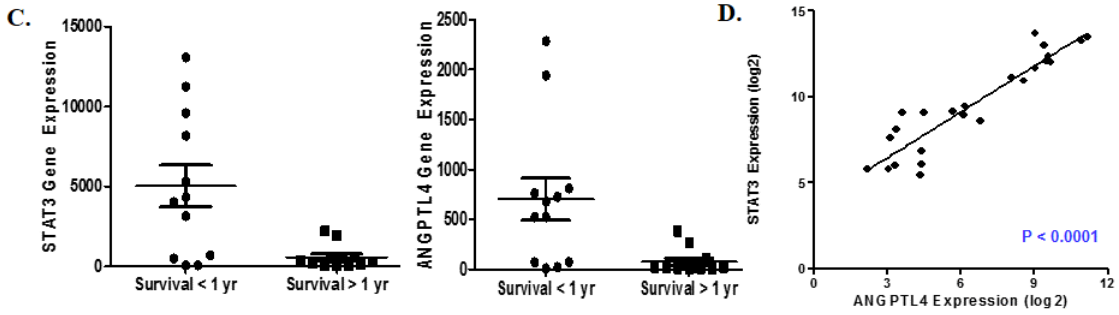
C.
STAT3 Gene Expression
Survival < 1 yr
Survival > 1 yr
ANGPTL4 Gene Expression
Survival < 1 yr
Survival > 1 yr
D.
STAT3 Expression (log2)
P < 0.0001
ANGPTL4 Expression (log 2)

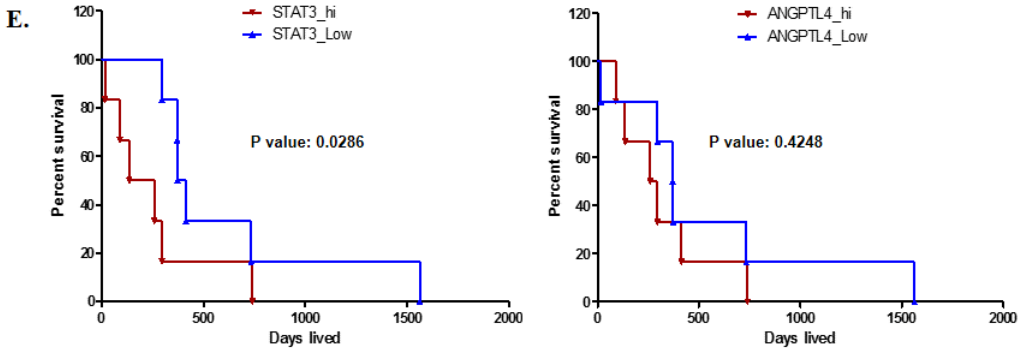
E.
STAT3_hi
STAT3_Low
Percent survival
P value: 0.0286
Days lived
ANGPTL4_hi
ANGPTL4_Low
Percent survival
P value: 0.4248
Days lived

Figure 4-4. Effects of selective STAT3 and VEGF inhibitors on adherent glioma CSCs.

A. Cells were treated with vehicle, WP1066 (50 μM) and/or Sorafenib (5 μM) and colocalization of STAT3 and ANGPTL4 was determined by immunostaining; Red-Angptl4, Green-Stat3, Blue-DAPI, White-Colocalization. **B**. GBM6 Ad-CSCs were treated with STAT3 (50uM WP1066) or VEGF (10uM Sorafenib) inhibitors for 6 hrs. RNA was prepared and the gene expression of ANGPTL4, VEGF-R1, VEGF-R2, CD133, SOX2 and Nestin was quantified by qPCR and normalized to actin expression (n=3). **C**. Proliferation of GBM6 monolayer and adherent CSC cultures was measured by MTT assay after treatment (72 hr) with WP1066 or Sorafenib at the indicated concentrations. **D**. Apoptosis of GBM6 monolayer and adherent CSC cultures was measured by AnnexinV staining after 48 hrs treatment with WP1066 (10uM) and/or Sorafenib (5uM).

A.

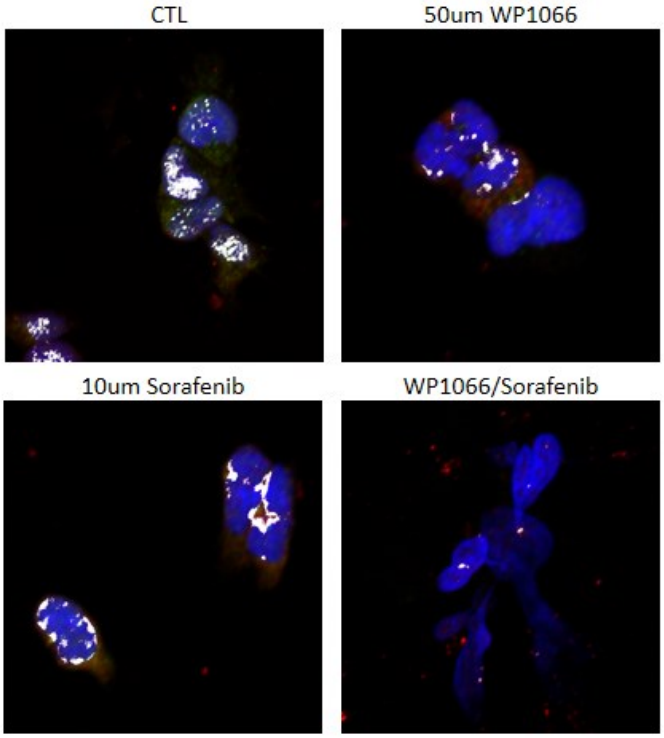
CTL
50um WP1066
10um Sorafenib
WP1066/Sorafenib

B.

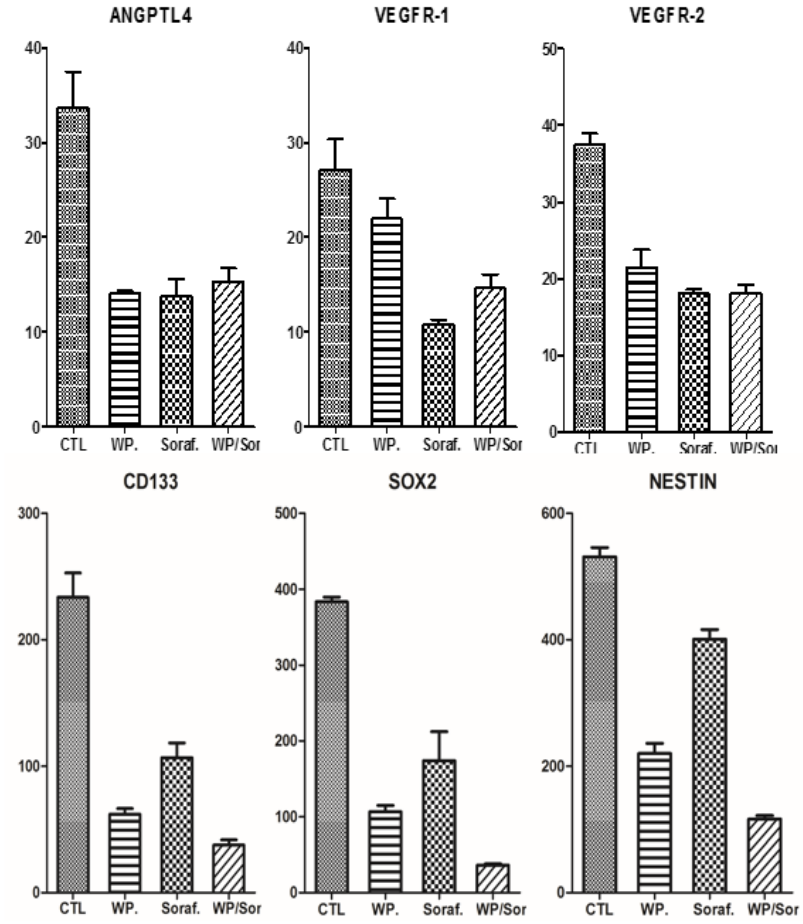
ANGPTL4
VEGFR-1
VEGFR-2
CD133
SOX2
NESTIN
CTL
WP.
Soraf.
WP/Sor

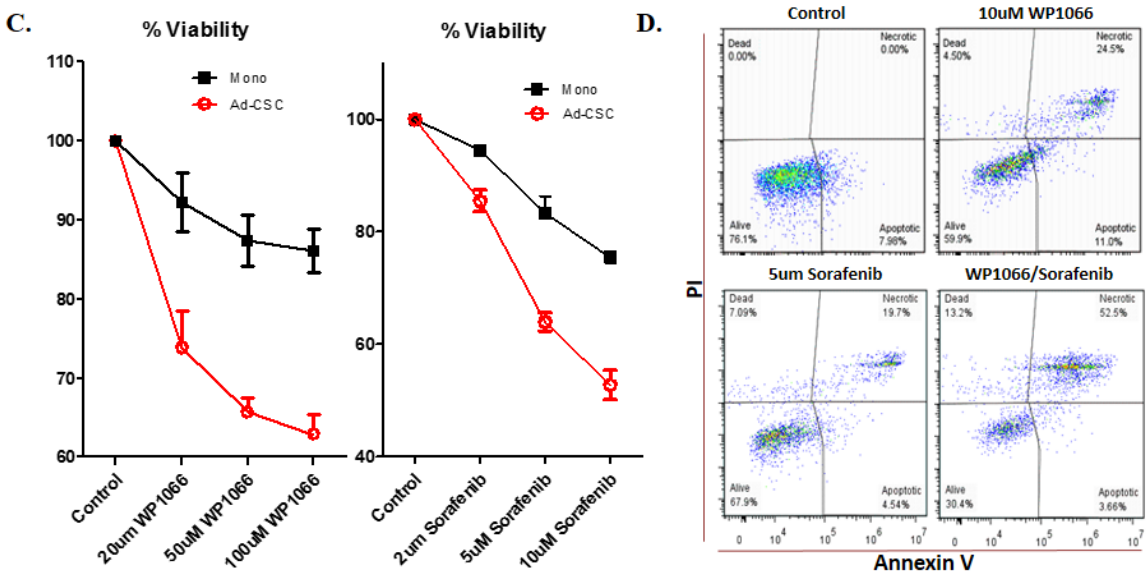

Figure 4-4. Continued.

Figure 4-2A by confocal microscopy, STAT3 and ANGPTL4 are colocalized in the nucleus of adherent CSCs. In contrast, treatment with WP1066 or Sorafenib markedly inhibits the colocalization of STAT3 and ANGPTL4 within the nucleus of GBM6 glioma CSCs. It is of interest that colocalization of STAT3 and ANPTL4 appears to be specifically at the nuclear membrane of cells. Furthermore, the combined treatment with these inhibitors prevents expression of STAT3 and ANPTL4, and results in a change in cellular morphology, such as the cell shrinkage and lifting, that is indicative of cells undergoing apoptosis.

To characterize the functional significance of blocking the STAT3 and ANGPTL4 pathways in CSCs, we examined the effects of WP1066 and Sorafenib treatment on the expression of genes involved in angiogenesis as well as in stem cell maintenance. **Figure 4-4B** reveals the significantly decreased expression of pro-angiogenic genes (ANGPTL4, VEGFR-1 and VEGFR-2) and stem cell markers (CD133, SOX2 and Nestin) upon STAT3 and VEGF inhibition. Both WP1066 and Sorafenib treatment had similar inhibitory effects on pro-angiogenic gene expression, but in combination had no greater effects than each drug alone. This result suggests that inhibition of STAT3-regulated ANGPTL4 is comparable to VEGF inhibition in GBM. In contrast, combined treatment with WP1066 and Sorafenib was found to significantly decrease the expression of genes associated with a stem cell signature in GBM6 cells.

We then examined the effects of WP1066 and Sorafenib on the cell viability in glioma monolayer and adherent CSC cultures. Varying concentrations of both inhibitors were tested by MTT assay and were found to induce a dose-dependent reduction in cell number in both glioma monolayers and adherent CSCs, but there was a markedly enhanced effect on adherent CSCs (**Figure 4-4C**). We then determined the effect of these inhibitors on the induction of apoptosis in adherent CSCs as determined by flow cytometry of Annexin V stained cells. In brief, cells in 6-well plates were treated with 10 μM WP1066, 5 μM Sorafenib or a combination of these inhibitors together for 48 hrs. As shown in **Figure 4-4D**, although both inhibitors induced detectable apoptosis in glioma adherent CSCs, there was a greater effect when these inhibitors were used in combination on adherent CSCs.

Effect of Treatment with STAT3 and VEGF Inhibitors on Mesenchymal GBM Tumor Progression

Since both STAT3 and ANGPTL4 have been associated with various steps of tumor progression, we then examined the effects of STAT3 and ANGPTL4 inhibition on Mesenchymal gliomagenesis. In brief, NSG mice were subcutaneously injected with GBM6 cells maintained as monolayer or adherent CSC cultures, and tumor volume was determined at weekly intervals by caliper measurement. At the first sign of tumor formation at day 20, intraperitoneal drug delivery was done every other day for two weeks using WP1066 (40 mg/kg) and Sorafenib (15 mg/kg). **Figure 4-5A** displays the effect of both drugs on tumor progression measured by xenogen imaging. The formation of GBM6 tumors was markedly suppressed by inhibition of STAT3 and ANGPTL4, with

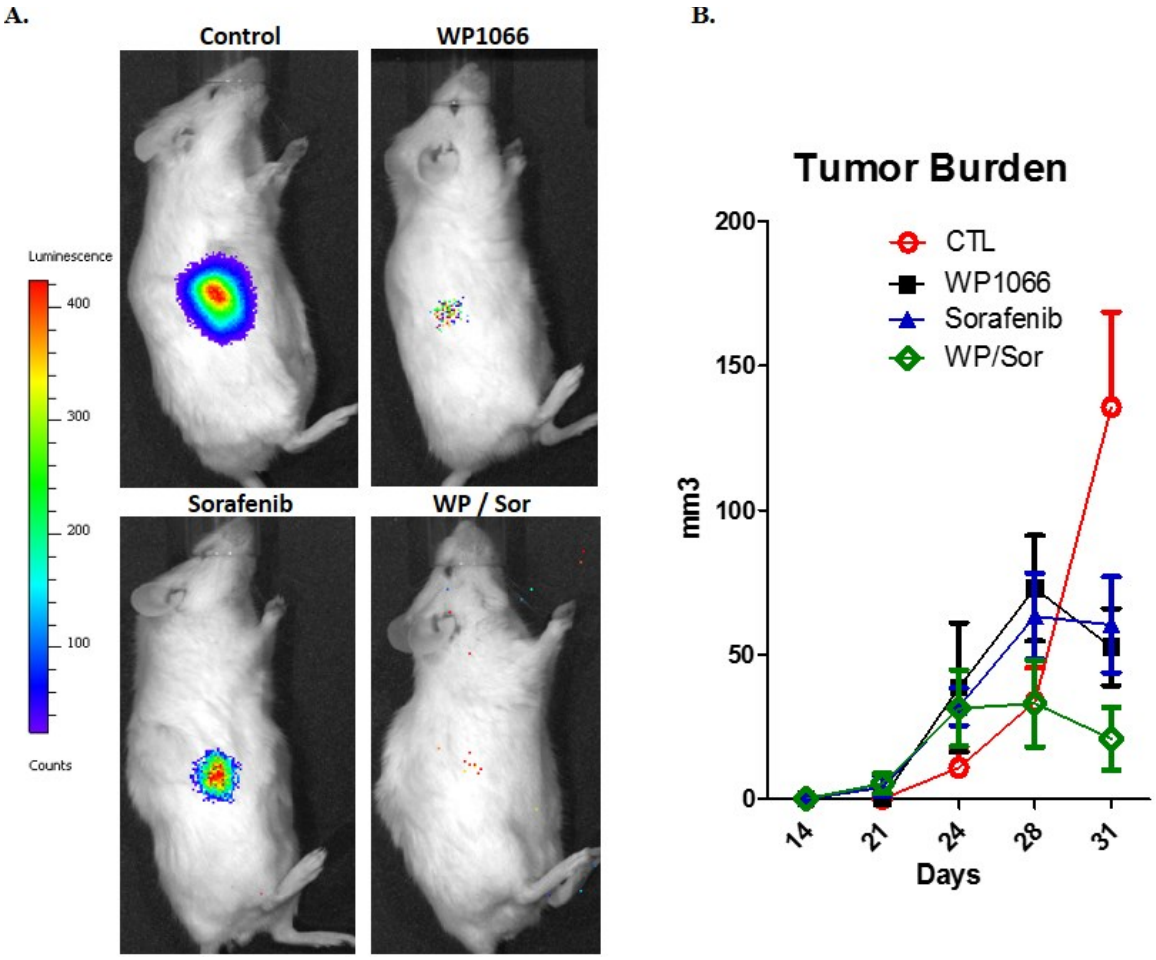

Figure 4-5 Efficacy of STAT3 and ANGPTL4 inhibitors *in vivo.*

Mice were subcutaneously injected with $1x10^6$ luciferase-tagged GBM6 cells grown as monolayers or adherent CSCs and upon first detection of tumor, mice were treated with WP1066 (40mg/kg), Sorafenib (20mg/kg) or in combination every other day beginning on day 21 after initial injection. **A.** Effect of drug treatment was measured by bioluminescence twice a week (representive images shown for Day 31) and **B.** tumor volume was measured twice a week by caliper measurement. (n=5 per condition)

the combined treatment of WP1066 and Sorafenib completely ablating glioma tumorigenesis. As shown in **Figure 4-5B**, tumor progression was dramatically decreased following treatment with WP1066 and Sorafenib alone, and the drug combination led to enhanced tumor regression. These results indicate the significance of elevated STAT3 and ANGPTL4 in GBM progression and the potential of selective STAT3 and ANGPTL4 inhibitors in targeting the CSC subpopulation of Mesenchymal GBM.

Discussion

Mesenchymal GBM is the most aggressive and deadly form of glioma, accounting for around 30% of GBM cases. Despite improved molecular characterization, aggressive surgery, radiation and chemotherapy, the median survival of patients remains only around 1 year. The ineffectiveness of current therapies may reflect the lack of potency on the CSC subpopulation, which remains viable and commonly leads to tumor regeneration. Although CSCs represent only a small population of cells within a tumor, their high tumor-initiating capacity and therapeutic resistance may play a critical role in driving GBM tumorigenesis. Therefore, it is imperative to identify biomarkers associated with CSCs in order to devise strategies to selectively target them and subsequently block GBM progression. In the present study, we describe a novel relationship between STAT3 and ANGPTL4 within the stem-like cell population of Mesenchymal GBM that drives tumor initiation and progression.

We previously performed microarray analysis on RNA prepared from GBM xenografts derived from bulk tumor cells and adherent CSCs and found elevated levels of both STAT3 and ANGPTL4 in aggressive Mesenchymal tumors formed from CSCs. These results are consistent with previous findings in Mesenchymal GBM, in which STAT3 was suggested to be a major regulator of mesenchymal transformation [56]. A robust angiogenesis gene signature, including ANGPTL4, has also been shown to correlate with the Mesenchymal subtype of GBM [125]. ANGPTL4 is a secreted, matricellular protein that provides signals to support many steps of tumor progression, especially angiogenesis [109, 169]. While ANGPTL4 is commonly activated by VEGF or HIF-1, studies have identified ANGPTL4 as being induced by constitutive activation of STAT3 [114]. This led us to evaluate the relationship of these proteins within Mesenchymal GBM CSCs. Constitutive activation of STAT3 and ANGPTL4 and their direct interaction was evidenced by confocal microscopy in certain cells throughout GBM xenografts, leading us to believe these cells represented the CSC subpopulation of the tumor. Upon isolation of CD133+ cells from GBM xenografts, STAT3 and ANGPTL4 were shown to be dramatically activated in CSCs when compared to the CD133- population. Furthermore, the colocalization of STAT3 and ANGPTL4 was also observed *in vitro* in glioma adherent CSCs but not bulk tumor cells, indicating the importance of STAT3 and ANGPTL4 to the CSC subpopulation of GBM. These results are supported by recent studies, which have identified the requirement of STAT3 for CSC proliferation and survival and the involvement of ANGPTL4 in maintenance of stem cell niches [80]. In addition, we identified direct crosstalk between STAT3 and ANGPTL4 within GBM CSCs by demonstrating the direct binding of STAT3 to the ANGPTL4 promoter. These

results are consistent with previous findings in breast and renal cell carcinoma, in which STAT3 was shown to activate ANGPTL4 by binding its promoter and interacting with HIF-1 and other coactivators [115].

STAT3 has been shown to activate ANGPTL4 directly or indirectly through transcriptional regulation of VEGF and HIF-1 in various human cancers, so we next examined the relationship of STAT3 and ANGPTL4 expression in GBM to patient prognosis and survival based on information in the TCGA database [27, 28]. High STAT3 and ANGPTL4 levels were observed in GBM samples when compared to normal brain and lower grade gliomas, and enhanced expression also correlated to short-term survival. Consistent with our findings, STAT3 is reported to be among the most frequently activated oncogenic proteins in multiple solid tumor types. More specifically, a large body of data has demonstrated activation of the typically quiescent STAT3 pathway as being crucial to tumorigenesis and a predictor of poor prognosis in many malignancies including gliomas [55]. ANGPTL4 has been identified as a prominent gene in *in vivo* hypoxia gene sets that predict poor outcome in multiple tumor types. In a study of several epithelial tumor types, ANGPTL4 levels increased as tumors progress from local to metastatic disease [107, 108]. In our studies, we found a strong relationship between poor patient performance and survival and enhanced expression of STAT3 and ANGPTL4 in GBM patients. Additionally, our studies revealed that several individual patients exhibited elevated expression of both STAT3 and ANGPTL4, while others were shown to have low levels of both genes. A direct correlation in expression levels of STAT3 and ANGPTL4 was found within human GBM samples. These results indicate that the co-expression of STAT3 and ANGPTL4 may have diagnostic and prognostic utility in GBM. Moreover, since ANGPTL4 is a secreted protein and detectable by ELISA, in future studies ANGPTL4 levels could be measured for a non-invasive test of tumor response and diagnosis.

Targeted small molecule inhibitors of STAT3 have previously been shown to inhibit CSC proliferation and tumorsphere formation as well as sensitize GBM stem cells to TMZ [81]. We examined the effects of the STAT3 inhibitor WP1066 and the indirect ANGPTL4 inhibitor Sorafenib, which targets VEGF signaling, on glioma CSCs and Mesenchymal GBM progression. WP1066 is a JAK-2 kinase inhibitor that blocks the tyrosine phosphorylation of STAT3, which is the transcriptionally active form of STAT3. It has been shown to have pro-apoptotic and anti-proliferative activity in a variety of tumor types, including glioma, and most importantly shown to cross the blood brain barrier [143, 170]. Sorafenib is a multitargeted tyrosine kinase inhibitor with anti-angiogenic properties that works by inhibiting VEGFR activation. It has proven efficacy for treatment of various cancers and is currently in clinical trials for GBM [171, 172]. In our study, both drugs blocked the interaction of STAT3 and ANGPTL4 in GBM stem cells and lead to a decrease in expression of pro-angiogenic genes as well as stem cell marker genes, which suggest an important combined role of STAT3 and ANGPTL4 in Mesenchymal GBM stem cell maintenance. In addition, combined treatment with WP1066 and Sorafenib resulted in an induction of apoptosis in GBM CSCs. We also studied the sensitivity of Mesenchymal GBM xenografts to these targeted drugs and found that both WP1066 and Sorafenib decreased cancer progression individually, while

combined treatment lead to complete tumor regression. The drugs have not been used in combination previously, but our individual results are similar to previous studies done with these inhibitors. WP1066 has been shown to significantly inhibit growth of malignant glioma xenografts by blocking STAT3 activation and subsequent pro-proliferative genes [170]. Interestingly, studies show that Sorafenib induced growth arrest and apoptosis of GBM cells by blocking VEGF and STAT3 signaling [173]. Taken together, we have identified a significant relationship between STAT3 and ANGPTL4 in GBM stem cells and their therapeutic value as biomarkers in targeting the CSC subpopulation of Mesenchymal GBM.

Summary

In conclusion, we characterized the molecular properties of Mesenchymal GBM xenografts derived from cancer stem-like cells and identified biomarkers associated with the CSC subpopulation of GBM. CD133+ cells isolated from tumor tissue expressed elevated levels of both STAT3 and ANGPTL4, and these proteins were found to colocalize within GBM stem cells. Aberrant STAT3 and ANGPTL4 expression was also found to correlate to short-term survival of human GBM patients, and a link in expression levels was observed between the genes in individual patient samples. The deregulated expression of these genes in glioma CSCs was sensitive to targeted kinase inhibitors, WP1066 and Sorafenib. Targeted therapy against STAT3 and ANGPTL4 was found to decrease stem cell marker expression within tumors and lead to tumor regression. The novel relationship between STAT3 and ANGPTL4 in Mesenchymal GBM and their therapeutic value as biomarkers in targeting the CSC subpopulation of GBM could be of utmost importance to an aggressive cancer that is ultimately untreatable.

CHAPTER 5. DISCUSSION

Constitutive Activation of STAT3, NF-κB and Notch Signaling in Glioma CSCs Promotes Tumorigenesis

Numerous studies support the idea that many types of malignancies, including glioblastoma, originate from a CSC population that is able to initiate and maintain tumors [8, 136]. Although CSCs only represent a small fraction of cells within a tumor, their high tumor-initiating capacity and therapeutic resistance drives tumorigenesis. Therefore, it is imperative to identify pathways associated with CSCs in order to devise strategies to selectively target them. In Chapter 2, we described a novel relationship between glioblastoma CSCs and the Notch pathway, which involves the constitutive activation of STAT3 and NF-κB signaling. Glioma CSCs were isolated and maintained *in vitro* using a previously described adherent culture system [77], and the biological properties were compared to traditional tumorsphere cultures of CSCs [132, 133]. GBM CSCs exhibited enhanced CD133, Sox2 and Nestin expression and were ~100 times more tumorigenic *in vivo* than monolayer cultured glioma cells. These findings are consistent with previous studies, in which 100-fold fewer CD133 positive cells of the murine GL261 glioma line were found to be sufficient to initiate tumors when injected intracranially into mice when compared to CD133 negative cells [139]. Taken together, these findings demonstrate that adherent glioma CSCs exhibit characteristics previously described for CSCs grown in suspension culture and thus provide a valuable model for studying glioma CSC behavior.

The STAT3 and NF-κB pathways have been linked to cancer, and they trigger critical target genes regulating cell proliferation and survival. Both pathways have been found to be constitutively active in a number of human cancers including glioma, but their role in the glioma CSC subpopulation is not well understood [140]. Aberrant nuclear expression of NF-κB has been found in a panel of GBM cell lines and constitutively high STAT3 activity has been observed in a number of glioma cell lines and correlated with poor prognosis [141, 142]. In this study, we identified that these pathways are dramatically activated in GBM stem cells, and that STAT3 and NF-κB proteins colocalize in the nuclei of glioma CSCs. Evidence of the functional significance of STAT3 and NF-κB activation in glioma CSCs was provided by the finding that some of their known target genes were overexpressed in adherent and tumorsphere CSCs relative to glioma monolayers. Since targeting these signaling pathways would be a novel approach in glioma treatment, we examined the effects of two STAT3 inhibitors, WP1066 and S3I-203, on GBM stem cells. The inhibitors blocked STAT3 tyrosine phosphorylation and led to the loss of nuclear colocalization of STAT3 and the p65 subunit of NF-κB. In addition, treatment with either STAT3 inhibitor resulted in a greater growth suppressive effect on glioma CSCs, suggesting that targeted therapy of these key pathways in glioma CSCs may be possible.

To further investigate potential biomarkers in glioma CSCs, microarray analysis revealed deregulation of the Notch signaling pathway. Notch is involved in cell fate decisions throughout brain development and in stem cell proliferation and maintenance,

and its role in glioma is firmly established [84]. We also defined molecular crosstalk between the STAT3, NF-κB and Notch signaling pathways in glioma CSCs. While STAT3 inhibitors reduced expression of Notch-related genes in GBM stem cells, they increased expression of the negative regulator of Notch, RBPJ. It has been previously reported that in the developing CNS there is crosstalk between Notch and STAT3 pathways, in which phosphorylation of STAT3 is mediated by the direct binding of several Hes family members (Notch effectors) to STAT3 [95]. Interestingly, activation of the Notch pathway led to serine phosphorylation of STAT3 in neural stem cells, but our studies revealed the constitutive activation of STAT3 in glioma CSCs as determined by its tyrosine phosphorylation lies upstream of the Notch pathway [134, 135]. In addition, Notch and NF-κB signaling pathways have been found to collaborate throughout normal brain development and regulate stem cell renewal and differentiation [94]. We hypothesize that the interactions of STAT3, NF-κB, and Notch signaling pathways that occur during normal brain development are deregulated in glioma CSCs. As shown in Chapter 2, there is crosstalk between these signaling pathways in the glioma CSC subpopulation that drives gliomagenesis. The constitutive activation of STAT3 and NF-κB signaling pathways, and the upregulation of the Notch pathway in glioma CSCs identifies novel therapeutic targets for the treatment of glioma. Future studies will be required to validate these findings *in vivo* and decipher the underlying molecular mechanisms.

Distinct CSC Populations Drive Tumor Heterogeneity and Subsequent GBM Subclassfication

Although GBM patients present uniform histological phenotypes, the molecular determinants of disease aggressiveness vary considerably between individual cases. Genomic profiling of GBM samples in the TCGA database has identified four subtypes, Classical, Neural, Proneural and Mesenchymal, which are thought to develop as a result of different CSC populations driving tumorigenesis [120]. Since few biomarkers show prognostic promise or predict therapeutic response, improved molecular understanding of the tumor-initiating cells that drive cancer heterogeneity will advance treatment strategies for the distinct molecular subclasses of GBM. In Chapter 3, we identified two distinct cancer stem-like cell populations that produce Classical or Mesenchymal GBM tumors but display identical histological features. Molecular characterization of GBM cells and their derived tumor tissue revealed a distinct difference in gene expression pattern between tumors derived from adherent CSC and tumorsphere cultures. Our findings support recent studies proposing that tumor heterogeneity is a result of CSCs that are able to self-renew and generate differentiated progeny that compose the bulk of the tumor. Initially, CD133 was proposed to be the robust marker of brain tumor stem cells, but recent studies have shown that CD133 does not consistently distinguish tumorigenic and non-tumorigenic glioma cells, suggesting that distinct CSC subpopulations exist to drive GBM tumorigenesis [161, 162].

To determine whether adherent CSCs and tumorspheres promote tumor heterogeneity corresponding to a specific subtype of GBM, we analyzed traditional

markers of the Classical, Neural, Proneural and Mesenchymal subtypes. Adherent CSC-derived tumors were found to promote a Mesenchymal GBM gene signature, while tumorspheres promoted the Classical GBM subtype like that of the bulk tumor cells. This is supported by previous findings, in which the genetic profile of tumorspheres was shown to closely resemble that of the tumor they were isolated from, and the CSCs also replicated the infiltrating growth patterns observed in primary tumors [174, 175]. To determine if this molecular heterogeneity is maintained in the conventional microenvironment of GBM, we performed intracranial injections of GBM6 cells. The tumor-initiating capacity and molecular heterogeneity of the GBM CSCs by orthotopic injection were found to closely resemble our previous findings by subcutaneous injection. The extensive heterogeneity at the cellular and molecular levels of GBM that are found in tumors produced by CSCs has great significance for the general outcome of the malignancy; it confounds our understanding of the disease and also contributes to tumor aggressiveness and poses obstacles to the design of effective therapies [163]. Therefore, establishing an adherent CSC culture method that exhibits a mesenchymal gene signature and promotes the initiation and progression of the aggressive Mesenchymal GBM subtype *in vivo*, provides a valuable model of the human disease for future studies.

All GBMs are distinguished pathologically from lower grade gliomas by the presence of necrosis and microvascular hyperplasia, but there is no distinction between molecular subtypes, which complicates prognosis and therapeutic strategies [164]. To study the pathology of the Classical and Mesenchymal GBM tumors derived from our different GBM6 cell cultures, each sample was stained for H&E analysis and the common GBM prognostic markers GFAP, S100, OLIG2, MAP2 and SYN. The Classical GBM tumors derived from bulk tumor cells and tumorspheres and the Mesenchymal tumors derived from adherent GBM stem cells were all diagnosed as High-Grade Glioma and displayed no differences in H&E staining or marker expression. These findings reveal the pathological likeness between the molecularly distinct Classical and Mesechymal xenografts derived from bulk tumor cells and adherent CSCs, respectively. It also demonstrates the importance of integrative histological and molecular classification of gliomas in establishing effective treatment regimens for GBM patients.

To identify novel genes specifically deregulated in Mesenchymal GBM tumors derived from adherent CSC cultures of GBM6 xenografts, we further analyzed our microarray data. The expression of STAT3 was shown be elevated in the more aggressive stem cell-derived tumors, which is consistent with our previous identification of STAT3 as a potential therapeutic target due to its constitutive activation in GBM stem cells [154]. STAT3 is a master regulator of genes involved in various steps of tumor progression, so we sought to identify pathways that STAT3 could potentially regulate within CSCs to promote gliomagenesis. IPA analysis revealed significant upregulation of several genes involved in angiogenesis, with ANGPTL4 being of great interest since our lab has observed elevated expression of ANGPTL4 in xenografts derived from CSCs in other cancer types [unpublished]. While previous reports suggest EGFR induces ANGPTL4 expression and promotes tumor angiogenesis in malignant gliomas, we found ANGPTL4 activation to be independent of EGFR upregulation in Mesenchymal GBM xenografts [165]. The important roles of STAT3 and ANGPTL4 in promoting GBM progression and

vascularization represent potential therapeutic targets in treating GBM and warrant further molecular characterization.

STAT3 and ANGPTL4 Interact and Function as Biomarkers of the CSC Subpopulation within GBM Tumors

Mesenchymal GBM is the most aggressive and deadly form of glioma, accounting for around 30% of GBM cases. The poor survival rate and ineffectiveness of current therapies may reflect the lack of drug potency on the CSC subpopulation. Therefore, it is imperative to identify biomarkers associated with CSCs in order to devise strategies to selectively target them and subsequently block GBM progression. In Chapter 4, we describe a novel relationship between STAT3 and ANGPTL4 within the stem cell population of Mesenchymal GBM that drives tumor initiation and progression. We previously performed microarray analysis and found elevated levels of both STAT3 and ANGPTL4 in aggressive Mesenchymal tumors formed from CSCs. These results are consistent with previous findings in Mesenchymal GBM, in which STAT3 was suggested to be a major regulator of mesenchymal transformation [56]. A robust angiogenesis gene signature, including ANGPTL4, has also been shown to correlate with the Mesenchymal subtype of GBM [125]. ANGPTL4 is a secreted, matricellular protein that provides signals to support many steps of tumor progression, especially angiogenesis [109, 169]. While ANGPTL4 is commonly activated by VEGF or HIF-1, studies have identified ANGPTL4 as being induced by constitutive activation of STAT3 [114]. This led us to evaluate the relationship of these proteins within Mesenchymal GBM CSCs. Constitutive activation and direct interaction of STAT3 and ANGPTL4 was found in cells throughout GBM xenografts, specifically in CD133+ CSCs when compared to the CD133- population. These results are supported by recent studies, which have identified the requirement of STAT3 for CSC proliferation and survival and the involvement of ANGPTL4 in maintenance of stem cell niches [80]. Additionally, previous findings in breast and renal cell carcinoma found that STAT3 activates ANGPTL4 by binding its promoter and interacting with HIF-1 and other coactivators [115].

STAT3 has been shown to activate ANGPTL4 directly or indirectly through transcriptional regulation of VEGF and HIF-1 in various human cancers, so we examined the relationship of STAT3 and ANGPTL4 expression in GBM to patient prognosis and survival in the TCGA database [27, 28]. High STAT3 and ANGPTL4 levels were observed in GBM samples when compared to normal brain and low-grade gliomas, and enhanced expression correlated to short-term survival. Consistent with our findings, STAT3 is reported to be among the most frequently activated oncogenic proteins in multiple solid tumor types. More specifically, a large body of data has demonstrated activation of the typically quiescent STAT3 pathway as being crucial to tumorigenesis and a predictor of poor prognosis in glioma [55]. ANGPTL4 has been identified as a prominent gene in *in vivo* hypoxia gene sets that predict poor outcome in multiple tumor types. In a study of several epithelial tumor types, ANGPTL4 levels increased as tumors progressed from local to metastatic disease [107, 108]. In our studies, we found a strong relationship between poor patient performance and survival and enhanced expression of

STAT3 and ANGPTL4 in GBM patients. Additionally, our studies revealed a direct correlation in expression levels of STAT3 and ANGPTL4 within human GBM samples. These results indicate that the co-expression of STAT3 and ANGPTL4 may have diagnostic and prognostic utility in GBM. Moreover, since ANGPTL4 is a secreted protein and detectable by ELISA, in future studies ANGPTL4 levels could be measured for a non-invasive test of tumor response and diagnosis.

Targeted small molecule inhibitors of STAT3 have previously been shown to inhibit CSC proliferation and tumorsphere formation as well as sensitize GBM stem cells to TMZ [81]. We examined the effects of the STAT3 inhibitor WP1066 and the indirect ANGPTL4 inhibitor Sorafenib, which targets VEGF signaling, on glioma CSCs and Mesenchymal GBM progression. WP1066 has been shown to have pro-apoptotic and anti-proliferative activity in glioma and most importantly shown to cross the blood brain barrier [143, 170]. Sorafenib has proven efficacy for treatment of various cancers and is currently in clinical trials for GBM [171, 172]. In our study, both drugs blocked the interaction of STAT3 and ANGPTL4 in GBM stem cells and lead to a decrease in expression of pro-angiogenic genes as well as stem cell marker genes, which suggest an important combined role of STAT3 and ANGPTL4 in Mesenchymal GBM stem cell maintenance. In addition, combined treatment with WP1066 and Sorafenib resulted in an induction of apoptosis in GBM CSCs. We also found that WP1066 and Sorafenib individually decreased Mesenchymal GBM cancer progression *in vivo*, while combined treatment lead to complete tumor regression. The drugs have not been used in combination previously, but our individual results are similar to previous studies done with these inhibitors. WP1066 has been shown to significantly inhibit growth of malignant glioma xenografts by blocking STAT3 activation and subsequent pro-proliferative genes [170]. Interestingly, studies show that Sorafenib induced growth arrest and apoptosis of GBM cells by blocking VEGF and STAT3 signaling [173]. Taken together, we have identified a significant relationship between STAT3 and ANGPTL4 in GBM stem cells and their therapeutic value as biomarkers in targeting the CSC subpopulation of Mesenchymal GBM.

Remaining Questions and Future Studies

While our molecular characterization of GBM cancer stem cells has led to the identification of distinct tumor initiating populations and novel therapeutic targets in treating GBM, further study must be done to verify these results. Most of the reports within this body of work were done using cells or tumor tissue derived from GBM6, which is a Classical GBM patient xenograft that exhibits overexpression of the VIII mutant of EGFR. It will be important to study additional patient-derived xenografts that contain amplified EGFR VIII (such as GBM39) as well as wild type EGFR (such as GBM10 and GBM12), which are patient-derived GMB xenografts from the laboratory of C. David James, UCSF. It will be important to establish adherent CSC cultures of these other xenografts to determine if this is truly a subpopulation of GBM stem cells that drives Mesenchymal GBM tumor initiation and progression. The upregulation and interaction of STAT3, NF-κB and ANGPTL4 signaling pathways will also need to be

verified in additional xenolines to confirm their role in stem cell maintenance and GBM tumor progression. While the relationship between STAT3 and NF-κB in cancer is well established, further characterization of the interaction between STAT3 and ANGPTL4 in GBM should be completed. Constitutive activation of STAT3 has been shown to activate ANGPTL4 in other cancers by binding its promoter and interacting with HIF-1 and other coactivators. Therefore, investigating the role of hypoxia and HIF-1 within glioma CSCs might lead to a better understanding of the novel relationship found between STAT3 and ANGPTL4 in GBM stem cells.

The aberrant activation of STAT3 and ANGPTL4 has previously been associated with Mesenchymal GBM, but their specific role in the CSC subpopulations of GBM warrants further investigation. To determine if STAT3 and ANGPTL4 activation drives the aggressive mesenchymal gene signature in GBM, gene knockdowns should be created in adherent CSCs to reveal the essential roles of STAT3 and ANGPTL4 in glioma tumor initiation and heterogeneity. Our lab has previously attempted to transduce GBM6 stem cells with a lentivirus-delivered shRNA against STAT3 and ANGPTL4, but knockdown resulted in widespread cell death. Currently, the lab is creating a doxycycline-dependent inducible knockdown system specific for these target genes to investigate the effect of diminished expression of STAT3 and ANGPTL4 on CSCs and tumor initiation. ANGPTL4 activity following inducible STAT3 knockdown will also be examined to determine if STAT3 is an essential regulator of ANGPTL4 signaling and subsequent tumor vascularization. This knockdown system will also be used to determine if knockdown of STAT3 or ANGPTL4 prevents the Mesenchymal gene signature observed in adherent GBM stem cells and their derived tumors.

Other genes differentially expressed between adherent CSCs and tumorspheres in our microarray analysis will be examined in future studies to determine if these genes also contribute to the mesenchymal gene signature. Our lab has recently identified Galectin-1, Annexin A1 and Major Vault Protein as being differentially expressed between the two GBM stem cell populations. These genes are involved in angiogenesis, stem cell maintenance and drug resistance respectively, and represent genes of interest that should be investigated further for their roles in CSCs that drive Classical or Mesenchymal GBM [176-178]. It will also be important to determine if these genes, along with STAT3, NF-κB and ANGPTL4, could serve as potential drug targets for treating mesenchymal GBM. The lab will soon be testing the efficacy of combined STAT3 and ANGPTL4 inhibition on intracranial Mesenchymal GBM tumors using WP1066 and Sorafenib. If these drugs cross the blood brain barrier and result in tumor regression, the combined treatment could eventually lead to clinical treatment regimens for GBM patients. Taken together, further investigation of these genes involved in glioma CSCs will give insight into the formation of distinct GBM subclasses and future therapeutic approaches in treating GBM.

LIST OF REFERENCES

1. Vaquerizas, J.M., et al., *A census of human transcription factors: function, expression and evolution.* Nat Rev Genet, 2009. **10**(4): p. 252-63.

2. Sellier, H., et al., *How should we define STAT3 as an oncogene and as a potential target for therapy?* JAKSTAT, 2013. **2**(3): p. e24716.

3. Accili, D. and K.C. Arden, *FoxOs at the crossroads of cellular metabolism, differentiation, and transformation.* Cell, 2004. **117**(4): p. 421-6.

4. Bain, G., et al., *E2A proteins are required for proper B cell development and initiation of immunoglobulin gene rearrangements.* Cell, 1994. **79**(5): p. 885-92.

5. Dynlacht, B.D., *Regulation of transcription by proteins that control the cell cycle.* Nature, 1997. **389**(6647): p. 149-52.

6. Libermann, T.A. and L.F. Zerbini, *Targeting transcription factors for cancer gene therapy.* Curr Gene Ther, 2006. **6**(1): p. 17-33.

7. Blume, A., T. Herdegen, and T. Unger, *Angiotensin peptides and inducible transcription factors.* J Mol Med (Berl), 1999. **77**(3): p. 339-57.

8. Marotta, L.L., et al., *The JAK2/STAT3 signaling pathway is required for growth of CD44(+)CD24(-) stem cell-like breast cancer cells in human tumors.* J Clin Invest, 2011. **121**(7): p. 2723-35.

9. Shostak, K. and A. Chariot, *NF-kappaB, stem cells and breast cancer: the links get stronger.* Breast Cancer Res, 2011. **13**(4): p. 214.

10. Kamran, M.Z., P. Patil, and R.P. Gude, *Role of STAT3 in cancer metastasis and translational advances.* Biomed Res Int, 2013. **2013**: p. 421821.

11. Yang, C.H., et al., *Direct association of STAT3 with the IFNAR-1 chain of the human type I interferon receptor.* J Biol Chem, 1996. **271**(14): p. 8057-61.

12. Akira, S., et al., *Molecular cloning of APRF, a novel IFN-stimulated gene factor 3 p91-related transcription factor involved in the gp130-mediated signaling pathway.* Cell, 1994. **77**(1): p. 63-71.

13. Zhong, Z., Z. Wen, and J.E. Darnell, Jr., *Stat3: a STAT family member activated by tyrosine phosphorylation in response to epidermal growth factor and interleukin-6.* Science, 1994. **264**(5155): p. 95-8.

14. Darnell, J.E., Jr., *Transcription factors as targets for cancer therapy.* Nat Rev Cancer, 2002. **2**(10): p. 740-9.

15. Turkson, J. and R. Jove, *STAT proteins: novel molecular targets for cancer drug discovery.* Oncogene, 2000. **19**(56): p. 6613-26.

16. Furqan, M., et al., *STAT inhibitors for cancer therapy.* J Hematol Oncol, 2013. **6**: p. 90.

17. Bowman, T., et al., *STATs in oncogenesis.* Oncogene, 2000. **19**(21): p. 2474-88.

18. Akira, S., *Roles of STAT3 defined by tissue-specific gene targeting.* Oncogene, 2000. **19**(21): p. 2607-11.

19. Yu, L.F., et al., *[The impact of decreased Stat3 activation on 5-fluorouracil resistance of human gastric cancer cell line]*. Zhonghua Nei Ke Za Zhi, 2004. **43**(12): p. 903-6.

20. Dang, C.V., *c-Myc target genes involved in cell growth, apoptosis, and metabolism.* Mol Cell Biol, 1999. **19**(1): p. 1-11.

21. Bhattacharya, S., R.M. Ray, and L.R. Johnson, *STAT3-mediated transcription of Bcl-2, Mcl-1 and c-IAP2 prevents apoptosis in polyamine-depleted cells.* Biochem J, 2005. **392**(Pt 2): p. 335-44.

22. Dechow, T.N., et al., *Requirement of matrix metalloproteinase-9 for the transformation of human mammary epithelial cells by Stat3-C.* Proc Natl Acad Sci U S A, 2004. **101**(29): p. 10602-7.

23. Suiqing, C., Z. Min, and C. Lirong, *Overexpression of phosphorylated-STAT3 correlated with the invasion and metastasis of cutaneous squamous cell carcinoma.* J Dermatol, 2005. **32**(5): p. 354-60.

24. Xie, T.X., et al., *Stat3 activation regulates the expression of matrix metalloproteinase-2 and tumor invasion and metastasis.* Oncogene, 2004. **23**(20): p. 3550-60.

25. Debidda, M., et al., *A role of STAT3 in Rho GTPase-regulated cell migration and proliferation.* J Biol Chem, 2005. **280**(17): p. 17275-85.

26. Teng, T.S., et al., *Stat3 promotes directional cell migration by regulating Rac1 activity via its activator betaPIX.* J Cell Sci, 2009. **122**(Pt 22): p. 4150-9.

27. Niu, G., et al., *Constitutive Stat3 activity up-regulates VEGF expression and tumor angiogenesis.* Oncogene, 2002. **21**(13): p. 2000-8.

28. Semenza, G.L., *Targeting HIF-1 for cancer therapy.* Nat Rev Cancer, 2003. **3**(10): p. 721-32.

29. Xu, Q., et al., *Targeting Stat3 blocks both HIF-1 and VEGF expression induced by multiple oncogenic growth signaling pathways.* Oncogene, 2005. **24**(36): p. 5552-60.

30. Sun, Z. and R. Andersson, *NF-kappaB activation and inhibition: a review.* Shock, 2002. **18**(2): p. 99-106.

31. Du, Z., et al., *Non-conventional signal transduction by type 1 interferons: the NF-kappaB pathway.* J Cell Biochem, 2007. **102**(5): p. 1087-94.

32. Tam, W.F., W. Wang, and R. Sen, *Cell-specific association and shuttling of IkappaBalpha provides a mechanism for nuclear NF-kappaB in B lymphocytes.* Mol Cell Biol, 2001. **21**(14): p. 4837-46.

33. Hayden, M.S. and S. Ghosh, *Shared principles in NF-kappaB signaling.* Cell, 2008. **132**(3): p. 344-62.

34. Garg, A. and B.B. Aggarwal, *Nuclear transcription factor-kappaB as a target for cancer drug development.* Leukemia, 2002. **16**(6): p. 1053-68.

35. Erl, W., et al., *Nuclear factor-kappa B regulates induction of apoptosis and inhibitor of apoptosis protein-1 expression in vascular smooth muscle cells.* Circ Res, 1999. **84**(6): p. 668-77.

36. Grilli, M. and M. Memo, *Nuclear factor-kappaB/Rel proteins: a point of convergence of signalling pathways relevant in neuronal function and dysfunction.* Biochem Pharmacol, 1999. **57**(1): p. 1-7.

37. Malek, S., T. Huxford, and G. Ghosh, *Ikappa Balpha functions through direct contacts with the nuclear localization signals and the DNA binding sequences of NF-kappaB.* J Biol Chem, 1998. **273**(39): p. 25427-35.

38. Aggarwal, B.B., *Nuclear factor-kappaB: the enemy within.* Cancer Cell, 2004. **6**(3): p. 203-8.

39. Beg, A.A. and D. Baltimore, *An essential role for NF-kappaB in preventing TNF-alpha-induced cell death.* Science, 1996. **274**(5288): p. 782-4.

40. Beg, A.A., et al., *Embryonic lethality and liver degeneration in mice lacking the RelA component of NF-kappa B.* Nature, 1995. **376**(6536): p. 167-70.

41. Van Antwerp, D.J., et al., *Suppression of TNF-alpha-induced apoptosis by NF-kappaB.* Science, 1996. **274**(5288): p. 787-9.

42. Wang, C.Y., M.W. Mayo, and A.S. Baldwin, Jr., *TNF- and cancer therapy-induced apoptosis: potentiation by inhibition of NF-kappaB.* Science, 1996. **274**(5288): p. 784-7.

43. Barkett, M. and T.D. Gilmore, *Control of apoptosis by Rel/NF-kappaB transcription factors.* Oncogene, 1999. **18**(49): p. 6910-24.

44. Guttridge, D.C., et al., *NF-kappaB controls cell growth and differentiation through transcriptional regulation of cyclin D1.* Mol Cell Biol, 1999. **19**(8): p. 5785-99.

45. Pahl, H.L., *Activators and target genes of Rel/NF-kappaB transcription factors.* Oncogene, 1999. **18**(49): p. 6853-66.

46. Iademarco, M.F., et al., *Characterization of the promoter for vascular cell adhesion molecule-1 (VCAM-1).* J Biol Chem, 1992. **267**(23): p. 16323-9.

47. van de Stolpe, A., et al., *12-O-tetradecanoylphorbol-13-acetate- and tumor necrosis factor alpha-mediated induction of intercellular adhesion molecule-1 is inhibited by dexamethasone. Functional analysis of the human intercellular adhesion molecular-1 promoter.* J Biol Chem, 1994. **269**(8): p. 6185-92.

48. Whelan, J., et al., *An NF kappa B-like factor is essential but not sufficient for cytokine induction of endothelial leukocyte adhesion molecule 1 (ELAM-1) gene transcription.* Nucleic Acids Res, 1991. **19**(10): p. 2645-53.

49. Chilov, D., et al., *Genomic organization of human and mouse genes for vascular endothelial growth factor C.* J Biol Chem, 1997. **272**(40): p. 25176-83.

50. Collart, M.A., P. Baeuerle, and P. Vassalli, *Regulation of tumor necrosis factor alpha transcription in macrophages: involvement of four kappa B-like motifs and of constitutive and inducible forms of NF-kappa B.* Mol Cell Biol, 1990. **10**(4): p. 1498-506.

51. Shakhov, A.N., et al., *Kappa B-type enhancers are involved in lipopolysaccharide-mediated transcriptional activation of the tumor necrosis factor alpha gene in primary macrophages.* J Exp Med, 1990. **171**(1): p. 35-47.

52. de la Iglesia, N., S.V. Puram, and A. Bonni, *STAT3 regulation of glioblastoma pathogenesis.* Curr Mol Med, 2009. **9**(5): p. 580-90.

53. Louis, D.N., et al., *The 2007 WHO classification of tumours of the central nervous system.* Acta Neuropathol, 2007. **114**(2): p. 97-109.

54. Stupp, R., et al., *Radiotherapy plus concomitant and adjuvant temozolomide for glioblastoma.* N Engl J Med, 2005. **352**(10): p. 987-96.

55. Abou-Ghazal, M., et al., *The incidence, correlation with tumor-infiltrating inflammation, and prognosis of phosphorylated STAT3 expression in human gliomas.* Clin Cancer Res, 2008. **14**(24): p. 8228-35.

56. Carro, M.S., et al., *The transcriptional network for mesenchymal transformation of brain tumours.* Nature, 2010. **463**(7279): p. 318-25.

57. Tchirkov, A., et al., *Interleukin-6 gene amplification and shortened survival in glioblastoma patients.* Br J Cancer, 2007. **96**(3): p. 474-6.

58. Repovic, P., et al., *Oncostatin-M induction of vascular endothelial growth factor expression in astroglioma cells.* Oncogene, 2003. **22**(50): p. 8117-24.

59. Brantley, E.C., et al., *Loss of protein inhibitors of activated STAT-3 expression in glioblastoma multiforme tumors: implications for STAT-3 activation and gene expression.* Clin Cancer Res, 2008. **14**(15): p. 4694-704.

60. Dasgupta, A., et al., *Stat3 activation is required for the growth of U87 cell-derived tumours in mice.* Eur J Cancer, 2009. **45**(4): p. 677-84.

61. Prasad, S.R., et al., *Common and uncommon histologic subtypes of renal cell carcinoma: imaging spectrum with pathologic correlation.* Radiographics, 2006. **26**(6): p. 1795-806; discussion 1806-10.

62. Korkolopoulou, P., et al., *Expression of nuclear factor-kappaB in human astrocytomas: relation to pI kappa Ba, vascular endothelial growth factor, Cox-2, microvascular characteristics, and survival.* Hum Pathol, 2008. **39**(8): p. 1143-52.

63. Wang, H., et al., *Analysis of the activation status of Akt, NFkappaB, and Stat3 in human diffuse gliomas.* Lab Invest, 2004. **84**(8): p. 941-51.

64. McCoy, M.K. and M.G. Tansey, *TNF signaling inhibition in the CNS: implications for normal brain function and neurodegenerative disease.* J Neuroinflammation, 2008. **5**: p. 45.

65. Otsuka, G., et al., *Inhibition of nuclear factor-kappaB activation confers sensitivity to tumor necrosis factor-alpha by impairment of cell cycle progression in human glioma cells.* Cancer Res, 1999. **59**(17): p. 4446-52.

66. Brown, R.E. and A. Law, *Morphoproteomic demonstration of constitutive nuclear factor-kappaB activation in glioblastoma multiforme with genomic correlates and therapeutic implications.* Ann Clin Lab Sci, 2006. **36**(4): p. 421-6.

67. Downward, J., *Mechanisms and consequences of activation of protein kinase B/Akt.* Curr Opin Cell Biol, 1998. **10**(2): p. 262-7.

68. Romashkova, J.A. and S.S. Makarov, *NF-kappaB is a target of AKT in anti-apoptotic PDGF signalling.* Nature, 1999. **401**(6748): p. 86-90.

69. Bredel, M., et al., *Tumor necrosis factor-alpha-induced protein 3 as a putative regulator of nuclear factor-kappaB-mediated resistance to O6-alkylating agents in human glioblastomas.* J Clin Oncol, 2006. **24**(2): p. 274-87.

70. Xie, T.X., et al., *Aberrant NF-kappaB activity is critical in focal necrosis formation of human glioblastoma by regulation of the expression of tissue factor.* Int J Oncol, 2008. **33**(1): p. 5-15.

71. Clarke, M.F., et al., *Cancer stem cells--perspectives on current status and future directions: AACR Workshop on cancer stem cells.* Cancer Res, 2006. **66**(19): p. 9339-44.

72. Huntly, B.J. and D.G. Gilliland, *Leukaemia stem cells and the evolution of cancer-stem-cell research.* Nat Rev Cancer, 2005. **5**(4): p. 311-21.

73. Li, Z., et al., *Turning cancer stem cells inside out: an exploration of glioma stem cell signaling pathways.* J Biol Chem, 2009. **284**(25): p. 16705-9.

74. Thon, N., et al., *Presence of pluripotent CD133+ cells correlates with malignancy of gliomas.* Mol Cell Neurosci, 2010. **43**(1): p. 51-9.

75. Reya, T., et al., *Stem cells, cancer, and cancer stem cells.* Nature, 2001. **414**(6859): p. 105-11.

76. Mather, J.P., *In vitro models.* Stem Cells, 2012. **30**(2): p. 95-9.

77. Pollard, S.M., et al., *Glioma stem cell lines expanded in adherent culture have tumor-specific phenotypes and are suitable for chemical and genetic screens.* Cell Stem Cell, 2009. **4**(6): p. 568-80.

78. Conti, L., et al., *Niche-independent symmetrical self-renewal of a mammalian tissue stem cell.* PLoS Biol, 2005. **3**(9): p. e283.

79. Sun, Y., et al., *CD133 (Prominin) negative human neural stem cells are clonogenic and tripotent.* PLoS One, 2009. **4**(5): p. e5498.

80. Villalva, C., et al., *STAT3 is essential for the maintenance of neurosphere-initiating tumor cells in patients with glioblastomas: a potential for targeted therapy?* Int J Cancer, 2011. **128**(4): p. 826-38.

81. Sherry, M.M., et al., *STAT3 is required for proliferation and maintenance of multipotency in glioblastoma stem cells.* Stem Cells, 2009. **27**(10): p. 2383-92.

82. Annabi, B., et al., *A MT1-MMP/NF-kappaB signaling axis as a checkpoint controller of COX-2 expression in CD133+ U87 glioblastoma cells.* J Neuroinflammation, 2009. **6**: p. 8.

83. Stein, S.J. and A.S. Baldwin, *Deletion of the NF-kappaB subunit p65/RelA in the hematopoietic compartment leads to defects in hematopoietic stem cell function.* Blood, 2013. **121**(25): p. 5015-24.

84. Lino, M.M., A. Merlo, and J.L. Boulay, *Notch signaling in glioblastoma: a developmental drug target?* BMC Med, 2010. **8**: p. 72.

85. Lee, H., et al., *Persistently activated Stat3 maintains constitutive NF-kappaB activity in tumors.* Cancer Cell, 2009. **15**(4): p. 283-93.

86. Yang, C.H., et al., *MicroRNA miR-21 regulates the metastatic behavior of B16 melanoma cells.* J Biol Chem, 2011. **286**(45): p. 39172-8.

87. Bray, S.J., *Notch signalling: a simple pathway becomes complex.* Nat Rev Mol Cell Biol, 2006. **7**(9): p. 678-89.

88. Wang, Z., et al., *Emerging role of Notch in stem cells and cancer.* Cancer Lett, 2009. **279**(1): p. 8-12.

89. Allenspach, E.J., et al., *Notch signaling in cancer.* Cancer Biol Ther, 2002. **1**(5): p. 466-76.

90. Dickson, B.C., et al., *High-level JAG1 mRNA and protein predict poor outcome in breast cancer.* Mod Pathol, 2007. **20**(6): p. 685-93.

91. Santagata, S., et al., *JAGGED1 expression is associated with prostate cancer metastasis and recurrence.* Cancer Res, 2004. **64**(19): p. 6854-7.

92. Miele, L., H. Miao, and B.J. Nickoloff, *NOTCH signaling as a novel cancer therapeutic target.* Curr Cancer Drug Targets, 2006. **6**(4): p. 313-23.

93. Ranganathan, P., K.L. Weaver, and A.J. Capobianco, *Notch signalling in solid tumours: a little bit of everything but not all the time.* Nat Rev Cancer, 2011. **11**(5): p. 338-51.

94. Ang, H.L. and V. Tergaonkar, *Notch and NFkappaB signaling pathways: Do they collaborate in normal vertebrate brain development and function?* Bioessays, 2007. **29**(10): p. 1039-47.

95. Kamakura, S., et al., *Hes binding to STAT3 mediates crosstalk between Notch and JAK-STAT signalling.* Nat Cell Biol, 2004. **6**(6): p. 547-54.

96. Ando, K., et al., *Induction of Notch signaling by tumor necrosis factor in rheumatoid synovial fibroblasts.* Oncogene, 2003. **22**(49): p. 7796-803.

97. Fernandez-Majada, V., et al., *Nuclear IKK activity leads to dysregulated notch-dependent gene expression in colorectal cancer.* Proc Natl Acad Sci U S A, 2007. **104**(1): p. 276-81.

98. Espinosa, L., et al., *IkappaBalpha and p65 regulate the cytoplasmic shuttling of nuclear corepressors: cross-talk between Notch and NFkappaB pathways.* Mol Biol Cell, 2003. **14**(2): p. 491-502.

99. Yang, Y.H., et al., *Suppression of the Raf/MEK/ERK signaling cascade and inhibition of angiogenesis by the carboxyl terminus of angiopoietin-like protein 4.* Arterioscler Thromb Vasc Biol, 2008. **28**(5): p. 835-40.

100. Wang, Y., et al., *Adiponectin modulates the glycogen synthase kinase-3beta/beta-catenin signaling pathway and attenuates mammary tumorigenesis of MDA-MB-231 cells in nude mice.* Cancer Res, 2006. **66**(23): p. 11462-70.

101. Wild, R., et al., *Quantitative assessment of angiogenesis and tumor vessel architecture by computer-assisted digital image analysis: effects of VEGF-toxin conjugate on tumor microvessel density.* Microvasc Res, 2000. **59**(3): p. 368-76.

102. Chen, Z. and Z.C. Han, *STAT3: a critical transcription activator in angiogenesis.* Med Res Rev, 2008. **28**(2): p. 185-200.

103. Wei, D., et al., *Stat3 activation regulates the expression of vascular endothelial growth factor and human pancreatic cancer angiogenesis and metastasis.* Oncogene, 2003. **22**(3): p. 319-29.

104. Bartoli, M., et al., *VEGF differentially activates STAT3 in microvascular endothelial cells.* FASEB J, 2003. **17**(11): p. 1562-4.

105. Hato, T., M. Tabata, and Y. Oike, *The role of angiopoietin-like proteins in angiogenesis and metabolism.* Trends Cardiovasc Med, 2008. **18**(1): p. 6-14.

106. Oike, Y., et al., *Angiopoietin-like proteins: potential new targets for metabolic syndrome therapy.* Trends Mol Med, 2005. **11**(10): p. 473-9.

107. Verine, J., et al., *Determination of angptl4 mRNA as a diagnostic marker of primary and metastatic clear cell renal-cell carcinoma.* PLoS One, 2010. **5**(4): p. e10421.

108. Zhu, P., et al., *Angiopoietin-like 4: a decade of research.* Biosci Rep, 2012. **32**(3): p. 211-9.

109. Chong, H.C., et al., *Matricellular proteins: a sticky affair with cancers.* J Oncol, 2012. **2012**: p. 351089.

110. Huang, R.L., et al., *ANGPTL4 modulates vascular junction integrity by integrin signaling and disruption of intercellular VE-cadherin and claudin-5 clusters.* Blood, 2011. **118**(14): p. 3990-4002.

111. Zhang, Z., et al., *Acquisition of anoikis resistance reveals a synoikis-like survival style in BEL7402 hepatoma cells.* Cancer Lett, 2008. **267**(1): p. 106-15.

112. Ma, T., et al., *Viral G protein-coupled receptor up-regulates Angiopoietin-like 4 promoting angiogenesis and vascular permeability in Kaposi's sarcoma.* Proc Natl Acad Sci U S A, 2010. **107**(32): p. 14363-8.

113. Li, H., et al., *Hypoxia-inducible factor 1 alpha-activated angiopoietin-like protein 4 contributes to tumor metastasis via vascular cell adhesion molecule-1/integrin beta1 signaling in human hepatocellular carcinoma.* Hepatology, 2011. **54**(3): p. 910-9.

114. Dauer, D.J., et al., *Stat3 regulates genes common to both wound healing and cancer.* Oncogene, 2005. **24**(21): p. 3397-408.

115. Pawlus, M.R., L. Wang, and C.J. Hu, *STAT3 and HIF1alpha cooperatively activate HIF1 target genes in MDA-MB-231 and RCC4 cells.* Oncogene, 2013.

116. Godard, S., et al., *Classification of human astrocytic gliomas on the basis of gene expression: a correlated group of genes with angiogenic activity emerges as a strong predictor of subtypes.* Cancer Res, 2003. **63**(20): p. 6613-25.

117. Rickman, D.S., et al., *Distinctive molecular profiles of high-grade and low-grade gliomas based on oligonucleotide microarray analysis.* Cancer Res, 2001. **61**(18): p. 6885-91.

118. van den Boom, J., et al., *Characterization of gene expression profiles associated with glioma progression using oligonucleotide-based microarray analysis and real-time reverse transcription-polymerase chain reaction.* Am J Pathol, 2003. **163**(3): p. 1033-43.

119. Nutt, C.L., et al., *Gene expression-based classification of malignant gliomas correlates better with survival than histological classification.* Cancer Res, 2003. **63**(7): p. 1602-7.

120. Verhaak, R.G., et al., *Integrated genomic analysis identifies clinically relevant subtypes of glioblastoma characterized by abnormalities in PDGFRA, IDH1, EGFR, and NF1.* Cancer Cell, 2010. **17**(1): p. 98-110.

121. Furnari, F.B., et al., *Malignant astrocytic glioma: genetics, biology, and paths to treatment.* Genes Dev, 2007. **21**(21): p. 2683-710.

122. Watanabe, K., et al., *Overexpression of the EGF receptor and p53 mutations are mutually exclusive in the evolution of primary and secondary glioblastomas.* Brain Pathol, 1996. **6**(3): p. 217-23; discussion 23-4.

123. Yan, H., et al., *IDH1 and IDH2 mutations in gliomas.* N Engl J Med, 2009. **360**(8): p. 765-73.

124. Thiery, J.P., *Epithelial-mesenchymal transitions in tumour progression.* Nat Rev Cancer, 2002. **2**(6): p. 442-54.

125. Phillips, H.S., et al., *Molecular subclasses of high-grade glioma predict prognosis, delineate a pattern of disease progression, and resemble stages in neurogenesis.* Cancer Cell, 2006. **9**(3): p. 157-73.

126. Zhu, Y., et al., *Neurofibromas in NF1: Schwann cell origin and role of tumor environment.* Science, 2002. **296**(5569): p. 920-2.

127. Bhat, K.P., et al., *Mesenchymal differentiation mediated by NF-kappaB promotes radiation resistance in glioblastoma.* Cancer Cell, 2013. **24**(3): p. 331-46.

128. Yang, C.H., et al., *Identification of CXCL11 as a STAT3-dependent gene induced by IFN.* J Immunol, 2007. **178**(2): p. 986-92.

129. Wei, L., et al., *NFkappaB negatively regulates interferon-induced gene expression and anti-influenza activity.* J Biol Chem, 2006. **281**(17): p. 11678-84.

130. Huang da, W., B.T. Sherman, and R.A. Lempicki, *Systematic and integrative analysis of large gene lists using DAVID bioinformatics resources.* Nat Protoc, 2009. **4**(1): p. 44-57.

131. Jensen, L.J., et al., *STRING 8--a global view on proteins and their functional interactions in 630 organisms.* Nucleic Acids Res, 2009. **37**(Database issue): p. D412-6.

132. Dontu, G., et al., *In vitro propagation and transcriptional profiling of human mammary stem/progenitor cells.* Genes Dev, 2003. **17**(10): p. 1253-70.

133. Lee, A., et al., *Isolation of neural stem cells from the postnatal cerebellum.* Nat Neurosci, 2005. **8**(6): p. 723-9.

134. Androutsellis-Theotokis, A., et al., *Notch signalling regulates stem cell numbers in vitro and in vivo.* Nature, 2006. **442**(7104): p. 823-6.

135. Fan, X., et al., *NOTCH pathway blockade depletes CD133-positive glioblastoma cells and inhibits growth of tumor neurospheres and xenografts.* Stem Cells, 2010. **28**(1): p. 5-16.

136. Mani, S.A., et al., *The epithelial-mesenchymal transition generates cells with properties of stem cells.* Cell, 2008. **133**(4): p. 704-15.

137. Ma, Y.H., et al., *Expression of stem cell markers in human astrocytomas of different WHO grades.* J Neurooncol, 2008. **86**(1): p. 31-45.

138. Liu, G., et al., *Analysis of gene expression and chemoresistance of CD133+ cancer stem cells in glioblastoma.* Mol Cancer, 2006. **5**: p. 67.

139. Wu, A., et al., *Persistence of CD133+ cells in human and mouse glioma cell lines: detailed characterization of GL261 glioma cells with cancer stem cell-like properties.* Stem Cells Dev, 2008. **17**(1): p. 173-84.

140. Grivennikov, S.I. and M. Karin, *Dangerous liaisons: STAT3 and NF-kappaB collaboration and crosstalk in cancer.* Cytokine Growth Factor Rev, 2010. **21**(1): p. 11-9.

141. Gill, J.S., et al., *Effects of NFkappaB decoy oligonucleotides released from biodegradable polymer microparticles on a glioblastoma cell line.* Biomaterials, 2002. **23**(13): p. 2773-81.

142. Mizoguchi, M., et al., *Activation of STAT3, MAPK, and AKT in malignant astrocytic gliomas: correlation with EGFR status, tumor grade, and survival.* J Neuropathol Exp Neurol, 2006. **65**(12): p. 1181-8.

143. Hussain, S.F., et al., *A novel small molecule inhibitor of signal transducers and activators of transcription 3 reverses immune tolerance in malignant glioma patients.* Cancer Res, 2007. **67**(20): p. 9630-6.

144. Hitoshi, S., et al., *Mammalian Gcm genes induce Hes5 expression by active DNA demethylation and induce neural stem cells.* Nat Neurosci, 2011. **14**(8): p. 957-64.

145. Liang, Y., et al., *Gene expression profiling reveals molecularly and clinically distinct subtypes of glioblastoma multiforme.* Proc Natl Acad Sci U S A, 2005. **102**(16): p. 5814-9.

146. Cancer Genome Atlas Research, N., *Comprehensive genomic characterization defines human glioblastoma genes and core pathways.* Nature, 2008. **455**(7216): p. 1061-8.

147. Dunn, G.P., et al., *Emerging insights into the molecular and cellular basis of glioblastoma.* Genes Dev, 2012. **26**(8): p. 756-84.

148. Eng, L.F., R.S. Ghirnikar, and Y.L. Lee, *Glial fibrillary acidic protein: GFAP-thirty-one years (1969-2000).* Neurochem Res, 2000. **25**(9-10): p. 1439-51.

149. Kahn, H.J., et al., *Role of antibody to S100 protein in diagnostic pathology.* Am J Clin Pathol, 1983. **79**(3): p. 341-7.

150. Hirokawa, N., S. Hisanaga, and Y. Shiomura, *MAP2 is a component of crossbridges between microtubules and neurofilaments in the neuronal cytoskeleton: quick-freeze, deep-etch immunoelectron microscopy and reconstitution studies.* J Neurosci, 1988. **8**(8): p. 2769-79.

151. Marie, Y., et al., *OLIG2 as a specific marker of oligodendroglial tumour cells.* Lancet, 2001. **358**(9278): p. 298-300.

152. Xie, Q., et al., *A highly invasive human glioblastoma pre-clinical model for testing therapeutics.* J Transl Med, 2008. **6**: p. 77.

153. Abdelzaher, E. *CNS Tumors Pathology - Glioblastoma Multiforme*. 2013 March 2012 [cited 2014 March 15]; Available from: http://www.pathologyoutlines.com/topic/cnstumorglioblastoma.html.

154. Garner, J.M., et al., *Constitutive activation of signal transducer and activator of transcription 3 (STAT3) and nuclear factor kappaB signaling in glioblastoma cancer stem cells regulates the Notch pathway.* J Biol Chem, 2013. **288**(36): p. 26167-76.

155. Lewis-Tuffin, L.J., et al., *Misregulated E-cadherin expression associated with an aggressive brain tumor phenotype.* PLoS One, 2010. **5**(10): p. e13665.

156. Liu, W.M., et al., *Lyn facilitates glioblastoma cell survival under conditions of nutrient deprivation by promoting autophagy.* PLoS One, 2013. **8**(8): p. e70804.

157. Okamura, T., et al., *NADPH/quinone oxidoreductase is a priority target of glioblastoma chemotherapy.* Int J Oncol, 2000. **16**(2): p. 295-303.

158. Brat, D.J., A.C. Bellail, and E.G. Van Meir, *The role of interleukin-8 and its receptors in gliomagenesis and tumoral angiogenesis.* Neuro Oncol, 2005. **7**(2): p. 122-33.

159. Strieter, R.M., et al., *Cancer CXC chemokine networks and tumour angiogenesis.* Eur J Cancer, 2006. **42**(6): p. 768-78.

160. Kleihues, P. and L.H. Sobin, *World Health Organization classification of tumors.* Cancer, 2000. **88**(12): p. 2887.

161. Chen, R., et al., *A hierarchy of self-renewing tumor-initiating cell types in glioblastoma.* Cancer Cell, 2010. **17**(4): p. 362-75.

162. Wang, J., et al., *CD133 negative glioma cells form tumors in nude rats and give rise to CD133 positive cells.* Int J Cancer, 2008. **122**(4): p. 761-8.

163. Bonavia, R., et al., *Heterogeneity maintenance in glioblastoma: a social network.* Cancer Res, 2011. **71**(12): p. 4055-60.

164. Rong, Y., et al., *'Pseudopalisading' necrosis in glioblastoma: a familiar morphologic feature that links vascular pathology, hypoxia, and angiogenesis.* J Neuropathol Exp Neurol, 2006. **65**(6): p. 529-39.

165. Katanasaka, Y., et al., *Epidermal growth factor receptor variant type III markedly accelerates angiogenesis and tumor growth via inducing c-myc mediated angiopoietin-like 4 expression in malignant glioma.* Mol Cancer, 2013. **12**: p. 31.

166. Le Jan, S., et al., *Angiopoietin-like 4 is a proangiogenic factor produced during ischemia and in conventional renal cell carcinoma.* Am J Pathol, 2003. **162**(5): p. 1521-8.

167. Minn, A.J., et al., *Genes that mediate breast cancer metastasis to lung.* Nature, 2005. **436**(7050): p. 518-24.

168. Yu, H. and R. Jove, *The STATs of cancer--new molecular targets come of age.* Nat Rev Cancer, 2004. **4**(2): p. 97-105.

169. Tan, M.J., et al., *Emerging roles of angiopoietin-like 4 in human cancer.* Mol Cancer Res, 2012. **10**(6): p. 677-88.

170. Iwamaru, A., et al., *A novel inhibitor of the STAT3 pathway induces apoptosis in malignant glioma cells both in vitro and in vivo.* Oncogene, 2007. **26**(17): p. 2435-44.

171. Lee, E.Q., et al., *Phase I/II study of sorafenib in combination with temsirolimus for recurrent glioblastoma or gliosarcoma: North American Brain Tumor Consortium study 05-02.* Neuro Oncol, 2012. **14**(12): p. 1511-8.

172. Wilhelm, S.M., et al., *Preclinical overview of sorafenib, a multikinase inhibitor that targets both Raf and VEGF and PDGF receptor tyrosine kinase signaling.* Mol Cancer Ther, 2008. **7**(10): p. 3129-40.

173. Yang, F., et al., *Sorafenib induces growth arrest and apoptosis of human glioblastoma cells through the dephosphorylation of signal transducers and activators of transcription 3.* Mol Cancer Ther, 2010. **9**(4): p. 953-62.

174. Galli, R., et al., *Isolation and characterization of tumorigenic, stem-like neural precursors from human glioblastoma.* Cancer Res, 2004. **64**(19): p. 7011-21.

175. Lee, J., et al., *Tumor stem cells derived from glioblastomas cultured in bFGF and EGF more closely mirror the phenotype and genotype of primary tumors than do serum-cultured cell lines.* Cancer Cell, 2006. **9**(5): p. 391-403.

176. Chen, J., et al., *High expressions of galectin-1 and VEGF are associated with poor prognosis in gastric cancer patients.* Tumour Biol, 2013.

177. Geary, L.A., et al., *CAF-secreted Annexin A1 Induces Prostate Cancer Cells to Gain Stem Cell-like Features.* Mol Cancer Res, 2014.

178. Scheffer, G.L., et al., *The drug resistance-related protein LRP is the human major vault protein.* Nat Med, 1995. **1**(6): p. 578-82.

VITA

Jo Meagan Garner was born in 1986 in Huntingdon, TN. She graduated with her Bachelor of Science from Tennessee Technological University in 2009 with a major in Biochemistry. After graduating, she entered the Integrated Program in Biomedical Sciences (IPBS) Cancer and Developmental Biology track at the University of Tennessee Health Science Center in August of 2009. She then joined Dr. Lawrence M. Pfeffer's laboratory studying the role of cancer stem-like cells in Glioblastoma initiation, progression and invasion. She graduated with the degree Doctor of Philosophy in May 2014 with a focus on cancer biology.